

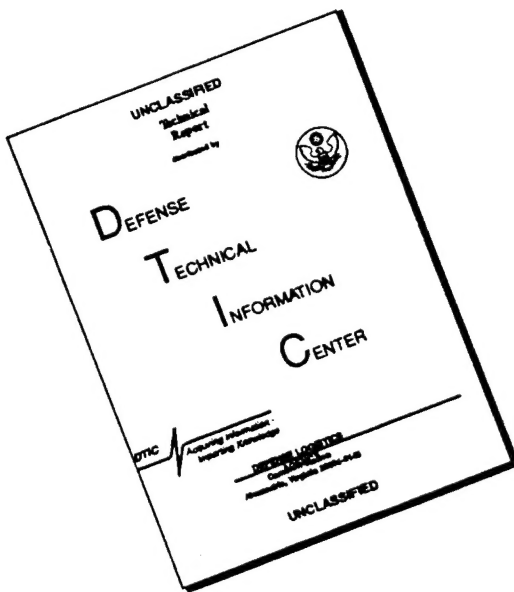
# REPORT DOCUMENTATION PAGE

*Form Approved  
OMB No. 0704-0188*

Public reporting burden for this collection of information is estimated to average 1 hour per response, including the time for reviewing instructions, searching existing data sources, gathering and maintaining the data needed, and completing and reviewing the collection of information. Send comments regarding this burden estimate or any other aspect of this collection of information, including suggestions for reducing this burden, to Washington Headquarters Services, Directorate for Information Operations and Reports, 1215 Jefferson Davis Highway, Suite 1204, Arlington, VA 22202-4302, and to the Office of Management and Budget, Paperwork Reduction Project (0704-0188), Washington, DC 20503.

<b>1. AGENCY USE ONLY (Leave blank)</b>			<b>2. REPORT DATE</b> 11 Dec 95	<b>3. REPORT TYPE AND DATES COVERED</b>	
<b>4. TITLE AND SUBTITLE</b> <i>Predicting Critical Strains, Pavement Life, and Overlay Requirements Using Pavement Deflection Measurements</i>			<b>5. FUNDING NUMBERS</b>		
<b>6. AUTHOR(S)</b>  Elaine M. Gallant					
<b>7. PERFORMING ORGANIZATION NAME(S) AND ADDRESS(ES)</b>  AFIT Student Attending:  University of Washington			<b>8. PERFORMING ORGANIZATION REPORT NUMBER</b>  96-021		
<b>9. SPONSORING/MONITORING AGENCY NAME(S) AND ADDRESS(ES)</b>  DEPARTMENT OF THE AIR FORCE AFIT/CI 2950 P STREET, BLDG 125 WRIGHT-PATTERSON AFB OH 45433-7765			<b>10. SPONSORING/MONITORING AGENCY REPORT NUMBER</b>		
<b>11. SUPPLEMENTARY NOTES</b>					
<b>12a. DISTRIBUTION / AVAILABILITY STATEMENT</b>  Approved for Public Release IAW AFR 190-1 Distribution Unlimited BRIAN D. GAUTHIER, MSgt, USAF Chief Administration			<b>12b. DISTRIBUTION CODE</b>		
<b>13. ABSTRACT (Maximum 200 words)</b>					
<b>14. SUBJECT TERMS</b>			<b>15. NUMBER OF PAGES</b> 153		
			<b>16. PRICE CODE</b>		
<b>17. SECURITY CLASSIFICATION OF REPORT</b>	<b>18. SECURITY CLASSIFICATION OF THIS PAGE</b>	<b>19. SECURITY CLASSIFICATION OF ABSTRACT</b>	<b>20. LIMITATION OF ABSTRACT</b>		

# **DISCLAIMER NOTICE**



**THIS DOCUMENT IS BEST  
QUALITY AVAILABLE. THE COPY  
FURNISHED TO DTIC CONTAINED  
A SIGNIFICANT NUMBER OF  
PAGES WHICH DO NOT  
REPRODUCE LEGIBLY.**

## GENERAL INSTRUCTIONS FOR COMPLETING SF 298

The Report Documentation Page (RDP) is used in announcing and cataloging reports. It is important that this information be consistent with the rest of the report, particularly the cover and title page. Instructions for filling in each block of the form follow. It is important to stay *within the lines* to meet *optical scanning requirements*.

**Block 1. Agency Use Only (Leave blank).**

**Block 2. Report Date.** Full publication date including day, month, and year, if available (e.g. 1 Jan 88). Must cite at least the year.

**Block 3. Type of Report and Dates Covered.**

State whether report is interim, final, etc. If applicable, enter inclusive report dates (e.g. 10 Jun 87 - 30 Jun 88).

**Block 4. Title and Subtitle.** A title is taken from the part of the report that provides the most meaningful and complete information. When a report is prepared in more than one volume, repeat the primary title, add volume number, and include subtitle for the specific volume. On classified documents enter the title classification in parentheses.

**Block 5. Funding Numbers.** To include contract and grant numbers; may include program element number(s), project number(s), task number(s), and work unit number(s). Use the following labels:

C - Contract	PR - Project
G - Grant	TA - Task
PE - Program Element	WU - Work Unit Accession No.

**Block 6. Author(s).** Name(s) of person(s) responsible for writing the report, performing the research, or credited with the content of the report. If editor or compiler, this should follow the name(s).

**Block 7. Performing Organization Name(s) and Address(es).** Self-explanatory.

**Block 8. Performing Organization Report Number.** Enter the unique alphanumeric report number(s) assigned by the organization performing the report.

**Block 9. Sponsoring/Monitoring Agency Name(s) and Address(es).** Self-explanatory.

**Block 10. Sponsoring/Monitoring Agency Report Number. (If known)**

**Block 11. Supplementary Notes.** Enter information not included elsewhere such as: Prepared in cooperation with...; Trans. of...; To be published in.... When a report is revised, include a statement whether the new report supersedes or supplements the older report.

**Block 12a. Distribution/Availability Statement.**

Denotes public availability or limitations. Cite any availability to the public. Enter additional limitations or special markings in all capitals (e.g. NOFORN, REL, ITAR).

**DOD** - See DoDD 5230.24, "Distribution Statements on Technical Documents."

**DOE** - See authorities.

**NASA** - See Handbook NHB 2200.2.

**NTIS** - Leave blank.

**Block 12b. Distribution Code.**

**DOD** - Leave blank.

**DOE** - Enter DOE distribution categories from the Standard Distribution for Unclassified Scientific and Technical Reports.

**NASA** - Leave blank.

**NTIS** - Leave blank.

**Block 13. Abstract.** Include a brief (*Maximum 200 words*) factual summary of the most significant information contained in the report.

**Block 14. Subject Terms.** Keywords or phrases identifying major subjects in the report.

**Block 15. Number of Pages.** Enter the total number of pages.

**Block 16. Price Code.** Enter appropriate price code (*NTIS only*).

**Blocks 17. - 19. Security Classifications.** Self-explanatory. Enter U.S. Security Classification in accordance with U.S. Security Regulations (i.e., UNCLASSIFIED). If form contains classified information, stamp classification on the top and bottom of the page.

**Block 20. Limitation of Abstract.** This block must be completed to assign a limitation to the abstract. Enter either UL (unlimited) or SAR (same as report). An entry in this block is necessary if the abstract is to be limited. If blank, the abstract is assumed to be unlimited.

Predicting Critical Strains, Pavement Life, and Overlay Requirements  
Using Pavement Deflection Measurements

by

Elaine M. Gallant

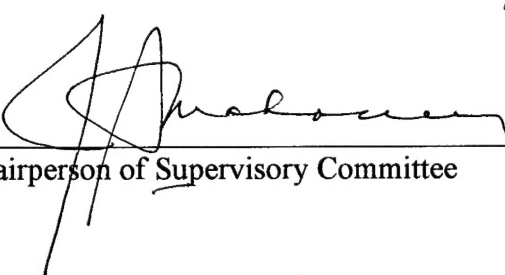
A thesis submitted in partial fulfillment  
of the requirements for the degree of

Master of Science in Civil Engineering

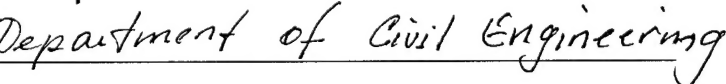
University of Washington

1995

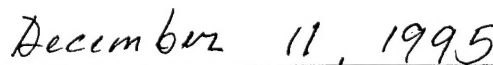
Approved by \_\_\_\_\_

  
Chairperson of Supervisory Committee

Program Authorized  
to Offer Degree \_\_\_\_\_

  
Department of Civil Engineering

Date \_\_\_\_\_

  
December 11, 1995

In presenting this thesis in partial fulfillment of the requirements for a Master's degree at the University of Washington, I agree that the library shall make its copies freely available for inspection. I further agree that extensive copying of this thesis is allowable only for scholarly purposes, consistent with "fair use" as prescribed in the U.S. Copyright Law. Any other reproduction for any purposes or by any means shall not be allowed without my written permission.

Signature \_\_\_\_\_

Date \_\_\_\_\_

## TABLE OF CONTENTS

	<u>Page</u>
List of Tables . . . . .	ii
List of Figures . . . . .	iv
Chapter 1: Introduction . . . . .	1
1.1 Background . . . . .	1
1.2 Scope . . . . .	2
1.3 Structure . . . . .	2
Chapter 2: Literature Review . . . . .	4
2.1 Introduction . . . . .	4
2.2 Nondestructive Testing . . . . .	4
2.3 Interpretation of NDT Data . . . . .	6
2.4 Design Procedures . . . . .	11
2.5 Sources of Error . . . . .	18
2.6 Significant Parameters Affecting NDT . . . . .	19
2.7 Developing Standard Procedures . . . . .	24
2.8 Methods Employed by SHAs and Other Agencies . . . . .	25
Chapter 3: Predicting Critical Strains and Pavement Life . . . . .	28
3.1 Introduction . . . . .	28
3.2 Methodology . . . . .	29
3.3 Results . . . . .	36
3.4 Case Study Comparison . . . . .	39
3.5 Conclusion . . . . .	50
Chapter 4: Load Adjustment . . . . .	52
4.1 Introduction . . . . .	52
4.2 Methodology . . . . .	53
4.3 Results . . . . .	60
4.4 Conclusion . . . . .	65
Chapter 5: Predicting Overlay Requirements . . . . .	66
5.1 Introduction . . . . .	66
5.2 Methodology . . . . .	66
5.3 Results . . . . .	68
5.4 Conclusion . . . . .	73
Chapter 6: Conclusions and Recommendations . . . . .	76
6.1 Conclusions . . . . .	76
6.2 Recommendations . . . . .	77
References . . . . .	79
Bibliography . . . . .	82
Appendix A: Data . . . . .	86
Appendix B: Graphs . . . . .	115
Appendix C: Regression Analysis . . . . .	124
Appendix D: Minitab Output . . . . .	128
Appendix E: Nondestructive Testing Devices . . . . .	137
Appendix F: Temperature Adjustment . . . . .	149

## LIST OF TABLES

Number	Page
2-1 State Highway Administration Deflection Equipment . . . . .	6
2-2 Summary of Deflection Basin Parameters . . . . .	8
2-3 Area Parameter Values for Typical Pavements . . . . .	9
2-4 Predictive Relationships for Subgrade Modulus . . . . .	10
2-5 Regression Equations Developed by Gomez-Achecar and Thompson .	17
3-1 Case Numbers for EVERSTRS Calculations. . . . .	34
3-2 Comparison of $\epsilon_t$ for Selected Case Numbers . . . . .	40
3-3 Comparison of $\epsilon_v$ for Selected Case Numbers . . . . .	41
3-4 Pavement Characteristics for Case Study Number One . . . . .	44
3-5 Comparison of Results for Predicting $\epsilon_t$ Using A & $E_{SG}$ . . . . .	45
3-6 Comparison of Results for Predicting $\epsilon_t$ Using $D_0$ & $E_{SG}$ . . . . .	46
3-7 Comparison of Results for Predicting $\epsilon_v$ Using A & $E_{SG}$ . . . . .	47
3-8 Comparison of Results for Predicting $\epsilon_v$ Using $D_0$ & $E_{SG}$ . . . . .	48
3-9 Comparison of Pavement Life Remaining for Fatigue Failure . . . . .	49
3-10 Comparison of Pavement Life Remaining for Rutting Failure . . . . .	50
4-1 Pavement Scenarios Used to Generate Load Adjustment Factors . . . . .	54
4-2 Error in Adjusting Area Parameter to 40 kN . . . . .	61
4-3 Error in Adjusting $D_0$ to 40 kN . . . . .	63
5-1 Comparison of Overlay Results - Case Study Number One . . . . .	70
5-2 Overlay Discrepancy Based on Seasonal Variation . . . . .	71
5-3 Overlay Discrepancy Based on Load Configuration . . . . .	72
5-4 Comparison of Overlay Results - Case Study Number Two . . . . .	74
6-1 Summary of Equations Developed in this Thesis . . . . .	77
A-1 Data Output from EVERSTRS . . . . .	89
A-2 EVERPAVE Output . . . . .	94
A-3 Comparison of Overlay Required EVERPAVE vs Equation . . . . .	105

Number	Page
D-1 Regression Equations for $\varepsilon_t$ and $\log \varepsilon_t$ . . . . .	128
D-2 Regression Equations for $\log \varepsilon_v$ . . . . .	128
D-3 Regression Equations for $\varepsilon_v$ . . . . .	129
D-4 Regression Equations for Area Parameter Load Adjustment . . . . .	129
D-5 Regression Equations for $D_0$ Load Adjustment . . . . .	130
D-6 Regression Equations for Slope of $D_0$ Adjustment for Load . . . . .	131
D-7 Regression Equations for Temperature Shift Factor for A . . . . .	132
D-8 Regression Equations for Area Temperature Shift Factor Calculation	133
D-9 Regression Equations for $D_0$ Temperature Shift Factor Calculation . .	134
D-10 Regression Equations for Overlay, N=327 . . . . .	135
D-11 Regression Equations for Overlay, N=360 . . . . .	135
F-1 Ranges of $E_{AC}$ Used vs Temperature . . . . .	150
F-2 Temperature Shift Factors for 1/A . . . . .	151
F-3 Temperature Shift Factors for $D_0$ . . . . .	152

## LIST OF FIGURES

Number	Page
2-1 Graphical Representation of Area Parameter . . . . .	9
2-2 Simplified Flow Chart for EVERCALC. . . . .	15
2-3 Agencies Use of Design Procedures . . . . .	25
2-4 Agencies Method of Asphalt Concrete Characterization . . . . .	26
2-5 Agencies Method of Base/Subbase Characterization . . . . .	26
2-6 Agencies Method of Subgrade Characterization . . . . .	27
3-1 Typical Deflection Basin . . . . .	28
3-2 Pavement Response Locations Used in Evaluating Load Effects . . . . .	33
3-3 Illustration of Area Parameter Limit for Prediction of Strain . . . . .	37
4-1 Load vs Area Parameter Graph . . . . .	55
4-2 Load vs $D_0$ Graph . . . . .	55
A-1 Sample EVERSTRS Output Sheet, page 1 . . . . .	87
A-2 Sample EVERSTRS Output Sheet, page 2 . . . . .	88
B-1 Typical Relationships Between Variables . . . . .	116
B-2 Area Parameter vs $\epsilon_v$ for All Subgrades . . . . .	117
B-3 Area Parameter vs $\epsilon_v$ for Subgrades with Modulus = 35 MPa . . . . .	118
B-4 Area Parameter vs $\epsilon_v$ for Subgrades with Modulus = 70 MPa . . . . .	118
B-5 Area Parameter vs $\epsilon_v$ for Subgrades with Modulus = 140 MPa . . . . .	119
B-6 Area Parameter vs $\epsilon_v$ for Subgrades with Modulus = 280 MPa . . . . .	119
B-7 Area Parameter vs $\epsilon_t$ for All Subgrades . . . . .	120
B-8 Area Parameter vs $\epsilon_t$ for Subgrades with Modulus = 35 MPa . . . . .	121
B-9 Area Parameter vs $\epsilon_t$ for Subgrades with Modulus = 70 MPa . . . . .	121
B-10 Area Parameter vs $\epsilon_t$ for Subgrades with Modulus = 140 MPa . . . . .	122
B-11 Area Parameter vs $\epsilon_t$ for Subgrades with Modulus = 280 MPa . . . . .	122
B-12 $D_0$ vs $\epsilon_v$ for All Subgrades . . . . .	123

Number	Page
B-13 D <sub>0</sub> vs ε <sub>t</sub> for All Subgrades . . . . .	123
C-1 Illustration of the “Best Fit” Line . . . . .	126
E-1 Typical FWD Configuration of Loading Plate and Geophones . . . . .	142
E-2 Illustration of FWD Deflection Basin . . . . .	143
E-3 First Point Measurement . . . . .	146
E-4 Second Point Measurement . . . . .	147
E-5 Variable Beam Angle and Height . . . . .	148

## ACKNOWLEDGEMENTS

A project of this size is not accomplished without the assistance and support of many individuals. I want to express my gratitude to Professor Joe Mahoney, my advisor, for his advice and expertise on this subject. I am particularly thankful for his consistent enthusiasm concerning the research efforts and the results achieved. Thank you to Professor Steve Kramer and Professor George Turkiyyah for being on my committee and providing insightful comments and critiques. I am very grateful to the U.S. Air Force for providing this opportunity and specifically to my previous boss, Mike Grenko, for providing computer support.

Thank you to my husband, Peter (my computer expert) and our son, Ryan (my data entry expert) for their patience while I worked nights and weekends on this project. Without their loving support I could not have completed this project. I also want to thank my mother for her support and encouragement throughout the past 28 years.

## **CHAPTER 1**

### **INTRODUCTION**

#### **1.1 BACKGROUND**

The pavement structure is the single most costly element of America's highway system (AASHTO Guide, 1993). It is not surprising then that Federal, State, and local Transportation Departments are continuously seeking advances in technology to reduce this cost. The development of mechanistic-empirical approaches for rehabilitation designs based on layered elastic theory is very promising. The falling weight deflectometer (FWD) is the device most often used to provide the field data necessary for mechanistic-empirical calculations. As mechanistic-empirical approaches and layered elastic theory design aids become more commonly used, pavement design will steadily transition from an art to a science based on accepted theory.

The ultimate goal is to accurately depict the remaining life of a given pavement section and to design an overlay that is neither over-conservative nor under-conservative. These analysis methods can also be used to prioritize pavements for rehabilitation based on scientific data as opposed to general rules-of-thumb. The pavement engineer will then have a clear picture of the priority for pavement overlays and an accurate measure of the thickness required to extend the life of the pavement.

Mechanistic design procedures are based on layered-elastic theory which supposes that pavements can be modeled as a multi-layered elastic structure placed on an elastic foundation. If pavements are modeled in this manner it is possible to calculate

stresses, strains and deflections due to traffic and/or environmental conditions at any point within or below the structure (AASHTO Guide, 1993). Because pavement performance is also affected by other parameters which cannot be directly modeled by mechanistic models, empirical correlations must be incorporated into the process. This is why it is referred to as a mechanistic-empirical design procedure.

### **1.2 SCOPE**

The goal of the research described in this thesis is to develop relationships using measurable pavement responses to loading to predict the current pavement life and the overlay requirements. The equations are designed to be used with any pavement nondestructive testing device that can measure the pavement deflection basin. The most popular device currently in use is the FWD. The most promising new technology is a laser rolling wheel deflectometer; prototypes are being developed by Quest Integrated and the Swedish National Road Administration.

### **1.3 STRUCTURE**

This thesis is structured as follows:

Chapter 1 is the Introduction.

Chapter 2 is the Literature Review. Its purpose is to describe previous research conducted, basic theories and applications, and current practices pertinent to this thesis.

Chapter 3 describes the research conducted and the methodology for developing predictive relationships for life remaining in the pavement structure.

Chapter 4 describes the research conducted and the methodology for developing an adjustment factor for load to adjust both Area Parameter and  $D_0$  to a standard load.

Chapter 5 describes the research conducted and the methodology for developing predictive relationships for the overlay required on a pavement system.

Chapter 6 provides some conclusions and recommendations for further research in this area.

The Appendices contain much of the data, charts, and equations that are important background to this thesis but were not necessary in the main text.

## **CHAPTER 2**

### **LITERATURE REVIEW**

#### **2.1 INTRODUCTION**

This chapter consolidates background information on nondestructive testing and design procedures using nondestructive testing results. Research efforts similar to that described in this thesis are also presented.

#### **2.2 NONDESTRUCTIVE TESTING**

Nondestructive testing (NDT) is a term used to describe many different techniques to analyze the properties of a material or structure without altering the in-situ properties of the material or structure in any way. For obvious reasons NDT is the preferred method to test a wide variety of structures from high-pressure steam lines in nuclear powered submarines to pavements. NDT is a growth area for many emerging technologies as greater accuracy and precision are required in a wide variety of industries. For the remainder of this thesis, NDT will refer only to the analysis of pavement structures, and more specifically to pavement surface deflection measurement devices.

The most reliable method for determining the material characteristics in an existing pavement system is to actually retrieve a sample by coring through every layer and conducting laboratory tests on each layer, but costs and time are a problem. In addition, samples of unstabilized material are very difficult to collect and preserve so in-situ properties are unaffected. For these reasons, different methods of nondestructive

testing have been developed in an effort to maximize the accuracy and reliability of the data while minimizing the cost to conduct the test.

Current NDT devices for analyzing pavement structures can be divided according to the types of loading placed on the pavement. Static deflection devices like the Benkleman Beam, the Plate Bearing Test and the LaCroix Deflectograph were the pioneering efforts in this field. Steady state deflection equipment (Dynaflect and Road Rater Models 400 and 2000) uses a vibratory load and is still used by many agencies (Mahoney et al. 1995; WSDOT Pavement Guide, 1995). Current state of the art technology utilizes an impact (or impulse) load which approximates a vehicular load on the pavement better than a static or vibratory load (ASTM D4694-87, 1989). These impact load devices are commonly referred to as Falling Weight Deflectometers (FWDs) and are manufactured by several companies worldwide including KUAB, Dynatest, Foundation Mechanics, and Phoenix. Over the last decade, the FWD has become the deflectometer of choice for most road authorities worldwide; hence there has been considerable analysis of FWD data (Mahoney, et al., 1995). Table 2-1 shows the past, current and predicted usage of the various NDT devices currently used in the United States. Appendix E provides an overview of several of the most common nondestructive testing devices; past, present, and future. Further information is available in a synthesis study of NDT devices by Smith and Lytton (1984)..

**Table 2-1 State Highway Administration (SHA) Deflection Equipment  
(WSDOT Pavement Guide, 1995)**

Device	Number of SHAs Using Device for Various Time Periods		
	mid-1980s	1990	mid-1990s (estimated)
Benkelman Beam	18	3	0-3
Dynaflect	18	11	5-10
Road Rater	5	4	2-6
FWD	5	30	30-40

### **2.3 INTERPRETATION OF NDT DATA**

NDT data is typically converted into different deflection basin parameters for use in analyzing the pavement. A summary of deflection basin parameters is found in the WSDOT Pavement Guide for Design Evaluation, and Rehabilitation (Feb. 1995) and is shown in Table 2-2.

Two important deflection basin parameters are  $D_0$  and Area Parameter. Because these are used extensively throughout this thesis, special attention will be paid to them here.  $D_0$  is the maximum deflection measured at the center of the load applied to the pavement. It is measured in units of length. The Area Parameter,  $A$ , is a measurement of the normalized area of a slice of the deflection basin from the center of the load to 90.5 cm (3 ft) from the center of the load. Because it is normalized by the  $D_0$  value, it

has units of length. It is calculated using the equation in Table 2-2, using the maximum deflections for  $D_0$ ,  $D_1$ ,  $D_2$ , and  $D_3$ . Figure 2-1 gives a graphical presentation of how Area Parameter is measured and what it actually represents. The maximum value to expect for Area Parameter is 915 mm (36.0 in) which would indicate all deflections were equal. This would represent an extremely stiff pavement system. The minimum value to expect for Area Parameter is 280 mm (11.1 in). The lower range of Area Parameter values indicate that the pavement is not acting significantly differently than the underlying layers (WSDOT Pavement Guide, 1995). Table 2-3 provides a guide to pavement type and condition typically associated with Area Parameter values.

Deflection basin parameters can be used in several sets of equations (shown in Table 2-3) to compute the subgrade elastic modulus. The accuracy of these methods is far better for the subgrade than for the surfacing layer (WSDOT Pavement Guide, 1995). Surfacing layer equations can be found in the WSDOT Pavement Guide (1995).

**Table 2-2 Summary of Deflection Basin Parameters (WSDOT Guide, 1995)**

Parameter	Formula	Measuring Device
Maximum Deflection	$D_0$	Benkelman Beam LaCroix Deflectograph FWD
Radius of Curvature	$R = r^2 / \{2D_0(D_0/D_r - 1)\}$ $r = 5''$	Curvaturometer
Spreadability	$S = 100[(D_0 + D_1 + D_2 + D_3)/5]/D_0$ $D_1 \dots D_3$ spaced 12" apart	Dynaflect
Area	$A = 6[1 + 2(D_1/D_0) + 2(D_2/D_0) + D_3/D_0]; 0, 1, 2, 3 \text{ ft}$	FWD
Shape Factors	$F_1 = (D_0 - D_2)/D_1$ $F_2 = (D_1 - D_3)/D_2$	FWD
Surface Curvature Index	$SCI = D_0 - D_r$ , where $r = 12''$ or $r = 20''$	Benkelman Beam Road Rater FWD
Base Curvature Index	$BCI = D_{24''} - D_{36''}$	Road Rater
Base Damage Index	$BDI = D_{12''} - D_{24''}$	Road Rater
Deflection Ratio	$Q_r = D_r/D_0$ , where $D_r \sim D_0/2$	FWD
Bending Index	$BI = D/a$ , where $a = \text{Deflection basin}$	Benkelman Beam
Slope of Deflection	$SD = \tan^{-1}(D_0 - D_r)/r$ $r = 24''$	Benkelman Beam

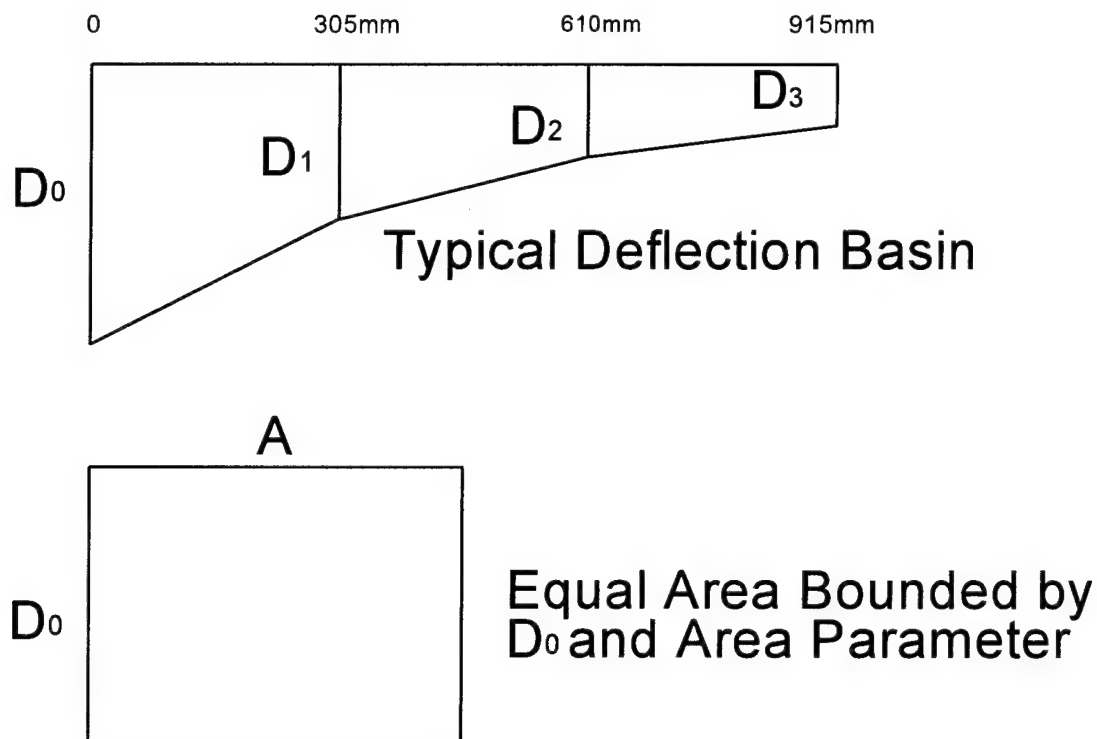


**Figure 2-1 Graphical Representation of Area Parameter  
(after WSDOT Pavement Guide)**

**Table 2-3 Area Parameter Values for Typical Pavements  
(after WSDOT Pavement Guide)**

Pavement	Area Parameter	
	mm	in
Thick ACP ( $\geq 107$ mm ACP)	530-760	21-30
Thin ACP ( $< 107$ mm ACP)	410-530	16-21
BST flexible pavement (relatively thin)	380-430	15-17
Weak BST	300-380	12-15

**Table 2-4 Predictive Relationships for Subgrade Modulus**

WSDOT	Two Layer	$E_{SG} = -466 + 0.00762 (P/D_3)$ $E_{SG} = -198 + 0.00577 (P/D_4)$ $E_{SG} = -371 + 0.00671 (2P/(D_3+D_4))$
WSDOT	Three Layer	$E_{SG} = -530 + 0.00877 (P/D_3)$ $E_{SG} = -111 + 0.00577 (P/D_4)$ $E_{SG} = -346 + 0.00676 (2P/(D_3+D_4))$
AASHTO		$E_{SG} = (P)(S_f)/(D_r)(r)$ $M_R = P(1-\mu^2)/(\pi)(D_r)(r)$
South African		$\log_{10}E_{SG} = 9727 - 0.989 \log_{10}\delta_{2000}$
CBR Correlation  *Valid for CBR values less than 10 only*		$E_{SG} (\text{psi}) = 1500(\text{CBR})$ $E_{SG} (\text{MPa}) = 10(\text{CBR})$

Definitions for variables used in Table 2-4:

- P = applied load (lbs) on 11.8 in. plate
- $E_{SG}$  = subgrade modulus (psi) ( $P_a$  for South African eqn.)
- $D_0$  = deflection beneath center of load plate (in.)
- $D_{0.67}$  = deflection 0.67 feet from center of load plate (in.)
- $D_1$  = deflection 1 foot from center of load plate (in.)
- $D_2$  = deflection 2 feet from center of load plate (in.)

$D_3$	=	deflection 3 feet from center of load plate (in.)
$D_4$	=	deflection 4 feet from center of load plate (in.)
$S_f$	=	subgrade modulus reduction factor based on Poisson's ratio, $\mu$
$D_r$	=	deflection measured $r$ feet from the center of load plate (in.)
$r$	=	distance from the applied load to $D_r$ (in.)
$M_R$	=	backcalculated subgrade resilient modulus (psi)
$\delta_{2000}$	=	deflection 2000 mm from the center of the load plate ( $\mu\text{m}$ )
CBR	=	California Bearing Ratio
$\mu$	=	Poisson's Ratio

## 2.4 DESIGN PROCEDURES

### 2.4.1 Empirical

An empirical design approach concerns itself only with the results observed in the laboratory or in the field. Correlations are made from large numbers of observations to create empirical relationships between inputs and results. Hveem and Carmany's equation for the thickness of asphalt pavement cover required is an example of an empirical pavement design (WSDOT Pavement Guide, 1993). The AASHTO process is another example of empirical design.

### 2.4.2 Mechanistic

Mechanistic approaches to design apply laws of physics and material properties to determine a structure's reaction to loading. Mechanistic design procedures for pavements rely on the assumption that a pavement can be modeled as a multi-layered

elastic or visco-elastic structure on a similar elastic/visco-elastic foundation. This assumption allows the calculation of stresses, strains, and deflections throughout the pavement structure and subgrade (AASHTO Guide, 1993).

#### **2.4.3 Mechanistic-Empirical**

As the name implies, a mechanistic-empirical approach incorporates elements of both empirical and mechanistic methods. The mechanistic component uses mathematical models to compute pavement reactions of interest while the empirical component relates these reactions to some measure of the performance of the pavement such as remaining life of the pavement (WSDOT Guide, 1995).

There are many benefits to using a mechanistic-empirical approach in pavement design. Because these methods are based on long established linear-elastic theory, they will model the pavement more correctly than the empirical equations which have been traditionally used for flexible pavement design (AASHTO Guide, 1993). Other benefits (WSDOT Guide, 1995) include:

- ability to accommodate changing load types
- better use of available materials
- ability to accommodate new materials
- improved reliability of performance predictions
- better defined role of construction
- improved definition of existing pavement layer properties
- ability to accommodate environmental and aging affects on materials

- material properties which relate better to actual pavement behavior and performance

#### **2.4.4 Backcalculation**

Backcalculation is a mechanistic-empirical evaluation which iteratively computes surface deflection basins for different moduli until the calculated basin matches a measured deflection basin within a preprogrammed tolerance. The layer moduli that produce the calculated deflection basin can be limited to certain ranges to ensure they make engineering sense (WSDOT Pavement Guide, 1995). Backcalculation is achieved by using different software programs designed to be used on standard microcomputers due to its calculation intensity. These programs usually use a linear-elastic analysis.

A successful analysis of a pavement based on a measured deflection basin depends on the accuracy of several input parameters, including the layer thicknesses and composition (which will dictate the initial moduli and Poisson's Ratio to be used) (Lytton, et al., 1990). When these parameters cannot be determined from construction records, core samples should be drilled. Some researchers and agencies have had success using seismic refraction studies or ground penetrating radar for determining layer thicknesses.

#### **2.4.5 Computer Programs**

The Federal Aviation Administration (FAA) has developed a program called LEDFAA which makes some standard assumptions concerning the materials and the structural model of the pavement system (FAA Workshop, 1995). These assumptions,

detailed below, are consistent with most other software programs using layered elastic theory:

- Multi-layer elastic system
- All layers are infinite in the lateral direction
- Each layer except the bottom layer has a constant, finite thickness
- Friction at the surface is not considered (surface shearing neglected)
- The bottom layer is infinite in depth
- Each layer consists of a homogenous and isotropic material
- The elastic modulus, E, and Poisson's ratio, V, for each layer are used to calculate the deflection basin (pavement response to loading)

The Washington State Department of Transportation has developed three computer programs to enhance their pavement management and design capability. EVERSTRS, a layered elastic analysis program, is used to estimate the stresses, strains and deflections within a layered pavement system due to a static load. EVERCALC, a pavement analysis computer program, is used to estimate the "elastic" moduli of pavement layers. Given the FWD load, sensor spacing, seed moduli (initial guesses) and layer thicknesses, EVERCALC computes an estimate of the actual moduli by iteratively comparing the computed deflection basin with the measured deflection basin until they match within given tolerance parameters. Figure 2-2 shows a simplified flow chart for EVERCALC. EVERPAVE, an empirical-mechanistic overlay design program, is used to

estimate the overlay thickness required for a pavement based on fatigue cracking criteria and rutting failure criteria. These programs are extremely useful tools, but should not replace the experience and judgment of a pavement engineer to verify the reasonability of the results.

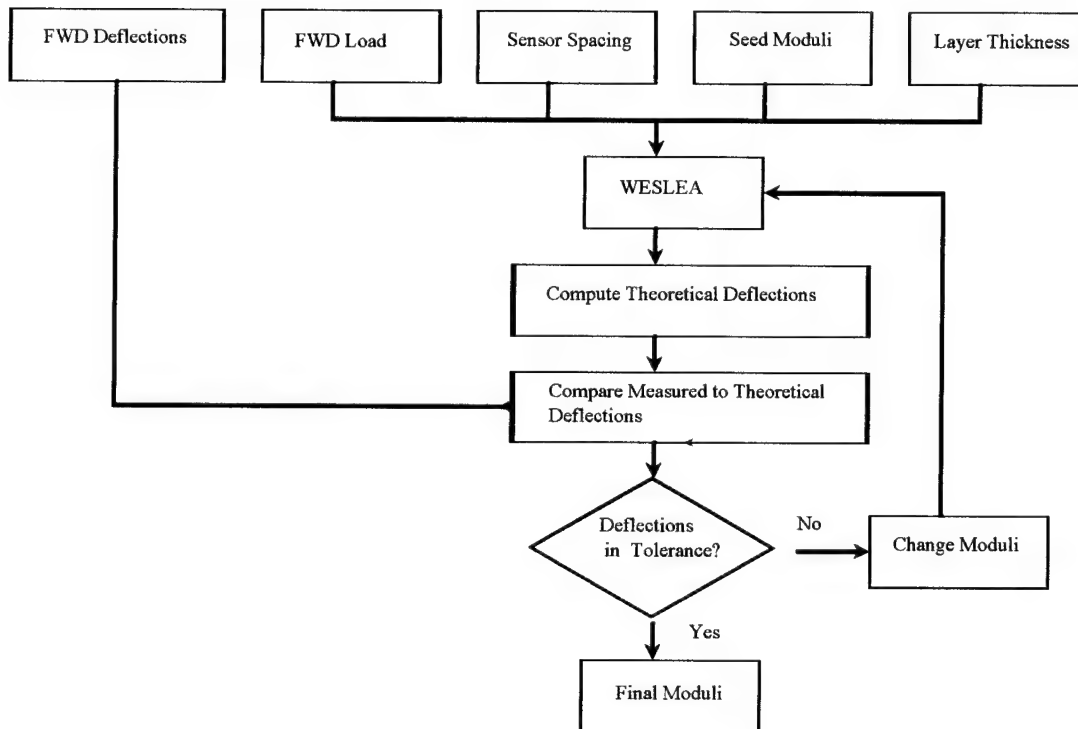


**Figure 2-2 Simplified Flow Chart for EVERCALC  
(after WSDOT Pavement Guide, 1995)**

#### **2.4.6 Regression Equations**

Regression equations (or algorithms) can be developed for data that correlates well enough to provide “predictive” relationships. Other researchers have studied and

created regression equations for the same or similar parameters that this thesis deals with. Some background information about regression and the meaning of some of the descriptors such as  $R^2$  and Root Mean Square Error (RMSE) are discussed in Section 3.2.2 and Appendix C.

Gomez-Achecar and Thompson (1986) developed regression equations relating pavement characteristics and deflections to certain strains, stresses and deflections. They are presented in Table 2-5. In general, the AC thickness and modulus must be known in addition to the subgrade modulus to use these equations. The  $R^2$  and RMSE are very good for the equations using the three independent variables just mentioned. The goal of this thesis is to create very similar relationships that do not require knowledge of the AC modulus or thickness.

Olle Andersson, Professor of Highway Engineering at the Royal Institute of Technology in Sweden, presented data from 140 different pavement scenarios (varying AC thickness, AC Modulus, Base Thickness, Base Modulus, Subgrade Modulus). His findings (Andersson, undated paper) include graphs indicating a linear relationship between the displacement at the center of the load and other displacement parameters for given AC modulus's and subgrade modulus's. No regression equations were proposed in this paper.

**Table 2-5 Regression Equations Developed  
by Gomez-Achecar and Thompson (1986)**

Equation	R <sup>2</sup>	RMSE
<u>Asphalt Strain</u> $\text{Log } \epsilon_{AC} = 5.746 - 1.589 \text{ Log } T_{AC} - 0.774 \text{ Log } E_{AC} - 0.097 \text{ Log } E_{Ri}$	0.967	0.083
<u>Subgrade Deviator Stress</u> $\text{Log } DEV = 2.744 - 1.138 \text{ Log } T_{AC} - 0.515 \text{ Log } E_{AC} + 0.289 \text{ Log } E_{Ri}$	0.976	0.053
<u>Surface Deflection</u> $\text{Log } D_0 = 3.135 - 0.895 \text{ Log } T_{AC} - 0.359 \text{ Log } E_{AC} - 0.287 \text{ Log } E_{Ri}$	0.984	0.033
<u>Subgrade Deflection</u> $\text{Log } DSUB = 3.090 - 0.979 \text{ Log } T_{AC} - 0.321 \text{ Log } E_{AC} - 0.306 \text{ Log } E_{Ri}$	0.983	0.037
<u>Subgrade Vertical Strain</u> $\text{Log } \epsilon_z = 4.022 - 1.680 \text{ Log } T_{AC} - 0.667 \text{ Log } E_{AC} - 0.165 \text{ Log } E_{Ri}$	0.944	0.110
<u>Asphalt Strain-Surface Deflection</u> $\text{Log } \epsilon_{AC} = 1.53 \text{ Log } D_0 + 0.319$	0.81	0.20
<u>Subgrade Stress Ratio-Surface Deflection</u> $\text{Log } S = 1.28 \text{ Log } D_0 - 2.21$	none given	none given

where:

$T_{AC}$  = Asphalt Concrete Thickness (inches)

$E_{AC}$  = Asphalt Concrete Modulus (ksi)

$E_{Ri}$  = Subgrade Modulus (ksi)

$\epsilon_{AC}$  = Asphalt Concrete Radial Tensile Strain (microstrain)

$DEV$  = Subgrade Deviator Stress,  $\sigma_1 - \sigma_3$  (psi)

$D_0$  = Surface Deflection (mils)

DSUB = Subgrade Deflection (mils)  
 $\epsilon_z$  = Subgrade Vertical Strain ( $\times 10^{-4}$ )  
 S = Subgrade Stress Ratio (subgrade deviator stress/unconfined compressive strength)

## **2.5 SOURCES OF ERROR**

There are two primary sources of error in the use of NDT data to compute layer moduli. These are random errors and systematic errors which are discussed in this section.

### **2.5.1 Random Errors**

Random errors are typically errors in the measurements themselves either due to the measurement sensors or the load cells. These errors cannot easily be predicted but they can be reduced by repeating measurements and averaging the results (Lytton, et al. 1990). For Laser rolling wheel deflectometers, random errors should not affect the results because of the vast amount of measurements which will be averaged over a small section of pavement.

### **2.5.2 Systematic Errors**

Systematic errors are by far the most troublesome because they are more difficult to correct, are numerous, and have the tendency to compound their effects. Systematic errors are the result of erroneous assumptions made in the backcalculation process. Lytton, et al (1990) described research which included the creation of an ‘expert system’ to be used in conjunction with a backcalculation computer program.

An engineer's knowledge of pavements is critical to the mechanistic-empirical process. This process cannot be used as a 'cookbook' to generate solutions without proper analysis of the results. The AASHTO Guide (1993) notes that good engineering judgment on the part of the designer will always be critical, especially since so many of the inputs to the design cannot be modeled properly by mechanistic models.

## **2.6 SIGNIFICANT PARAMETERS AFFECTING NDT**

Pavement systems react very differently to different loading conditions. The magnitude and the rate of loading can dramatically alter the pavement response (deflection). Since most NDT measures the pavement's response to loading in order to estimate the pavement strength properties, it is extremely important to keep the loading conditions consistent.

### **2.6.1 Stress Sensitivity of Pavement Materials**

The most significant factors that affect the response of the asphalt-concrete layer(s) are the rate or frequency of loading and the temperature (Hoffman and Thompson, 1981). The AC layer is not greatly influenced by the stress imposed on it.

The unbound materials often found in the base course, subbase and subgrade have been found to be sensitive to the stress exerted upon them. Generally, the modulus of fine-grained materials decrease with increasing stresses while the modulus of granular materials increase with increasing applied stress (Newcomb, 1986). Since the unstabilized base course, subbase and/or subgrade can respond in a nonlinear fashion

with regards to applied stress, the modulus may be calculated by either of two equations (WSDOT Guide, 1995):

$$E = K_1(\theta)^{K_2}$$

or

$$E = K_3(\sigma_d)^{K_4}$$

where:

$E$  = Layer Modulus

$K_1 \dots K_4$  = Regression Constants

$\theta$  = Sum of the principal stresses ( $\sigma_1 + \sigma_2 + \sigma_3$ )

$\sigma_d$  = Difference between major and minor principal stresses ( $\sigma_1 - \sigma_3$ )

The laboratory method typically used to compute the regression constants is a repeated load triaxial test on disturbed samples which are recompacted (Newcomb, 1986; Hoffman and Thompson, 1981).

Studies conducted on lime and cement treated materials (Hoffman and Thompson, 1981) indicate that their resilient response lies somewhere between a completely bonded material (elastic) and the unbound raw material (nonlinear) and depend a great deal on factors including mix proportions, curing time, method of testing and others.

### **2.6.2 Variations in Loading Type and Duration**

Three different mathematical formulations can be used to determine the response of a pavement system under different loading conditions. The are (Hoffman and Thompson, 1986):

1. Layered Theory: Does not consider time or mass
2. Visco-elastic: Considers time only
3. Dynamic: Considers time and mass

One model should not be used to predict results for another. They are different models and are not interchangeable. The research described in this thesis used the layered theory.

During the 1950s and 1960s researchers noted that pavement surface deflections decrease as vehicle speeds increase (Hoffman and Thompson, 1981). Laser Rolling Wheel Deflectometers will experience this effect; consequently, dynamic analysis methods should be developed to properly interpret the data generated by these machines.

### **2.6.3 Temperature Effects**

Because asphalt properties are highly temperature-dependent, the temperature of the asphalt layer affects the deflections measured by any NDT device. Many researchers have attempted to explain and predict the relationship between temperature and deflection. It is very important to adjust deflections to a standard temperature before attempting to use the deflections in any kind of established analysis or design. Previous

research has yielded several important general conclusions, some of which are outlined here.

The Canadian Good Roads Association (Sebastyan, 1961) determined that:

1. Temperature variations could not be correlated with mix design characteristics. A linear relationship was assumed between temperature and deflection. For this linear relationship, a slope of 0.002 inches per 10 degrees Fahrenheit (pavement surface temperature) worked well for a variety of pavements.
2. No temperature effects could be seen on pavement systems with very thick bases.

Welch (1961) further concluded that the "deflection correction factor in inches for a weak base was considerably higher than that for a stronger base".

During the AASHO Road Test (Benkelman, et al, 1962) the following conclusions were made:

1. Temperature has the greatest effect on deflection in lower temperature ranges.
2. Very little temperature effect is experienced when the average pavement temperature is above 26.7 °C (80 °F).

In addition to conclusions made based on observations of test sites, Meyerhoff proposed the following mathematical relationship between deflection and temperature based on a two-layer elastic system (Meyerhoff, 1962):

$$d = \frac{0.52W}{E_s \left( \frac{E_p}{E_s} \right)^{\frac{1}{3}} t}$$

where  $d$  = deflection in inches

W	=	Wheel load in pounds
$E_s$	=	Subgrade Elastic Modulus
$E_p$	=	Pavement Elastic Modulus
t	=	Pavement Thickness in inches

Kingham (1969), summarized the significant findings from many research efforts as follows:

1. Surface pavement temperatures do not correlate well to deflection for asphalt layers greater than 3 inches. Mean temperature throughout the slab provides a better correlation for these thicker pavements.
2. Pavements with high deflections experience greater temperature effects (thin pavements, weak subgrade, etc.).
3. Temperature vs. deflection relationships are curvilinear for large temperature ranges (greater than  $4.4^{\circ}\text{C}$  ( $40^{\circ}\text{F}$ )). For smaller temperature ranges, such as those experienced in a 24 hour period, the relationship can be reasonably modeled as a linear relationship.
4. Field measurements do not fully support theoretical models for temperature effects.

Theory should not be the only input to a temperature correction procedure.

Kingham went on to outline a temperature conversion procedure which can be used to normalize measured deflections to  $21.1^{\circ}\text{C}$  ( $70^{\circ}\text{F}$ ).

The Asphalt Institutes' Manual Series No. 17, "Asphalt Overlays for Highway and Street Rehabilitation", (1983) included a discussion of adjusting a Representative Rebound Deflection (RRD) to a standard temperature. The RRD was based on

Benkelman Beam results. The manual provides a figure which provides a temperature adjustment factor for Full-Depth and three-layered asphalt concrete pavements. Thickness of the untreated aggregate base and mean pavement temperature must be known to use this chart.

A temperature adjustment can be made to Asphalt Concrete Modulus,  $E_{AC}$  with the following equation (WSDOT Pavement Guide, 1995):

$$E_{AC} = e^{9.1242 - 0.04456(T)}$$

where  $E_{AC}$  = AC Modulus (MPa)

T = mean asphalt concrete temperature (degrees Celsius)

## **2.7 DEVELOPING STANDARD PROCEDURES**

In 1986, Harold Von Quintas presented a first draft of a "Standard Practice for Calculating In-Situ Resilient Modulus of Pavement Materials" in an attempt to develop a standard for a procedure that is gaining acceptance and continues to evolve (May and Von Quintas, 1994). Seven drafts and six years later the work on the proposed standard was put on hold until after the 1993 Symposium "Nondestructive Testing of Pavements and Backcalculation of Moduli" sponsored by the American Society for Testing and Materials (ASTM). To date, there seems to be very little agreement on when and how to standardize backcalculation procedures.

## **2.8 METHODS EMPLOYED BY STATE HIGHWAY ADMINISTRATIONS AND OTHER AGENCIES**

In 1991 a National Cooperative Highway Research Program (NCHRP) survey was conducted to quantify state and Canadian Province standard practices in design (WSDOT Guide, 1995). Figures 2-3 to 2-6 show pertinent results concerning methods used by SHAs and other agencies to determine different pavement parameters. The data to create these charts came from the WSDOT Pavement Guide, Volume 2, 1995.

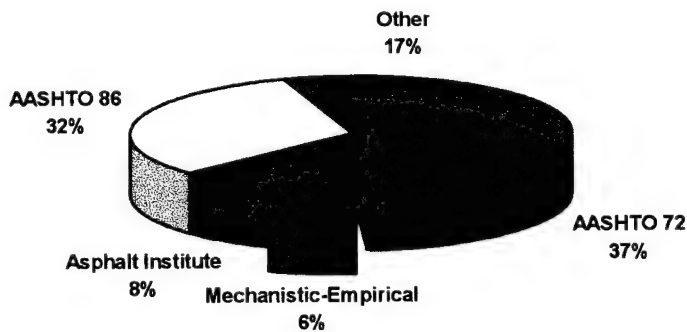


**Figure 2-3 Agencies Use of Design Procedures**

Percentages are based on 63 agencies reporting.

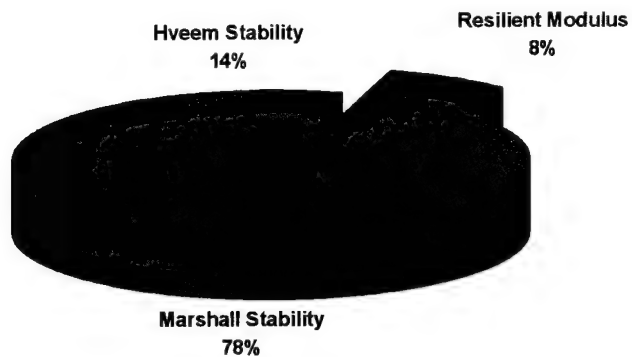


**Figure 2-4 Agencies Method of Asphalt Concrete Characterization**

Percentages based on 51 agencies, updated to include WSDOT.



**Figure 2-5 Agencies Method of Base/Subbase Characterization**

Percentages based on 27 agencies reporting use of a specific test and associated strength or stiffness criterion. The remainder of the agencies tend to use grading requirements.

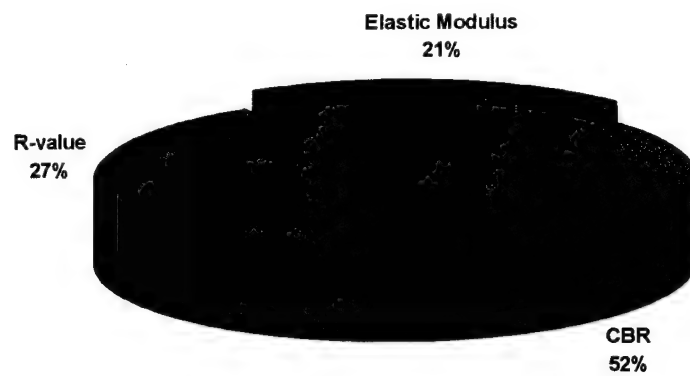


**Figure 2-6 Agencies Method of Subgrade Characterization**

Percentages based on 48 agencies reporting (updated to include WSDOT).

## CHAPTER 3

### PREDICTING CRITICAL STRAINS AND PAVEMENT LIFE

#### **3.1 INTRODUCTION**

The pavement manager is concerned with the life remaining in any given pavement section. A powerful tool, then, is the ability to estimate the pavement life remaining based on deflection basin parameters. The most fundamental of these deflection basin parameters are the Area Parameter and  $D_0$ . The Area Parameter is a normalized width of the deflection basin (refer to Figure 2-1) and  $D_0$  is the pavement surface deflection at the center of the applied load.

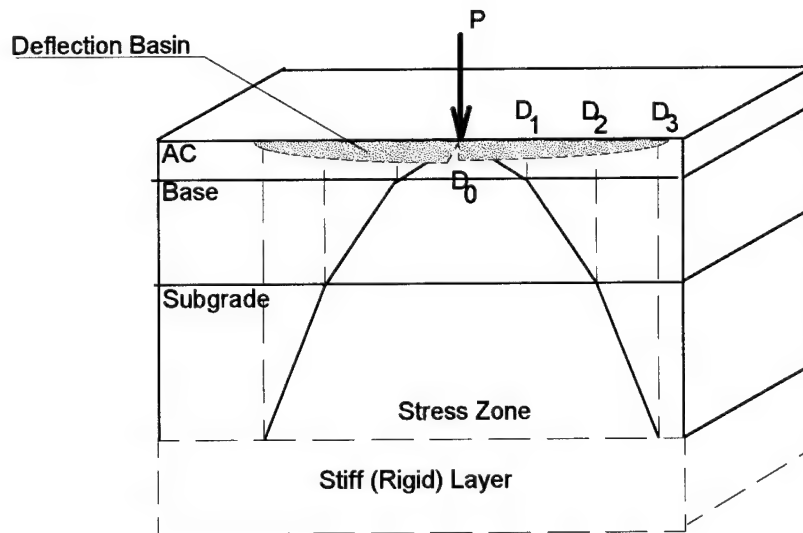


**Figure 3-1 Typical Deflection Basin (after WSDOT Pavement Guide, 1995)**

### **3.2 METHODOLOGY**

The goal of the research discussed in this chapter is to develop predictive relationships that can predict critical strains and pavement life using only  $D_0$ , Area Parameter and subgrade modulus ( $E_{SG}$ ). With such relationships, there would be no need to know the layer thicknesses, AC modulus, or base modulus to estimate the critical strains and thereby the pavement life remaining. These relationships would also be independent of the pavement temperature because they would be based on data generated at a wide range of AC stiffnesses representing a wide range of pavement temperatures.

#### **3.2.1 Data Generation**

In order to generate data for analysis, a matrix of different pavement scenarios was established (see Table 3-1). Three parameters were chosen to be variable in the pavement scenarios and all other parameters were kept constant. The variable parameters were subgrade modulus, asphalt concrete modulus and asphalt concrete thickness. The constant parameters were:

Poisson's Ratio, AC layer:	0.35
Poisson's Ratio, Base layer:	0.40
Poisson's Ratio, Subgrade layer:	0.45
Base Modulus:	207 MPa
Base Thickness:	20 cm
Load	40 kN
Tire Pressure	690 MPa

Table 3-1 shows the 120 combinations of variable parameters and indicates which pavement scenarios (according to ‘case number’) correspond to which combinations. For example, pavement scenario (case number) 34 represents a Subgrade Modulus of 70 MPa, an AC Modulus of 5520 MPa, and an AC Thickness of 10 cm. Initially only 80 pavement scenarios were chosen. Case Numbers 81-120 were added because additional data points were needed to further investigate trends that were identified using the initial 80 data points.

Each pavement scenario was analyzed using WSDOT’s EVERSTRS Program to estimate the deflections and the critical strains needed to predict the number of loads to failure for both the rutting criteria and the AC fatigue criteria. Figure 3-2 provides a view of the key locations of concern for pavement response. Locations 2 and 4 are the critical strains evaluated in this thesis. A sample EVERSTRS output can be found in Appendix A along with a compilation of the critical outputs for every pavement scenario.

**Note:** throughout this thesis, the negative sign normally associated with vertical compressive strain in the subgrade is omitted. A negative sign indicates a case in which the strain at the top of the subgrade is predicted to be in tension instead of in compression.

The estimations of  $D_0$ ,  $D_1$ ,  $D_2$ ,  $D_3$ ,  $\epsilon_t$  (horizontal tensile strain at bottom of AC layer), and  $\epsilon_v$  (vertical compressive strain at the top of the subgrade layer) were transferred to a spreadsheet where the Area Parameter,  $N_f$  for Rutting, and  $N_f$  for AC Fatigue could be calculated. Different parameters were plotted against each other to see

if any relationships could be seen. The results were very promising and showed a significant relationship between key measured or calculated parameters and those critical strains required for computing pavement life. Appendix B contains the graphs that include all 120 pavement scenarios.

The pavement scenarios with an AC thickness of 40 cm create outlying points on some of the graphs presented in Appendix B. Looking at Figures B-3 to B-6 and Figures B-8 to B-11, there are several points on each graph that have a combination of low strain and low Area Parameter or  $D_0$ . These points that do not fall on the curve are the very thick 40 cm pavements.

The equations used to calculate loads to failure,  $N_f$  are:

Rutting Criteria :

$$N_f = \left[ \frac{1.05 * 10^{-2}}{\varepsilon_v} \right]^{4.4843}$$

where  $N_f$  = allowable number of 80 kN single axle loads to ensure that rutting at the pavement surface does not exceed 12.7 mm.

$\varepsilon_v$  = vertical compressive strain at the top of the subgrade

AC Fatigue Criteria:

$$N_f = N_{f(lab)} * (\text{shiftfactor})$$

$$\text{where } \log N_{f(lab)} = 14.82 - 3.291 \log\left(\frac{\varepsilon_t}{10^{-6}}\right) - 0.854 \log\left(\frac{E_{AC}}{10^3}\right)$$

where  $N_f$  = number of 80 kN 4 layer (psi)

The shift factor for the AC fatigue criteria equation is generally accepted to be between 4 and 10 (WSDOT Pavement Guide, 1995).

### **3.2.2 Regression Analysis**

Regression creates an equation which predicts the variation of one parameter based on the values of one or more other parameters. Appendix C provides more detailed information on regression analysis. The equation developed through linear regression typically follows the form of:

$$y = a_0 + a_1x_1 + a_2x_2 + a_3x_3, \dots + a_nx_n$$

where  $y$  is the dependent variable (the predicted value)

$x_1..x_n$  are the independent variables (the known values)

$a_0..a_n$  are constants determined by the relationship between the independent and dependent variables.

The relationship is easiest to visualize when there is one independent variable. The equation is providing the “best fit” line between the dependent and independent variable. The first constant is the  $y$ -intercept, while the second constant is the slope of the line.

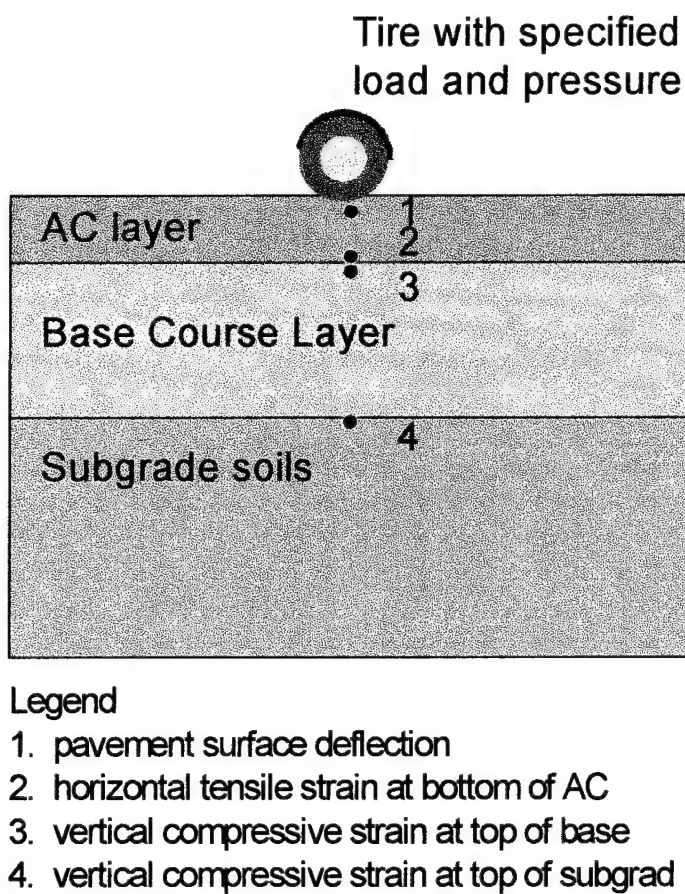


**Figure 3-2 Pavement Response Locations Used in Evaluating Load Effects  
(after WSDOT Pavement Guide, 1995)**

**Table 3-1 Case Numbers for EVERSTRS Calculations**

Subgrade Modulus = 35 MPa		AC Thickness					
		2.5 cm	3.75 cm	5 cm	10 cm	20 cm	40 cm
AC Modulus	690 MPa	81	82	1	2	3	4
	1,380 MPa	83	84	5	6	7	8
	2,760 MPa	85	86	9	10	11	12
	5,520 MPa	87	88	13	14	15	16
	11,040 MPa	89	90	17	18	19	20
Subgrade Modulus = 70 MPa		AC Thickness					
AC Modulus	690 MPa	91	92	21	22	23	24
	1,380 MPa	93	94	25	26	27	28
	2,760 MPa	95	96	29	30	31	32
	5,520 MPa	97	98	33	34	35	36
	11,040 MPa	99	100	37	38	39	40
Subgrade Modulus = 140 MPa		AC Thickness					
AC Modulus	690 MPa	101	102	41	42	43	44
	1,380 MPa	103	104	45	46	47	48
	2,760 MPa	105	106	49	50	51	52
	5,520 MPa	107	108	53	54	55	56
	11,040 MPa	109	110	57	58	59	60
Subgrade Modulus = 280 MPa		AC Thickness					
AC Modulus	690 MPa	111	112	61	62	63	64
	1,380 MPa	113	114	65	66	67	68
	2,760 MPa	115	116	69	70	71	72
	5,520 MPa	117	118	73	74	75	76
	11,040 MPa	119	120	77	78	79	80

There are several important descriptors of a regression equation which give an indication of how well the equation will predict the dependent variable. The Coefficient of Determination is annotated as R-Squared or  $R^2$ .  $R^2$  can be described as the fraction of the variation in the dependent variable that is explained by the regression equation (Ryan, et.al., 1985).  $R^2$  can range from 0% to 100% with the latter indicating a perfect fitted line. Another important descriptor is the Root Mean Square Error (RMSE) which is a measure of how much the observed dependent variable values differ from the average value on the “best fit” line. RMSE is the standard deviation of the “best-fit” or regression equation line (Mahoney, 1994). An often overlooked descriptor for a regression equation is the number of observed values used, designated as N. Intuitively, the larger N is, the more weight a predictive relationship should be given.

Regression analysis provides an equation which describes a straight line fit. Often, variables relate to each other in a curvilinear manner which does not work well with a direct correlation of the variables. In this case, a transformation is done on one or more of the variables so that they relate to each other in a linear relationship. The most common transformations are the log, inverse, square, or square root of the variable.

All of the data generated for the 120 pavement scenarios was entered into the statistical software program, Minitab. Regression equations were computed using different transformations of the variables in different combinations. The equations with the highest  $R^2$  and lowest RMSE are presented in the following section while the remainder of the equations developed can be found in Appendix D.

### **3.3 RESULTS**

#### **3.3.1 Tensile Strain Restriction**

Note that the equations presented in the next two sections for tensile strain at the bottom of the AC layer only have an N value of 41. That means only 41 of the 120 pavement scenarios were used to generate these equations. This is because the relationships involving  $\epsilon_t$  were discretely curvilinear only for Area Parameters greater than 500 (41 cases). This also happens to be the region in which the tensile strain would tend to be more critical than the vertical compressive strain in the subgrade. Figure 3-3 shows the relationship of strain at the bottom of the AC layer to Area Parameter for a subgrade modulus of 35 MPa. As can be seen, a strain of 200 would predict the Area Parameter to be approximately 440 or 620 depending on which side of the crest one looks. The equations discussed above used only those points to the right of the crest, with the Area Parameter greater than or equal to 500. Refer to Table 2-3 to see that these are relatively strong pavements. These are the pavements for which AC fatigue is expected to be more critical than rutting failure.

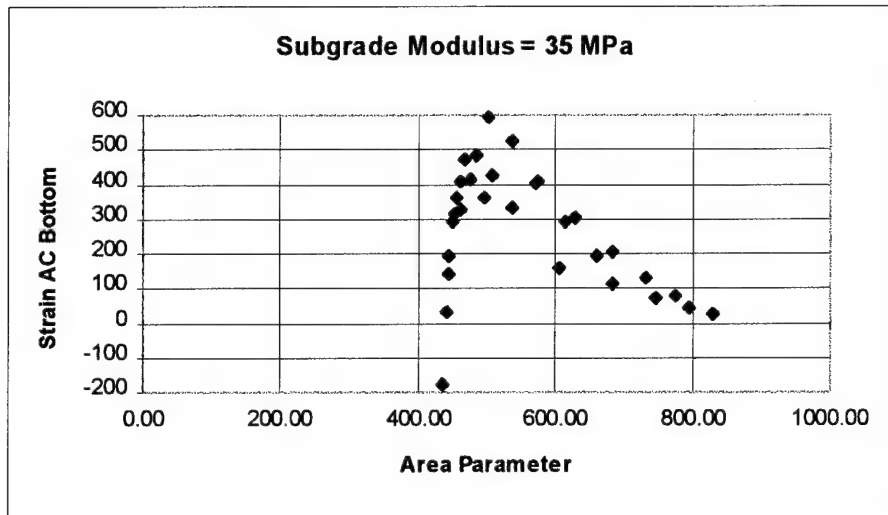


**Figure 3-3 Illustration of Area Parameter Limit for Prediction of Strain at the Bottom of the AC Layer**

### 3.3.2 Using Area Parameter

The best equations for predicting the critical strains,  $\epsilon_t$  and  $\epsilon_v$ , using Area Parameter, A, and subgrade modulus,  $E_{SG}$ , as calculated on Minitab are:

$$\log \epsilon_t = 5.91 - 0.00353A - 0.877\log E_{SG}$$

$$R^2 = 89.3\% \quad RMSE = 0.1358 \quad N = 41$$

and

$$\log \epsilon_v = 7.04 - 0.00339A - 1.34\log E_{SG}$$

$$R^2 = 94.4\% \quad RMSE = 0.1148 \quad N = 120$$

where A is in mm and  $E_{SG}$  is in MPa and is calculated using one of the closed form equations presented in Table 2-4. These equations both have strong  $R^2$  values showing a strong relationship between the dependent variable and the independent variables.

### **3.3.3 Using $D_0$**

The best equations for predicting the critical strains,  $\varepsilon_t$  and  $\varepsilon_v$ , using deflection at the center of the load,  $D_0$ , and subgrade modulus,  $E_{SG}$ , as calculated on Minitab are:

$$\log \varepsilon_t = -4.23 + 1.80 \log D_0 + 0.898 \log E_{SG}$$

$$R^2 = 97.6\% \quad RMSE = 0.0647 \quad N = 41$$

and

$$\varepsilon_v = -511 + 1.97D_0 + 0.788E_{SG}$$

$$R^2 = 96.0\% \quad RMSE = 163.9 \quad N = 120$$

where  $D_0$  is in micrometers and  $E_{SG}$  is in MPa and is calculated using one of the closed form equations presented in Table 2-4. These equations show that  $D_0$  is an even better predictor for critical strains than Area Parameter.

### **3.3.4 Illustration of Equation Results Using Sampling of Case Numbers**

Thirteen pavement scenarios from Table 3-1 were chosen to calculate strains using the equations presented in this Chapter. These strains were then compared to the strains that were predicted by EVERSTRS. The equations require knowledge of  $D_0$ , Area Parameter, and  $E_{SG}$ .  $D_0$  and Area Parameter were taken from the deflections estimated by EVERSTRS (See Table A-1 in Appendix A for a complete listing of these deflections).  $E_{SG}$  was calculated from the deflections using two of the closed form equations presented in Table 2-4. The AASHTO equation was used in conjunction with the deflection at two feet while the WSDOT three layer equation was used in conjunction

with the deflection at three feet. The other equations can also be used to calculate  $E_{SG}$  from deflection measurements. The subgrade modulus calculated from the deflection at three feet produced a smaller error in predicting  $\epsilon_t$  while the subgrade modulus calculated from  $D_2$  resulted in a smaller error in predicting  $\epsilon_v$ .

Table 3-2 presents the results of the comparisons for the tensile strain at the bottom of the AC layer and Table 3-3 presents the results of the comparisons for the vertical compressive strain at the top of the subgrade. Table 3-2 only contains the six case numbers which had an Area Parameter greater than 500 mm. The equation presented by Gomez-Achecar and Thompson (1986) for Asphalt strain (see Table 2-5) was also calculated for these six case numbers to see how well it would predict the tensile strain; the average error was 66%.

For the case numbers presented in Tables 3-2 and 3-3, the Area Parameter equation appears to be the better predictor for  $\epsilon_v$  and  $\epsilon_t$ . While these errors, ranging from -7 to +30 percent, are by no means negligible, they are certainly reasonable estimators considering no information concerning the pavement structure and layer properties is required.

### **3.4 CASE STUDY COMPARISON**

Volume 3 of the WSDOT Pavement Guide includes four case studies depicting actual pavement rehabilitation projects. Case Study Number One will be used to compare EVERSTRS predicted strains with the strains predicted by the regression equations presented herein. The pavement characteristics at each core location are

presented in Table 3-4. The thicknesses were established from as-built drawings and core samples. The asphalt, base, and subgrade moduli were back-calculated using EVERCALC with no stiff layer considered. Two core locations (MP 208.50 and MP 209.00) were not used in this comparison because the root mean square errors were large enough to consider the data unreliable. The  $E_{AC}$  is the actual backcalculated modulus for the AC at the insitu field temperatures.

**Table 3-2 Comparison of  $\varepsilon_t$  as Predicted by EVERSTRS and the Predictive Equations for Selected Case Numbers**

Case No.	$\varepsilon_t$ EVERSTRS	$E_{SG}$ calculated with $D_2$			
		$\varepsilon_t$ Equation using $D_0$	% difference	$\varepsilon_t$ Equation using A	% difference
2	361	532	+47	659	+83
7	303	244	-19	214	-29
16	43	75	+74	33	-23
38	176	182	+3	173	-2
40	23	41	+78	19	-17
58	161	156	-3	174	+8
		Average Error	+30	Average Error	+3
Case No.	$\varepsilon_t$ EVERSTRS	$E_{SG}$ calculated with $D_3$			
		$\varepsilon_t$ Equation using $D_0$	% difference	$\varepsilon_t$ Equation using A	% difference
2	361	586	+62	600	+66
7	303	246	-19	212	-30
16	43	66	+53	38	-12
38	176	210	+19	151	-14
40	23	37	+31	20	-13
58	161	197	+22	139	-14
		Average Error	+28	Average Error	-3

**Table 3-3 Comparison of  $\epsilon_v$  as Predicted by EVERSTRS and the Predictive Equations for Selected Case Numbers**

Case No.	$\epsilon_v$ EVERSTRS	$E_{SG}$ calculated with $D_2$			
		$\epsilon_v$ Equation using $D_0$	% difference	$\epsilon_v$ Equation using A	% difference
2	2577	2081	-19	2106	-18
7	733	1091	+49	676	-8
9	2189	2288	+5	2442	+12
16	119	154	+29	85	-29
25	1745	1592	-9	1988	+14
30	922	911	-1	884	-4
38	546	545	0	415	-24
40	58	-100	-272	35	-40
49	1069	964	-10	1141	+7
58	371	253	-32	303	-18
65	709	837	+18	753	+6
90	2076	2178	+5	2198	+6
99	1885	1636	-13	2051	+9
		Average Error	-19	Average Error	-7
Case No.	$\epsilon_v$ EVERSTRS	$E_{SG}$ calculated with $D_3$			
		$\epsilon_v$ Equation using $D_0$	% difference	$\epsilon_v$ Equation using A	% difference
2	2577	2084	-19	1826	-29
7	733	1091	+49	669	-9
9	2189	2291	+5	2071	-5
16	119	147	+24	103	-13
25	1745	1604	-8	1490	-15
30	922	922	0	680	-26
38	546	554	+1	336	-38
40	58	-110	-290	40	-31
49	1069	992	-7	827	-23
58	371	281	-24	214	-42
65	709	891	+26	558	-21
90	2076	2181	+5	1871	-10
99	1885	1647	-13	1548	-18
		Average Error	-19	Average Error	-22

### **3.4.1 Prediction of Critical Strains**

The information presented in Table 3-4 was used to estimate the critical strains using EVERSTRS. The regression equations were then calculated for each core location. The values of  $D_0$  presented in the WSDOT manual were used in the regression equations. Area Parameter was calculated using the equation presented in Table 2-2 using the deflections presented in the WSDOT manual. The deflection values were already normalized to a standard load of 40 kN which is consistent with the parameters of the predictive equations. If these values had not already been normalized for load, the procedure developed in Chapter 4 would have been used to normalize  $D_0$  and Area Parameter. The subgrade modulus required as an input to the predictive equations was calculated using the closed form equation:  $E_{SG} = -530 + 0.00877(P/D_3)$  where  $E_{SG}$  is in psi, P is the load in pounds, and  $D_3$  is in inches. Conversions were made from the metric units used in this thesis to the U. S. Customary units for this equation. Once  $E_{SG}$  was calculated, it was converted back to MPa.

Tables 3-5 and 3-6 present the results for the strain at the bottom of the AC layer ( $\epsilon_t$ ). Tables 3-7 and 3-8 present the results for the strain at the top of the subgrade layer ( $\epsilon_v$ ). The bold values in Tables 3-5 and 3-6 indicate that the equation should not be used for this core location because the Area Parameter is less than 500 mm. Recall, the predictive equations for  $\epsilon_t$  are valid only for Area Parameter values greater than 500 mm

(see Figure 3-4). These bold values are not included in the calculation of the average numerical and percent differences presented at the bottom of the tables.

The results indicate that the  $D_0$  equation better predicts  $\varepsilon_t$  (-6% error) while the Area Parameter equation better predicts  $\varepsilon_v$  (+17% error). Again, the margin of error is not insignificant, but it does show promise as a pavement management tool.

### **3.4.2 Prediction of Pavement Life Remaining**

The critical strains predicted in the last section ( $\varepsilon_t$  and  $\varepsilon_v$ ) are among the inputs required to calculate the pavement life remaining (measured in number of ESAL loads). Refer to Section 3.2.1 for the equations to calculate pavement life remaining ( $N_f$ ) for rutting and fatigue failure modes. The pavement life remaining was calculated for WSDOT Case Study Number One using the critical strains predicted by EVERSTRS and the critical strains predicted by the predictive relationships presented in this Chapter.

For each mode of failure, the pavement life remaining was calculated based on the critical strains predicted by EVERSTRS and the predictive relationship (using  $D_0$  or A) that most closely matched the EVERSTRS strain. The results of this comparison were very promising and are presented in Table 3-9 for fatigue failure and in Table 3-10 for rutting failure. In most cases, the predicted life remaining using the critical strain predicted by the predictive equation is of the same order of magnitude as the predicted life remaining using the critical strain predicted by EVERSTRS.

**Table 3-4 Pavement Characteristics for Case Study Number One  
(after WSDOT Pavement Guide, 1995)**

Core Location (Mile Post)	Layer Thickness		Selected Layer Moduli No Stiff Layer No Temperature Adjustment		
	AC (cm)	Base (cm)	AC (MPa)	Base (MPa)	Subgrade (MPa)
207.85	13.4	45.7	3640	115	82
208.00	15.2	45.7	2881	121	101
209.05	10.7	30.5	3736	41	59
209.40	14.9	33.5	1331	34	52
209.80	16.5	39.6	3125	86	117
210.00	11.3	36.6	6556	95	72
210.50	9.8	36.6	17036	115	119
211.00	22.9	36.6	6576	148	139
211.50	28.3	36.6	4608	81	256
212.00	29.9	36.6	2887	34	97
212.50	22.9	36.6	6886	36	122

**Table 3-5 Comparison of Results for Predicting  $\varepsilon_t$  Using Area Parameter &  $E_{SG}$** 

Core Location	Using Area Parameter and $E_{SG}$			
	$\varepsilon_t$ EVERSTRS	$\varepsilon_t$ EQUATION	numerical difference	percent difference
207.85	287	159	-128	-45
208.00	283	170	-113	-40
209.05	480	370	-110	<b>-23</b>
209.40	707	379	-328	-46
209.80	261	156	-105	-40
210.00	248	207	-41	-17
210.50	137	113	-24	-17
211.00	83	53	-30	-36
211.50	81	55	-26	-32
212.00	127	65	-62	-49
212.50	94	63	-31	-33
		<b>Average</b>	-91	-36

**Table 3-6 Comparison of Results for Predicting  $\varepsilon_t$  Using  $D_0$  &  $E_{SG}$** 

Core Location	Using $D_0$ and $E_{SG}$			
	$\varepsilon_t$ EVERSTRS	$\varepsilon_t$ EQUATION	numerical difference	percent difference
207.85	287	246	-41	-14
208.00	283	241	-42	-15
209.05	480	544	+64	+13
209.40	707	579	-128	-18
209.80	261	234	-27	-10
210.00	248	265	+17	+7
210.50	137	181	+44	+32
211.00	83	75	-8	-10
211.50	81	74	-7	-9
212.00	127	103	-24	-19
212.50	94	91	-3	-3
	Average		-22	-6

**Table 3-7 Comparison of Results for Predicting  $\varepsilon_v$  Using Area Parameter &  $E_{SG}$** 

Core Location	Using Area Parameter and $E_{SG}$			
	$\varepsilon_v$ EVERSTRS	$\varepsilon_v$ EQUATION	numerical difference	percent difference
207.85	311	296	-15	-5
208.00	256	287	+31	+12
209.05	639	820	+181	+28
209.40	648	909	+261	+40
209.80	227	258	+31	+14
210.00	402	421	+19	+5
210.50	236	182	-54	-23
211.00	108	83	-25	-23
211.50	51	73	+22	+42
212.00	98	133	+35	+36
212.50	77	121	+44	+57
		Average	+48	+17

**Table 3-8 Comparison of Results for Predicting  $\varepsilon_v$  Using  $D_0$  &  $E_{SG}$** 

Core Location	Using $D_0$ and $E_{SG}$			
	$\varepsilon_v$ EVERSTRS	$\varepsilon_v$ EQUATION	numerical difference	percent difference
207.85	311	492	+181	+58
208.00	256	418	+162	+63
209.05	639	1303	+664	+104
209.40	648	1510	+862	+133
209.80	227	387	+160	+70
210.00	402	617	+215	+53
210.50	236	265	+29	+12
211.00	108	0	-108	-100
211.50	51	-10	-61	-120
212.00	98	166	+68	+69
212.50	77	97	+20	+26
		<b>Average</b>	+199	+33

**Table 3-9 Comparison of Pavement Life Remaining for Fatigue Failure Criteria**

Core Location	N <sub>f</sub> Lab No Shift Factor based on EVERSTRS prediction	N <sub>f</sub> Lab No Shift Factor based on predictive equation prediction	Percent difference
207.85	25,469	42,300	+66
208.00	32,569	55,261	+70
209.05	4,584	3,037	-34
209.40	3,095	5,971	+93
209.80	39,657	56,807	+43
210.00	24,919	20,034	-20
210.50	77,724	31,080	-60
211.00	911,725	1,272,692	+40
211.50	1,338,522	1,802,222	+35
212.00	454,203	904,942	+99
212.50	581,972	647,531	+11
	Average Difference		+31

**Table 3-10 Comparison of Pavement Life Remaining for Rutting Failure Criteria**

Core Location	$N_f$ based on EVERSTRS prediction	$N_f$ based on predictive equation prediction	Percent difference
207.85	7,143,874	8,916,733	+25
208.00	17,098,133	10,240,930	-40
209.05	282,821	92,428	-67
209.40	265,628	58,228	-78
209.80	29,315,170	16,511,743	-44
210.00	2,259,895	1,837,177	-19
210.50	24,624,639	78,955,256	+221
211.00	819,854,957	2,669,914,071	+226
211.50	23,711,674,966	4,748,106,725	-80
212.00	1,267,547,032	322,278,446	-75
212.50	3,737,909,781	492,475,622	-87
	Average Difference		-2

### **3.5 CONCLUSION**

The regression equations developed in this chapter are designed to provide an approximate estimate of the critical strains in the pavement structure. These critical

strains can then be used to predict the pavement's remaining life. These estimates are not for use as a design tool.

Area Parameter and  $D_0$  must be normalized to a 40 kN load in order to use these equations and are not adjusted for temperature as presently configured. The ranges of AC stiffness used in the data generation provides for a range of temperatures. The regression equations that predict  $\varepsilon_t$  can only be used with pavement sections with an Area Parameter greater than 500 mm. Pavements with an Area Parameter less than 500 mm often fail due to rutting, although fatigue failure may also control for these pavements. Rutting failure is not typical for pavements with an Area Parameter greater than 500 mm.

## **CHAPTER 4**

### **LOAD ADJUSTMENT**

#### **4.1 INTRODUCTION**

When testing a section of pavement, two very important factors can affect the deflections that will be measured: load and temperature. As the load increases, the deflections will increase for the same pavement. Deflections also increase as AC temperature increases. For these reasons, test results must be adjusted to some standard load and temperature to make any comparisons valid. This chapter describes the process used to develop load adjustment factors for Area Parameter and  $D_0$ . The process used to develop a temperature adjustment is detailed in Appendix F because temperature adjustment is not required with the equations developed in this thesis.

The load adjustment must be used with the predictive equations developed in Chapters 3 and 5. The temperature adjustment should not be used with these equations because of the range of AC stiffnesses (hence temperatures) inherent in the data used to develop the equations.

A load adjustment is required if the testing will use other than a standard 40 kN load. Deflections and the Area Parameter calculated by those deflections will increase as the load is increased for the same pavement.

## **4.2 METHODOLOGY**

### **4.2.1 Data Generation**

The initial 120 pavement scenarios that were created to establish relationships between pavement response and critical strains were created at a single wheel load of 40 kN. In order to develop relationships between pavement response and load, 10 pavement scenarios were chosen to run additional EVERSTRS calculations. The pavement scenarios were chosen over a range of pavement thicknesses, pavement moduli, and subgrade moduli and are listed in Table 4-1. A complete listing of the EVERSTRS output values for these 10 pavement scenarios at loads of 20, 30, 40, 50, 60, 70, and 80 kN can be found in Appendix A.

When the values of Area Parameter and  $D_0$  were plotted against load, as can be seen in Figures 4-1 and 4-2, the variation of Area Parameter and  $D_0$  were approximately linear with changes in load. Equations relating Area Parameter and  $D_0$  with load were developed using the regression analysis software program Minitab and are discussed in the following section.

**Table 4-1 Pavement Scenarios Used to Generate Load Adjustment Factors**

Case No.	AC Thickness (cm)	AC Modulus (MPa)	Subgrade Modulus (MPa)
1	5	690	35
10	10	2760	35
13	5	5520	35
40	40	11040	70
50	10	2760	140
55	20	5520	140
65	5	1380	280
70	10	2760	280
89	2.5	11040	35
115	2.5	2760	280

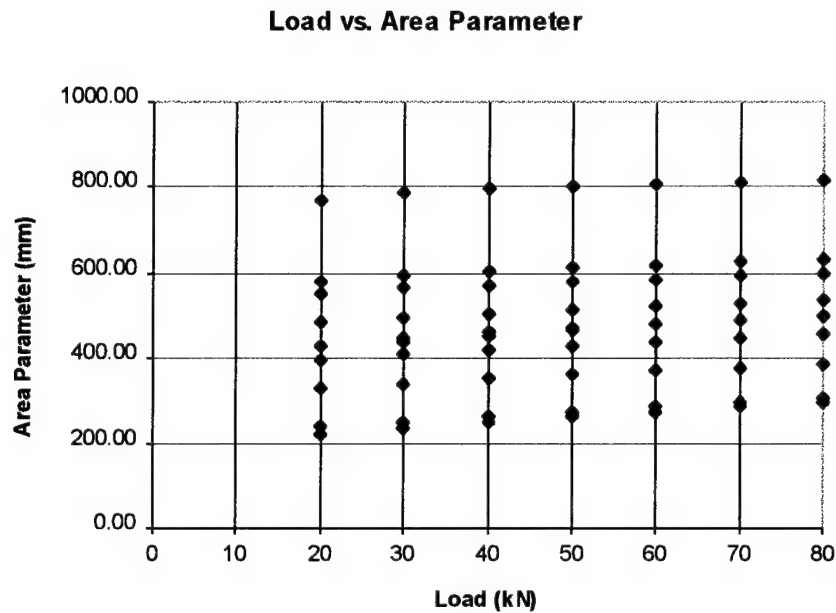


**Figure 4-1 Load vs Area Parameter Graph**

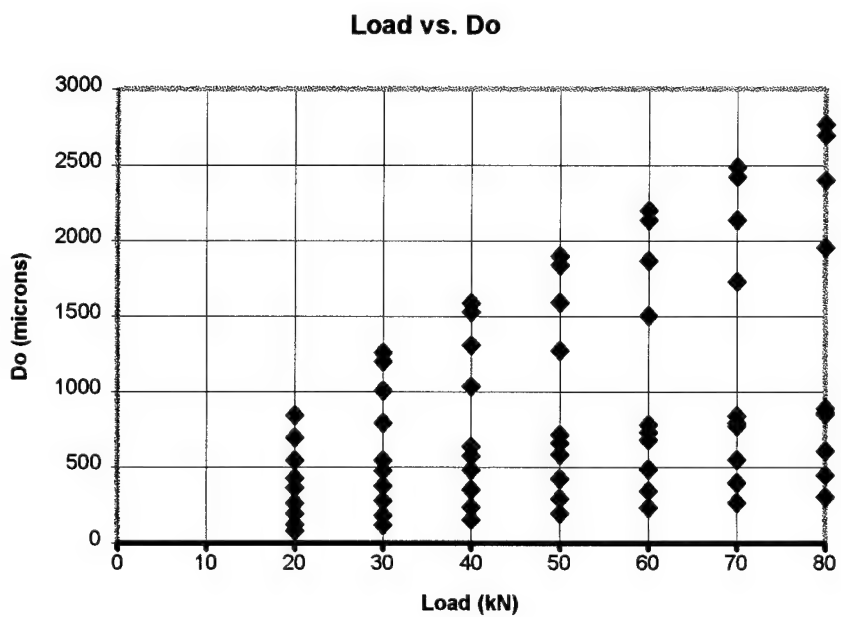


**Figure 4-2 Load vs  $D_0$  Graph**

#### **4.2.2 Regression Analysis**

The variation for both Area Parameter and  $D_0$  was estimated as a function of load only. In mathematical terms, the variation of Area Parameter and  $D_0$  due to load is the slope of the “best fit” line for each pavement scenario. The slope for each of the pavement scenarios is fairly constant for Area Parameter, while the slope of the line for  $D_0$  can be seen to increase with increasing y-intercept values. The Area Parameter variation was the most straightforward to determine.

##### **4.2.2.1 Area Parameter**

The values of load vs Area Parameter for each pavement scenario was analyzed using the Minitab computer program. For each case, a regression equation was generated for Area Parameter with Load as the single predictor. The equations were of the form:

$$A = (\text{intercept}) + (\text{slope})(\text{Load})$$

The resulting regression equations all had an  $R^2$  greater than 90% and can be found in Appendix D. The intercept ranged in value from 201 mm to 761 mm, but for the purpose of establishing a load adjustment factor the intercept is not important. The slope ranged in value from 0.715 to 1.37. The differences in the slope seemed to be random, so an average slope was calculated and used as the load adjustment factor for Area Parameter. The average slope, and thus the load adjustment factor is 1.069. The equation to adjust an Area Parameter for load is:

$$A_{\text{adjusted to } 40\text{kN}} = A_{\text{Load}} + (40 - \text{Load})(1.069)$$

As an example, if an FWD test conducted using a 20 kN load produced an Area Parameter of 450, the Area Parameter adjusted to 40 kN would be calculated as follows:

$$A_{\text{adjusted to } 40\text{kN}} = 450 + (40 - 20)(1.069)$$

$$A_{40\text{kN}} = 471.38$$

If the actual load is greater than 40 kN, Area Parameter will be shifted to a lower value, while the opposite is true for loads less than 40 kN. Refer to Figure 4-1 for a visual representation of this trend.

#### **4.2.2.2 Deflection at the Center of the Load**

Again, the values of Load vs  $D_0$  were analyzed using the Minitab computer program to find the regression equation describing the “best-fit” line for each pavement scenario. These equations were of the form:

$$D_0 = (\text{intercept}) + (\text{slope})(\text{Load})$$

The regression equations had excellent  $R^2$  values; all exceeded 98% and three were perfect fits with an  $R^2$  of 100%. These equations can be found in Appendix D. The intercept values ranged from 8 to 316 microns. The slope values ranged from 3.76 to 31.0. The slope values increased as the intercept values increased. This relationship created the opportunity to approximate the slope (load adjustment factor) rather than use an average as was done for the Area Parameter load adjustment factor.

The slope values were entered into Minitab and correlated with the values of  $D_0$  at each load. Seven regression equations were developed of the form:

$$\text{slope} = (\text{pintercept}) + (\text{pslope})(D_0)_{\text{Load}}$$

Pintercept and pslope are the intercept and slope from the equations relating the slope pictured in Figure 4-2 to  $D_0$  at each load. The goal was to predict slope using load only, pintercept and pslope were correlated with Load which resulted in the following regression equations:

$$\frac{1}{\text{pslope}} = 8.51 + 0.97(\text{Load}) \quad \text{for all loads}$$

$$R^2 = 99.9\% \qquad \text{RMSE} = 0.5917 \qquad N = 7$$

which can be simplified as:

$$\text{pslope} = \frac{1}{(8.51 + 0.970(\text{Load}))}$$

and

$$\text{pintercept} = -1.27 + 0.00758(\text{Load}) \quad \text{for loads 30-80 kN}$$

$$R^2 = 97.4\% \qquad \text{RMSE} = 0.02611 \qquad N = 6$$

$$\text{pintercept} = -0.91 \quad \text{for 20 kN load}$$

The pintercept equation was limited to the 30-80 kN loads because the value for the 20 kN load was severely out of line with the other values. The regression equation for pintercept which included the 20 kN load had an  $R^2$  of 75.4%.

An example to see how these equations come together is appropriate. Given a FWD test done at 65 kN and a measured  $D_0$  of 890  $\mu\text{m}$ , what should the  $D_0$  load adjustment factor be? Given the load, first calculate the pintercept and pslope:

$$\text{pintercept} = -1.27 + 0.00758(65 \text{ kN})$$

$$\text{pintercept} = -0.78$$

$$\text{pslope} = \frac{1}{(8.51 + 0.970(65 \text{ kN}))}$$

$$\text{pslope} = 0.0140$$

The calculated pintercept and pslope are then inserted into the equation for the  $D_0$  load adjustment factor:

$$\text{slope} = \text{pintercept} + \text{pslope}(D_0)_{\text{Load}}$$

$$\text{slope} = -0.78 + 0.0140(890)$$

$$D_0 \text{ load adjustment factor} = \text{slope} = 11.68$$

The adjusted  $D_0$  could then be calculated using the following equation:

$$(D_0)_{40\text{kN}} = (D_0)_{\text{Load}} + (40 - \text{Load})(D_0)_{\text{SF}}$$

where  $(D_0)_{\text{SF}}$  is the  $D_0$  load adjustment factor, or “shift factor”. The adjusted  $D_0$  would be:

$$(D_0)_{40\text{kN}} = (890) + (40 - 65)(11.68)$$

$$(D_0)_{40\text{kN}} = 598 \mu\text{m}$$

The procedure to adjust  $D_0$  for load is more complicated than that for Area Parameter. In summary the steps are:

1. Calculate pintercept and pslope. Input required: Load used in testing.
2. Calculate  $D_0$  load adjustment factor. Input required:  $D_0$  measured in testing.
3. Calculate adjusted  $D_0$ .

### **4.3 RESULTS**

The previous section described the process to adjust Area Parameter and  $D_0$  to a standard load of 40 kN. How well these parameters can be adjusted significantly impacts their use in predicting critical strains necessary to calculate life left in the pavement structure. Table 4-2 shows how well Area Parameter was shifted for load for the 10 pavement scenarios used to generate the initial data. Column 3 shows Area Parameter calculated by EVERSTRS for that Case Number at 40 kN load, column 5 shows Area Parameter calculated by EVERSTRS for that Case Number at the load indicated in column 2, and column 4 shows Area Parameter adjusted to 40 kN using the process outlined in this chapter. On average, the shifted value of Area Parameter is within 1% of the actual Area Parameter measured at 40 kN. Table 4-3 shows how well  $D_0$  was shifted for load for the same 10 pavement scenarios. On average, the error in shifting  $D_0$  to 40 kN is 6.4%. These comparisons use only theoretical data created by the EVERSTRS computer program; however, results should be comparable for FWD data since EVERSTRS was created based on FWD data.

**Table 4-2 Error in Adjusting Area Parameter to 40 kN**

Case No.	Load (kN)	A calculated at 40 kN	A adjusted to 40 kN	A calculated at X load	Percent Difference
1	20	455.09	439.16	417.78	3.50%
1	30	455.09	449.44	438.75	1.24%
1	50	455.09	457.93	468.62	0.62%
1	60	455.09	458.94	480.32	0.85%
1	70	455.09	458.61	490.68	0.77%
1	80	455.09	457.28	500.04	0.48%
10	20	572.80	574.77	553.39	0.34%
10	30	572.80	575.01	564.32	0.39%
10	50	572.80	569.27	579.96	0.62%
10	60	572.80	564.91	586.29	1.38%
10	70	572.80	559.95	592.02	2.24%
10	80	572.80	554.53	597.29	3.19%
13	20	505.98	505.39	484.01	0.12%
13	30	505.98	506.59	495.90	0.12%
13	50	505.98	504.23	514.92	0.35%
13	60	505.98	501.66	523.04	0.85%
13	70	505.98	498.46	530.53	1.49%
13	80	505.98	494.76	537.52	2.22%
40	20	794.85	791.75	770.37	0.39%
40	30	794.85	796.13	785.44	0.16%
40	50	794.85	790.83	801.52	0.51%
40	60	794.85	785.25	806.63	1.21%
40	70	794.85	778.64	810.71	2.04%
40	80	794.85	771.35	814.11	2.96%
50	20	421.64	418.25	396.87	0.80%
50	30	421.64	421.34	410.65	0.07%
50	50	421.64	420.51	431.20	0.27%
50	60	421.64	418.47	439.85	0.75%
50	70	421.64	415.77	447.84	1.39%
50	80	421.64	412.58	455.34	2.15%

**Table 4-2 Error in Adjusting Area Parameter to 40 kN, continued**

Case No.	Load (kN)	A calculated at 40 kN	A adjusted to 40 kN	A calculated at X load	Percent Difference
55	20	605.71	601.33	579.95	0.72%
55	30	605.71	605.98	595.29	0.04%
55	50	605.71	602.99	613.68	0.45%
55	60	605.71	598.84	620.22	1.13%
55	70	605.71	593.75	625.82	1.97%
55	80	605.71	588.00	630.76	2.92%
65	20	264.36	260.27	238.89	1.55%
65	30	264.36	262.86	252.17	0.57%
65	50	264.36	265.22	275.91	0.33%
65	60	264.36	265.69	287.07	0.50%
65	70	264.36	265.88	297.95	0.57%
65	80	264.36	265.87	308.63	0.57%
70	20	352.01	349.22	327.84	0.79%
70	30	352.01	351.75	341.06	0.07%
70	50	352.01	351.03	361.72	0.28%
70	60	352.01	349.28	370.66	0.78%
70	70	352.01	347.00	379.07	1.42%
70	80	352.01	344.31	387.07	2.19%
89	20	460.24	451.92	430.54	1.81%
89	30	460.24	457.33	446.64	0.63%
89	50	460.24	461.47	472.16	0.27%
89	60	460.24	461.47	482.85	0.27%
89	70	460.24	460.52	492.59	0.06%
89	80	460.24	458.81	501.57	0.31%
115	20	250.86	245.29	223.91	2.22%
115	30	250.86	248.59	237.90	0.90%
115	50	250.86	252.52	263.21	0.66%
115	60	250.86	253.57	274.95	1.08%
115	70	250.86	254.34	286.41	1.39%
115	80	250.86	254.87	297.63	1.60%
				Total Error	61.53%
				Average Error (excluding 40 kN load)	1.03%

**Table 4-3 Error in Adjusting  $D_0$  to 40 kN**

Case Number	Load (kN)	$D_0$ calculated at Load	$D_0$ calculated at 40 kN	$D_0$ adjusted to 40 kN	Percent Difference
1	20	906.10	1589.13	1537.20	3.27%
1	30	1259.69	1589.13	1584.20	0.31%
1	40	1589.13	1589.13	1589.13	0.00%
1	50	1901.36	1589.13	1576.76	0.78%
1	60	2200.60	1589.13	1557.15	2.01%
1	70	2489.10	1589.13	1534.01	3.47%
1	80	2768.73	1589.13	1509.14	5.03%
10	20	544.45	1037.40	916.40	11.66%
10	30	794.55	1037.40	995.38	4.05%
10	40	1037.40	1037.40	1037.40	0.00%
10	50	1274.13	1037.40	1059.55	2.13%
10	60	1505.75	1037.40	1070.62	3.20%
10	70	1732.64	1037.40	1074.56	3.58%
10	80	1955.37	1037.40	1073.60	3.49%
13	20	697.14	1307.67	1178.50	9.88%
13	30	1009.56	1307.67	1267.56	3.07%
13	40	1307.67	1307.67	1307.67	0.00%
13	50	1594.13	1307.67	1323.42	1.20%
13	60	1871.01	1307.67	1326.38	1.43%
13	70	2139.40	1307.67	1321.61	1.07%
13	80	2400.48	1307.67	1311.95	0.33%
40	20	82.66	158.93	123.69	22.17%
40	30	121.01	158.93	142.76	10.17%
40	40	158.93	158.93	158.93	0.00%
40	50	196.54	158.93	170.98	7.58%
40	60	233.95	158.93	180.11	13.33%
40	70	271.16	158.93	186.88	17.59%
40	80	308.22	158.93	191.59	20.55%
50	20	266.05	484.11	438.50	9.42%
50	30	378.26	484.11	468.41	3.24%
50	40	484.11	484.11	484.11	0.00%
50	50	584.75	484.11	491.09	1.44%
50	60	681.05	484.11	493.17	1.87%
50	70	773.50	484.11	491.99	1.63%
50	80	862.57	484.11	488.43	0.89%

**Table 4-3 Error in Adjusting  $D_0$  to 40 kN, continued**

Case Number	Load (kN)	Do calculated at Load	Do calculated at 40 kN	Do adjusted to 40 kN	Percent Difference
55	40	239.58	239.58	239.58	0.00%
55	50	294.01	239.58	251.35	4.91%
55	60	347.57	239.58	259.67	8.39%
55	70	400.33	239.58	265.33	10.75%
55	80	452.38	239.58	268.78	12.19%
65	20	365.45	574.91	609.13	5.95%
65	30	479.46	574.91	596.52	3.76%
65	40	574.91	574.91	574.91	0.00%
65	50	657.40	574.91	551.00	4.16%
65	60	730.38	574.91	527.71	8.21%
65	70	795.94	574.91	505.62	12.05%
65	80	855.65	574.91	484.73	15.69%
70	20	200.13	353.73	325.34	8.03%
70	30	279.93	353.73	343.93	2.77%
70	40	353.73	353.73	353.73	0.00%
70	50	422.68	353.73	357.45	1.05%
70	60	487.63	353.73	357.74	1.13%
70	70	549.07	353.73	355.68	0.55%
70	80	607.47	353.73	351.83	0.54%
89	20	845.31	1528.74	1432.85	6.27%
89	30	1199.06	1528.74	1507.45	1.39%
89	40	1528.74	1528.74	1528.74	0.00%
89	50	1840.40	1528.74	1526.49	0.15%
89	60	2138.11	1528.74	1513.40	1.00%
89	70	2424.19	1528.74	1494.59	2.23%
89	80	2700.61	1528.74	1472.66	3.67%
115	20	431.79	636.36	723.01	13.62%
115	30	545.54	636.36	680.17	6.88%
115	40	636.36	636.36	636.36	0.00%
115	50	712.45	636.36	596.39	6.28%
115	60	779.64	636.36	562.20	11.65%
115	70	839.36	636.36	531.99	16.40%
115	80	893.75	636.36	505.13	20.62%
Total Percentage Error					383.68%
Average Percentage Error (excluding 40 kN loads)					6.39%

#### **4.4 CONCLUSION**

The load shift factors presented in this chapter were developed using the data created for this thesis. Any shift factor can be used with the various equations presented in this thesis as long as the pavement engineer has confidence in the system being used. The critical point is to adjust pavement responses to a standard load (40 kN) before using the relationships presented throughout this thesis. Temperature shift factors are presented in Appendix F; however, these shift factors should not be used with the equations presented in this thesis because temperature variation was included in the data used to develop the equations.

## **CHAPTER 5**

### **PREDICTING OVERLAY REQUIREMENTS**

#### **5.1 INTRODUCTION**

Chapter 3 outlined the steps taken to estimate life remaining in a pavement using measurable pavement responses and parameters that can be directly calculated from those responses, namely: deflection at the center of the load ( $D_0$ ), Area Parameter (A), and subgrade elastic modulus ( $E_{SG}$ ). Another powerful tool is the ability to predict the overlay required for a pavement system based on those parameters and the number of equivalent single axle loads (ESALS) the pavement needs to be designed for. This chapter discusses the research conducted to develop relationships that can predict the overlay required based on these readily available parameters.

#### **5.2 METHODOLOGY**

##### **5.2.1 Data Generation**

A layered elastic analysis was performed for each of the 120 pavement scenarios originally shown in Table 3-1. The analysis reported in this chapter was done using EVERPAVE 4.0. The input parameters that were held constant for this analysis were:

Design Tire Load	40000 N
Tire Pressure	690 kPa
Dual Spacing	0 cm (i.e., a single tire was used)
Fatigue Shift Factor, New AC	10

Fatigue Shift Factor, Old AC	10
Seasonal Variation	All seasons at 25 degrees Celsius
Lane Distribution Factor	1.0
Minimum Overlay	0.5 cm (a value of 0 is not allowed by the program)

Each case was analyzed for total design traffic (80 kN ESALS) of 1, 5, and 10 million. The overlay thickness required and the damage levels for fatigue damage on the new AC, fatigue damage of the old AC and rutting damage on the subgrade were recorded. These values can be found in Appendix A, Table A-2. The overlays were significantly greater than typically expected and the reasons for this will be described in Section 5.3.

### **5.2.2 Regression Analysis**

Pavement scenarios that resulted in an overlay requirement of 0.5 cm only due to the program requirement that some minimum overlay be considered were removed for the regression analysis of the data. This was done because these values tended to skew the data. Pavements with a wide range of deflection responses will need the minimum overlay dictated by EVERPAVE.

The results from the EVERPAVE analyses were entered into the Minitab computer program to run the regression analysis. Regression analysis was done using  $D_0$ , Area Parameter,  $E_{SG}$ , and ESALS as independent variables. The overlay thickness required was the dependent variable. All of the equations calculated using these

variables in various transformations can be found in Appendix D. The best equation found was:

$$\text{Overlay} = -541 + 84.9\log D_0 + 82.4\log A + 54.3\log E_{SG} + 14.5\log ESALS$$

$$R^2 = 95.7\%$$

$$RMSE = 2.239$$

$$N = 327$$

where overlay is in cm,  $D_0$  and Area Parameter are in  $\mu\text{m}$  and mm respectively,  $E_{SG}$  is in MPa and ESALS is in millions.

### **5.3 RESULTS**

When the overlay equation was compared with the overlay predicted by EVERPAVE for the 327 cases analyzed, the overall results were very promising. On average there was a 13% difference from the overlay predicted from the equation compared to the overlay predicted by EVERPAVE (refer to Appendix A, Table A-3 for the complete listing of the comparisons). The absolute difference on average was 1.4 cm. This shows that, given constant parameters, overlay can be predicted fairly well from  $D_0$ , Area Parameter,  $E_{SG}$ , and ESALS without knowing the composition of the pavement system. Once the equation was compared with some of the case studies in the WSDOT Pavement Guide, however, it became clear that some of the simplifying assumptions created an overprediction of the overlay. Two Case Studies discussed in the WSDOT Pavement Guide were used to compare overlay results.

#### **5.3.1 Case Study Number One**

Case Study Number One in the WSDOT Pavement Guide covers the section of State Route 395 from Mile Post 207.81 to Mile Post 212.67. The pavement guide

determined the required overlay using three methods. The first method is WSPMS SCOPER which is a component analysis approach partially based on the Asphalt Institutes Component Analysis procedure. The second method is DARWin, the computerized version of the pavement design models in AASHTO's "Guide for Design of Pavement Structures 1993". The third and final method is using EVERPAVE 4.0, the mechanistic-empirical overlay design procedure developed by WSDOT.

Table 5-1 shows the comparison of the results from the three methods used in the pavement guide along with the results using the overlay equation presented in this chapter. No temperature adjustment was made for this comparison. The last four core locations may have shown an overlay requirement due only to the minimum requirement imposed by the computer program. For this reason, these core locations were not included in the computation of the average difference between EVERPAVE and the predictive equation. The average overlay thickness difference between the EVERPAVE results and the Equation result is 20.6 cm. The two primary factors which may be contributing to this difference are the seasonal effects and the load configuration chosen.

The overlay equation is based on EVERPAVE data which was executed with no seasonal variation and an average temperature of 25 degrees Celsius. This would represent a climate about the equivalent of Miami, Florida. In order to quantify the effect on the results, the first nine core locations were recalculated with EVERPAVE; the only change being the seasonal effects were held to the constant 25 degrees Celsius. The

results are shown in Table 5-2. The average difference in overlays due to temperature difference was an increase of 6.4 cm.

**Table 5-1 Comparison of Overlay Results - Case Study Number One  
(No Temperature Adjustment)**

Core Location	WSPMS overlay (cm)	AASHTO overlay (cm)	EVERPAVE overlay (cm)	Equation overlay (cm)
207.85	7.1	0	5	25.8
208	5.5	0	4	23.4
208.5	5.6	0	1	15.4
209	14.7	12.7	9.5	36
209.05	15.5	13.2	10	34.2
209.4	14.3	13.5	11	35.3
209.8	6.5	0	3.5	23
210	11..8	5.8	6	25.3
210.5	9	0	3.5	20.2
211	0	0	1(0)	11.2
211.5	0	0	1(0)	9.1
212	0	0	1(0)	17.4
212.5	0	0	1(0)	15

**Table 5-2 Overlay Discrepancy Based on Seasonal Variation**

Core Location	EVERPAVE w/ seasonal variation (cm)	Recalculation @ 25°C EVERPAVE (cm)	Difference (cm)
207.85	5.0	11.5	6.5
208.00	4.0	11.5	7.5
208.50	1.0	6.0	5.0
209.00	9.5	16.0	6.5
209.05	10.0	16.5	6.5
209.40	11.0	19.0	8.0
209.80	3.5	10.0	6.5
210.00	6.0	11.0	5.0
210.50	3.5	10.0	6.5

Another significant difference results from the way the tire load was modeled. In developing the data used to develop the overlay equation, the load was modeled as a single 40 kN load rather than dual tires loaded to 20 kN each and spaced 35.6 cm apart which is more typical of the assumption used in the original WSDOT case study. The single load was used because EVERPAVE analyzes pavement much faster with a single load rather than a dual load. Several of the original case scenarios were recalculated with a dual load, all other parameters were held constant. The results are shown in Table 5-3.

**Table 5-3 Overlay Discrepancy Based on Load Configuration**

Case No	Single Tire Overlay (cm)	Dual Tire Overlay (cm)	Difference (cm)
1	34.0	19.0	15.0
10	26.0	11.5	14.5
31	12.5	0	>12.5
74	17.0	3.5	13.5
81	35.0	20.5	14.5
85	33.5	19.0	14.5
94	28.0	14.0	14.0
100	25.0	11.0	14.0
108	26.0	11.5	14.5
120	22.0	9.0	13.0

The average difference due to the load configuration is 14.2 cm. This added with the difference due to temperature (6.4 cm) combines for a total average difference of 20.6 cm. This is also the average difference that was found between the EVERPAVE results and the overlay equation results in Table 5-1.

### **5.3.2 Case Study Number Two**

Case Study Number Two in the WSDOT Pavement Guide covers the section of Washington State Route 7 from Mile Post 0.00 to Mile Post 16.82. Again, the pavement guide determined the overlay required using three methods.

Table 5-4 shows the comparison of the results from the three methods used in the pavement guide along with the results using the overlay equation presented in this chapter. No temperature adjustment was made for this comparison.

The average difference between the EVERPAVE results and the overlay equation results is 24.06 cm. This is a 3.5 cm increase over the average difference for Case Study Number One. Again, the two primary factors contributing to this difference are the seasonal effects and the tire spacing chosen.

### **5.4 CONCLUSION**

The overlay equation developed from the 360 cases calculated by EVERPAVE shows a high correlation of the data. This indicates that the overlay required could be reasonably *estimated* using only  $D_0$ , Area Parameter,  $E_{SG}$ , and ESALS. This equation would be an extremely useful tool for prioritizing pavements for rehabilitation. It would also give an early estimation of the extent of overlay required. The particular equation developed in this thesis, however, severely overestimates the overlay required when compared with previous case studies presented in the WSDOT Pavement Guide. The two factors contributing to this overestimation are the seasonal temperature and load configuration used when developing the data. A similar overlay equation developed

using standard seasonal variation and load configuration for a region would provide more reasonable results. The consistency of the overlay equation results developed in this chapter are very promising, indicating further development would be worthwhile.

**Table 5-4 Comparison of Overlay Results - Case Study Number Two  
(No Temperature Adjustment)**

Core Location	WSPMS overlay (cm)	AASHTO overlay (cm)	EVERPAVE overlay (cm)	Equation overlay (cm)
0.23	4.9	0	0.5	16.5
0.43	2.4	-	-	9.9
0.98	8.2	8.1	4.5	26.2
1.83	0	0	0.5	15.1
2.38	0	0	0.5	19.3
3.68	5.2	8.9	4.0	24.8
4.08	7.1	7.4	2.0	22.4
4.48	3.0	3.3	0.5	18.7
5.03	8.6	6.9	1.0	21.2
5.63	5.5	8.9	1.5	26.1
6.13	8.8	2.5	0.5	15.6
6.48	9.8	15.0	7.0	30.7
7.18	7.9	9.7	2.0	25.7
7.73	5.2	5.8	2.5	24.8
8.23	8.2	3.8	0.5	19.4

**Table 5-4 Comparison of Overlay Results - Case Study Number Two  
(No Temperature Adjustment), continued...**

Core Location	WSPMS overlay (cm)	AASHTO overlay (cm)	EVERPAVE overlay (cm)	Equation overlay (cm)
8.78	10.1	11.4	4.5	28.5
9.48	10.7	13.0	4.0	34.6
9.98	13.4	14.7	8.0	35.0
10.58	11.3	13.7	6.0	36.2
10.98	10.7	10.7	7.0	29.2
11.63	10.7	10.7	7.5	30.7
12.18	9.8	14.7	5.5	36.8
12.53	9.4	11.4	5.0	31.5
13.03	9.8	7.4	1.5	26.6
13.53	9.4	8.4	1.0	23.0
14.53	7.3	7.6	0.5	21.7
15.08	7.6	9.1	3.5	24.8
15.68	8.2	15.0	8.0	30.2
16.03	0	5.1	1.0	23.3
16.55	0	3.0	0.5	18.8

## CHAPTER 6

### CONCLUSIONS AND RECOMMENDATIONS

#### **6.1 CONCLUSIONS**

General conclusions concerning the research presented in the previous chapters are included here.

- Critical strains ( $\varepsilon_t$  and  $\varepsilon_v$ ) can be estimated using only  $E_{SG}$  and Area Parameter or  $D_0$ .  
From these critical strains, pavement life remaining can be estimated.
- Overlay required can be estimated using Area Parameter,  $D_0$ ,  $E_{SG}$ , and ESALS given consistent seasonal variation and load configuration.
- Area Parameter and  $D_0$  must be adjusted to a standard load (40 kN) to use the equations presented in this thesis. Temperature adjustments are not required.
- The equations presented are estimations and should be used at the pavement management level, not the design level. More rigorous methods are required for design purposes.
- The equations developed and presented in this thesis are summarized in Table 6-1.

**Table 6-1 Summary of Equations Developed in this Thesis**

<b>Equation</b>	<b>R<sup>2</sup></b>	<b>RMSE</b>	<b>N</b>
$\log \varepsilon_t = 5.91 - 0.00353A - 0.877\log E_{SG}$	89.3	0.1358	41
$\log \varepsilon_t = -4.23 + 1.8\log D_0 + 0.898\log E_{SG}$	97.6	0.0647	41
$\log \varepsilon_v = 7.04 - 0.00339A - 1.34\log E_{SG}$	94.4	0.1148	120
$\varepsilon_v = -511 + 1.97D_0 + 0.788E_{SG}$	96.0	163.9	120
overlay = $-541 + 84.9\log D_0 + 82.4\log A + 54.3\log E_{SG} + 14.5\log ESALS$	95.7	2.239	327

## **6.2 RECOMMENDATIONS**

The pavement scenarios used to create the data in this thesis ranged in AC thickness from 2.5 cm to 40 cm. The very thick 40 cm pavements do not correlate as well as the pavements 20 cm and thinner. The predictive equations could be reformulated without the very thick pavements which should increase the R<sup>2</sup> and decrease the RMSE. Of course this would also limit the range of pavements the equations could be applied to.

Additional case study comparisons should be made for both the critical strain and the overlay predictive equations. A wide range of pavements should be compared with these equations; however, the pavements should be within the range of variable pavement parameters used in this research (see Table 3-1).

The critical strain equations could be recalculated using an array of pavement scenarios that include variations in base moduli and thickness. Another variation that could be attempted would be to limit the AC moduli to the equivalent for 25 °C. This would create a regression equation that would need to be adjusted for temperature. A comparison could be made between these types of equations to determine which is a better predictor of critical strains.

Further research is required for the overlay equation. An overlay equation could be developed using a more standard seasonal variation and a dual load configuration. Several seasonal variations could be tried to see if there is a correlation between average annual air temperature and additional overlay required.

The equations presented in this thesis represent many hours of data generation and manipulation. As they exist now, they can be used as an approximate estimation of the pavement condition and the extent of overlay required. It is hoped that further research will result in better predictive relationships that can be used with confidence for prioritizing pavement rehabilitation projects.

## REFERENCES

AASHTO Guide for Design of Pavement Structures, American Association of State Highway and Transportation Officials, 1993.

Andersson, Olle, "Comparison of Measured and Calculated Deflection Basins and Appropriate Deflection Parameters", Royal Institute of Technology, S-10044 Stockholm, Sweden, undated.

Asphalt Institute, The, Asphalt Overlays for Highway and Street Rehabilitation, Manual Series No. 17, June 1983.

ASTM D4694-87: Standard Test Method for Deflections with a Falling Weight Type Impulse Load Device. 1989 Annual Book of ASTM Standards, Sect. 4, Construction, Vol. 04.03 Road and Paving Materials; Traveled Surface Characteristics.

Benkelman, A. C., Kingham, R. I., and Fang, H. Y., "Selected Special Studies", The AASHO Road Test, Proceedings of a Conference Held May 16-18, 1962, Highway Research Board Special Report 73, 1962.

Bush, A. J., Hall, J.W., and Harr, M. E., "Nondestructive Airfield Pavement Testing Using LASER Technology", AIAA-83-1601, International Air Transportation Conference, June 1-3, 1983, Montreal, Canada.

FAA Pavements Workshop Notes, FAA Pavements Workshop, Seattle, WA, 27 April 1995.

Gomez-Achecar, M. and Thompson, Marshall R., "ILLI-PAVE Based Response Algorithms for Full-Depth Asphalt Concrete Flexible Pavements" University of Illinois at Urbana, Illinois, Submitted for the 1986 Annual Meeting of the Transportation Research Board, Washington, D. C. January 1986.

Hoffman, M. S. and Thompson, M. R., "Mechanistic Interpretation of Nondestructive Pavement Testing Deflections", Report No. UILU-ENG-2010, Illinois Department of Transportation, Springfield, Illinois, June 1981.

Johnson, R. F., Rolling Weight Deflectometer Final Report - Phase II SBIR, Quest Technical Report No. 637, December 1994.

Kingham, R. Ian, "A New Temperature-Correction Procedure for Benkelman-Beam Rebound Deflections" Research Report 69-1, The Asphalt Institute, College Park, Maryland 20740, February 1969.

Lytton, R. L., Germann, F. P., Chou, Y. J., and Stoffels, S. M., "Determining Asphaltic Concrete Pavement Structural Properties By Nondestructive Testing", National Cooperative Highway Research Program Report 327, Transportation Research Board National Research Council, Washington, D.C., June 1990.

Mahoney, Joe P., "Statistical Methods for WSDOT Pavement and Material Applications", Report No. WA-RD 315.1, Washington State Department of Transportation, Washington State Transportation Center (TRAC), Interim Report, Feb 1994.

Mahoney, Joe P., Kramer, Steven and Turkiyyah, George, "Draft Procedures for Analysis of Pavement Response for the High-Speed Road Deflection Tester" Proposal prepared for Vagverket, Swedish National Road Administration. Jan 1995.

May, Richard W. and Von Quintus, Harold L., "The Quest for a Standard Guide to NDT Backcalculation" Nondestructive Testing of Pavements and Backcalculation of Moduli (Second Volumn), ASTM STP 1198, Harold L. Von Quintas, Albert J. Bush, III, and Gilbert Y. Baladi, Eds., American Society for Testing and Materials, Philadelphia, 1994.

Meyerhoff, G. G., "Preliminary Analysis of Benkelman Beam Deflections and Flexible Pavement Design", Proceedings, Canadian Good Roads Association, 1962.

Newcomb, David E., "Development and Evaluation of a Regression Method to Interpret Dynamic Pavement Deflections", PhD Dissertation, University of Washington, 1986.

Ryan, Barbara F., Joiner, Brian L., and Ryan, Thomas A. Jr., Minitab Handbook, Second Edition, Duxbury Press, Boston, 1985.

Sebastyan, G. Y., "The Effect of Temperature on Deflection and Rebound of Flexible Pavements Subjected to the Standard CGRA Benkelman Beam Test", Proceedings of the Canadian Good Roads Association, September 1961.

Smith, Roger E. and Lytton, Robert L. "Synthesis Study of Nondestructive Testing Devices for Use in Overlay Thickness Design of Flexible Pavements" Federal Highway Administration, Report No. FHWA/RD-83/097, April 1984.

Welsh, D. A., "The Use of the Benkelman Beam in Municipal Street Design, Maintenance and Construction", Proceedings of the Canadian Good Roads Association, September 1961.

WSDOT Pavement Guide for Design, Evaluation, and Rehabilitation, Feb 1995

## BIBLIOGRAPHY

AASHTO Guide for Design of Pavement Structures, American Association of State Highway and Transportation Officials, 1993.

Andersson, Olle, "Comparison of Measured and Calculated Deflection Basins and Appropriate Deflection Parameters", Royal Institute of Technology, S-10044 Stockholm, Sweden, undated.

Asphalt Institute, The, Asphalt Overlays for Highway and Street Rehabilitation, Manual Series No. 17, June 1983.

ASTM D4694-87: Standard Test Method for Deflections with a Falling Weight Type Impulse Load Device. 1989 Annual Book of ASTM Standards, Sect. 4, Construction, Vol. 04.03 Road and Paving Materials; Traveled Surface Characteristics

ASTM D4695-87: Guide for General Pavement Deflection Measurements. 1989 Annual Book of ASTM Standards, Sect. 4, Construction, Vol. 04.03 Road and Paving Materials; Traveled Surface Characteristics

Baladi, G.Y., and Harr, M.E., "Nondestructive Pavement Evaluation: the Deflection Beam", Transportation Research Board 666

Benkelman, A. C., Kingham, R. I., and Fang, H. Y., "Selected Special Studies", The AASHO Road Test, Proceedings of a Conference Held May 16-18, 1962, Highway Research Board Special Report 73, 1962.

Bush, A. J., Hall, J.W., and Harr, M. E., "Nondestructive Airfield Pavement Testing Using LASER Technology", AIAA-83-1601, International Air Transportation Conference, June 1-3, 1983, Montreal, Canada

Bush, Albert J. III and Cox, Cary, B. "Evaluation of Laser Profile and Deflection Measuring System" DOT/FAA/PM-84/24, Geotechnical Laboratory Department of the Army, Waterways Experiment Station, Corps of Engineers, Vicksburg, Mississippi. Sept 1984 Final Report

FAA Pavements Workshop Notes, FAA Pavements Workshop, Seattle, WA, 27 April 1995

Gomez-Achecar, M. and Thompson, Marshall R., "ILLI-PAVE Based Response Algorithms for Full-Depth Asphalt Concrete Flexible Pavements" University of Illinois at Urbana, Illinois, Submitted for the 1986 Annual Meeting of the Transportation Research Board, Washington, D. C. January 1986.

Hoffman, M. S. and Thompson, M. R., "Mechanistic Interpretation of Nondestructive Pavement Testing Deflections", Report No. UILU-ENG-2010, Illinois Department of Transportation, Springfield, Illinois, June 1981.

Homsi, Abdullah, "An Explicit Relationship Between Asphalt Pavement Deflections and Service Life: An Approach to Practical Overlay Design" Department of Highway Engineering, Royal Institute of Technology, Stockholm, Sweden, 1985.

Horak, E. "The Use of Surface Deflection Basin Measurements in the Mechanistic Analysis of Flexible Pavements" Proceedings vol 1, Sixth International Conference Structural Design of Asphalt Pavements, University of Michigan, Ann Arbor, Michigan, USA, 1987.

Johnson, R. F., Rolling Weight Deflectometer Final Report - Phase II SBIR, Quest Technical Report No. 637, December 1994.

Jung, Friedrich W. "Direct Calculation of Maximum Curvature and Strain in AC Layers of Pavements from Load Deflection Basin Measurements" Ontario Ministry of Transportation, Research and Development Branch. Paper No. 870089, undated.

Jung, Friedrich W. "Numerical Deflection Basin Interpretation and Temperature Adjustment in Non-Destructive Testing of Flexible Pavements" Ontario Ministry of Transportation, Research and Development Branch. Paper No. 881087, December 1988.

Kingham, R. Ian, "A New Temperature-Correction Procedure for Benkelman-Beam Rebound Deflections" Research Report 69-1, The Asphalt Institute, College Park, Maryland 20740, February 1969.

Kramer, Steven, Notes taken from class lectures, CESM 562, Winter Quarter, 1995, University of Washington, Seattle WA.

Krarup, Jorgen, "Measured and Calculated Pavement Response in the Danish Road Testing Machine" Vehicle-Road Interaction, Bohdan T. Kulakowski, Editor STP 1225 ASTM.

Lee, S. W., Mahoney, J. P., and Jackson, N. C., "Verification of Backcalculation of Pavement Moduli", Transportation Research Record 1196, Transportation Research Board National Research Council, Washington, D.C., 1988.

Lytton, R. L., Germann, F. P., Chou, Y. J., and Stoffels, S. M., "Determining Asphaltic Concrete Pavement Structural Properties By Nondestructive Testing", National Cooperative Highway Research Program Report 327, Transportation Research Board National Research Council, Washington, D.C., June 1990.

Mahoney, Joe P., "Statistical Methods for WSDOT Pavement and Material Applications", Report No. WA-RD 315.1, Washington State Department of Transportation, Washington State Transportation Center (TRAC), Interim Report, Feb 1994.

Mahoney, Joe P., Kramer, Steven and Turkiyyah, George, "Draft Procedures for Analysis of Pavement Response for the High-Speed Road Deflection Tester" Proposal prepared for Vagverket, Swedish National Road Administration. Jan 1995.

Markow, Michael J., Hedrick, J. Karl, Brademeyer, Brian D., and Abbo, Edward, "Analyzing the Interactions Between Dynamic Vehicle Loads and Highway Pavements," Transportation Research Record 1196, Transportation Research Board National Research Council, Washington D.C., 1988.

Maser, K., Brademeyer, B., and Littlefield, R., "Pavement Condition Diagnosis Based on Multisensor Data," Transportation Research Record 1196, Transportation Research Board National Research Council, Washington, D.C., 1988.

May, Richard W. and Von Quintus, Harold L., "The Quest for a Standard Guide to NDT Backcalculation" Nondestructive Testing of Pavements and Backcalculation of Moduli (Second Volumn), ASTM STP 1198, Harold L. Von Quintas, Albert J. Bush, III, and Gilbert Y. Baladi, Eds., American Society for Testing and Materials, Philadelphia, 1994.

Melia, Marilyn Kennedy, "How to Improve Work-Zone Safety", Traffic Safety, v. 94 pp. 6-9 May/June 1994.

Meyerhoff, G. G., "Preliminary Analysis of Benkelman Beam Deflections and Flexible Pavement Design", Proceedings, Canadian Good Roads Association, 1962.

Newcomb, David E., "Development and Evaluation of a Regression Method to Interpret Dynamic Pavement Deflections", PhD Dissertation, University of Washington, 1986.

Pierce, Linda, Discussion at her office, Washington Department of Transportation Materials Laboratory, Tumwater, WA. 2 May 1995.

Ryan, Barbara F., Joiner, Brian L., and Ryan, Thomas A. Jr., Minitab Handbook, Second Edition, Duxbury Press, Boston, 1985.

Sebastyan, G. Y., "The Effect of Temperature on Deflection and Rebound of Flexible Pavements Subjected to the Standard CGRA Benkelman Beam Test", Proceedings of the Canadian Good Roads Association, September 1961.

Smith, Roger E. and Lytton, Robert L. "Synthesis Study of Nondestructive Testing Devices for Use in Overlay Thickness Design of Flexible Pavements" Federal Highway Administration, Report No. FHWA/RD-83/097, April 1984.

Spangler, Elson B., and Schell, Harold J., "Non-Contact, Nondestructive Determination of Pavement Deflection Under a Moving Load", FHWA Report OH-92/006, 2 Mar 1992.

Tholen, Olle, "Falling Weight Deflectometer - A Device for Bearing Capacity Measurement: Properties and Performance" Department of Highway Engineering Royal Institute of Technology, Stockholm, Sweden, 1980.

Welsh, D. A., "The Use of the Benkelman Beam in Municipal Street Design, Maintenance and Construction", Proceedings of the Canadian Good Roads Association, September 1961.

WSDOT Pavement Guide for Design, Evaluation, and Rehabilitation, Feb 1995.

## **APPENDIX A DATA**

Figures A-1 and A-2 show a sample output for the computer program EVERSTRS. Each of the 120 pavement scenarios was analyzed using EVERSTRS. The key results are listed in Table A-1. This includes the deflections at each sensor, the Area Parameter calculated from these deflections and the strains at the bottom of the asphalt-concrete layer and at the top of the subgrade. Table A-2 presents the EVERPAVE results for the 120 pavement scenarios at three different levels of ESALs required. The overlay required and the percent of damage accumulated for rutting and AC fatigue are shown in this table. Table A-3 is a comparison of the EVERPAVE prediction of overlay required (as shown in Table A-2) and the overlay predicted by the overlay equation presented in Chapter 5.

<b>Layered Elastic Analysis by EVERSTRS 4.0</b>								
Title: Input 2 No of Layers: 3		No of Loads: 1		No of X-Y Evaluation Points: 4				
Layer	Poisson's Ratio	Thickness (cm)	Moduli(1) (MPa)					
1	.35	10.000	690.00					
2	.40	20.000	207.00					
3	.45		35.00					
Load No	X-Position (cm)	Y-Position (cm)	Load (N)	Pressure (kPa)	Radius (cm)			
1	.00	.00	40000.0	690.00	13.584			
Location No: 1		X-Position (cm): .000	Y-Position (cm): .000					
Normal Stresses								
Z-Position (cm)	Layer	Sxx (kPa)	Syy (kPa)	Szz (kPa)	Syz (kPa)	Sxz (kPa)	Sxy (kPa)	
9.999	1	410.93	410.93	-403.32	.00	.00	.00	
20.000	2	68.01	68.01	-172.81	.00	.00	.00	
30.001	3	-5.18	-5.18	-66.44	.00	.00	.00	
.001	1	-1246.43	-1246.43	-690.00	.00	.00	.00	
Normal Strains and Deflections								
Z-Position (cm)	Layer	Exx (10^-6)	Eyy (10^-6)	Ezz (10^-6)	Ux (microns)	Uy (microns)	Uz (microns)	
9.999	1	591.69	591.69	-1001.41	.00	.00	1258.04	
20.000	2	531.07	531.07	-1097.69	.00	.00	1120.12	
30.001	3	772.77	772.77	-1764.99	.00	.00	1015.54	
.001	1	-824.18	-824.18	264.50	.00	.00	1302.61	
Principal Stresses and Strains								
Z-Position (cm)	Layer	S1 (kPa)	S2 (kPa)	S3 (kPa)	E1 (10^-6)	E2 (10^-6)	E3 (10^-6)	
9.999	1	-403.32	410.93	410.93	-1001.41	591.69	591.69	
20.000	2	-172.81	68.01	68.01	-1097.69	531.07	531.07	
30.001	3	-66.44	-5.18	-5.18	-1764.99	772.77	772.77	
.001	1	-1246.43	-1246.43	-690.00	-824.18	-824.18	264.50	
Location No: 2								
X-Position (cm): .000		Y-Position (cm): 30.500						
Normal Stresses								
Z-Position (cm)	Layer	Sxx (kPa)	Syy (kPa)	Szz (kPa)	Syz (kPa)	Sxz (kPa)	Sxy (kPa)	
9.999	1	15.31	-120.64	-15.67	-61.75	.00	.00	
20.000	2	36.58	-3.41	-26.21	-58.24	.00	.00	
30.001	3	-4.32	-14.02	-29.21	-15.01	.00	.00	
.001	1	-206.56	-13.19	.00	-0.01	.00	.00	
Normal Strains and Deflections								
Z-Position (cm)	Layer	Exx (10^-6)	Eyy (10^-6)	Ezz (10^-6)	Ux (microns)	Uy (microns)	Uz (microns)	
9.999	1	91.33	-174.66	30.71	.00	27.86	810.70	
20.000	2	239.94	-36.51	-190.70	.00	71.35	802.28	
30.001	3	432.44	30.54	-598.82	.00	131.89	773.49	
.001	1	-292.67	85.65	111.47	.00	-89.26	803.22	
Principal Stresses and Strains								
Z-Position (cm)	Layer	S1 (kPa)	S2 (kPa)	S3 (kPa)	E1 (10^-6)	E2 (10^-6)	E3 (10^-6)	
9.999	1	-149.20	12.89	15.31	-230.53	86.59	91.33	
20.000	2	-74.15	36.58	44.53	-514.95	239.94	287.73	
30.001	3	-38.43	-4.80	-4.32	-980.90	412.62	432.44	
.001	1	-206.56	-13.19	.00	-292.67	85.65	111.47	
Location No: 3		X-Position (cm): .000	Y-Position (cm): 61.000					

Figure A-1 Sample EVERSTRS Output Sheet, page 1

<b>Layered Elastic Analysis by EVERSTRS 4.0</b>							
Z-Position (cm)	Layer	Normal Stresses					
		Sxx (kPa)	Syy (kPa)	Szz (kPa)	Syz (kPa)	Sxz (kPa)	Sxy (kPa)
9.999	1	-7.75	-26.67	-2.57	-14.55	.00	.00
20.000	2	9.34	-13.54	-6.92	-14.07	.00	.00
30.001	3	-2.80	-10.08	-9.45	-6.87	.00	.00
.001	1	-60.84	32.73	.00	.00	.00	.00
Z-Position (cm)	Layer	Normal Strains and Deflections					
		Exx (10^-6)	Eyy (10^-6)	Ezz (10^-6)	Ux (microns)	Uy (microns)	Uz (microns)
9.999	1	3.61	-33.43	13.73	.00	2.20	517.79
20.000	2	84.65	-70.06	-25.33	.00	51.64	517.20
30.001	3	171.15	-130.50	-104.46	.00	104.40	513.27
.001	1	-104.78	78.30	14.26	.00	-63.92	516.30
Z-Position (cm)	Layer	Principal Stresses and Strains					
		S1 (kPa)	S2 (kPa)	S3 (kPa)	E1 (10^-6)	E2 (10^-6)	E3 (10^-6)
9.999	1	-33.52	-7.75	4.27	-46.81	3.61	27.12
20.000	2	-24.68	4.23	9.34	-145.46	50.07	84.65
30.001	3	-16.65	-2.89	-2.80	-402.49	167.54	171.15
.001	1	-60.84	.00	32.73	-104.78	14.26	78.30
Location No: 4		X-Position (cm): .000			Y-Position (cm): 91.500		
Z-Position (cm)	Layer	Normal Stresses					
		Sxx (kPa)	Syy (kPa)	Szz (kPa)	Syz (kPa)	Sxz (kPa)	Sxy (kPa)
9.999	1	-5.25	-7.38	-.84	-3.13	.00	.00
20.000	2	1.99	-11.14	-2.29	-3.64	.00	.00
30.001	3	-1.42	5.70	-3.23	-3.05	.00	.00
.001	1	-20.78	32.95	.00	.00	.00	.00
Z-Position (cm)	Layer	Normal Strains and Deflections					
		Exx (10^-6)	Eyy (10^-6)	Ezz (10^-6)	Ux (microns)	Uy (microns)	Uz (microns)
9.999	1	-3.45	-7.60	5.19	.00	-3.15	354.25
20.000	2	35.54	-53.23	6.64	.00	32.52	354.85
30.001	3	74.25	-103.04	-.74	.00	67.94	355.72
.001	1	-46.83	58.30	-6.17	.00	-42.85	354.27
Z-Position (cm)	Layer	Principal Stresses and Strains					
		S1 (kPa)	S2 (kPa)	S3 (kPa)	E1 (10^-6)	E2 (10^-6)	E3 (10^-6)
9.999	1	-8.63	-5.25	.42	-10.06	-3.45	7.65
20.000	2	-12.44	.98	1.99	-62.06	15.47	35.54
30.001	3	-7.75	-1.42	-1.17	-188.24	74.25	84.46
.001	1	-20.78	.00	32.95	-46.83	-6.17	58.30

**Figure A-2 Sample EVERSTRS Output Sheet, page 2**

**Table A-1 Data Output from EVERSTRS**

Case No.	Do (μm)	D1 (μm)	D2 (μm)	D3 (μm)	A (mm)	Strain Subgrade top (10-6)	H. Strain AC bottom (10-6)
1	1589.13	875.9	527.88	348.66	455.09	2576.61	360.66
2	1302.61	803.22	516.3	354.27	502.60	1764.99	591.69
3	961.25	661.62	477.74	353.15	569.67	942.49	400.24
4	674.14	463.52	379.63	313.3	604.44	393.84	160.37
5	1499.90	854.50	522.61	349.67	467.78	2394.77	471.07
6	1165.17	778.10	510.11	354.68	535.78	1519.22	522.98
7	799.12	611.82	461.53	350.2	628.58	733.26	303.46
8	512.18	400.41	343.89	293.88	682.78	279.26	113.29
9	1408.41	838.84	518.03	349.96	483.91	2189.20	485.38
10	1037.40	748.18	504.83	355.68	572.80	1258.73	409.25
11	667.21	552.20	437.64	343.61	683.07	541.52	207.72
12	397.60	338.50	302.41	267.4	746.22	187.01	72.53
13	1307.67	826.50	515.24	350.43	505.98	1942.84	427.18
14	911.64	706.32	497.48	357.4	614.63	993.75	291.18
15	553.08	484.42	403.38	329.81	732.54	379.09	131.69
16	311.56	280.51	258.56	235.64	795.04	119.48	43.41
17	1194.72	810.49	514.34	351.87	535.28	1654.59	335.04
18	786.87	648.90	482.64	357.82	660.01	744.02	192.44
19	453.36	413.54	359.99	306.82	775.59	252.89	78.97
20	245.14	228.93	216.09	201.85	831.21	73.76	24.86
21	1104.64	479.38	259.87	167.68	379.51	1866.10	408.53
22	906.84	458.03	260.61	171.09	422.70	1289.17	587.44
23	675.37	395.4	255.06	176.24	485.73	696.44	380.95
24	493.57	288.08	217.54	168.78	516.76	296.10	146.549
25	1041.85	474.05	259.02	168.22	391.47	1745.03	479.68

**Table A-1 Data Output from EVERSTRS, Cont.**

Case No.	Do (μm)	D1 (μm)	D2 (μm)	D3 (μm)	A (mm)	Strain Subgrade top (10-6)	H. Strain AC bottom (10-6)
26	797.47	451.25	260.53	171.9	457.30	1112.70	502.18
27	543.03	369.51	251.84	177.89	551.09	544.08	283.17
28	357.66	248.99	200.87	162.63	605.07	212.49	102.92
29	972.94	471.58	258.27	168.49	407.44	1598.27	472.03
30	697.39	440.02	261.66	173.32	496.95	921.73	384.48
31	441.87	335.98	244.31	178.79	614.35	403.52	191.55
32	268.16	210.83	179.68	151.94	682.62	144.08	65.91
33	893.44	470.98	258.36	168.8	430.01	1416.57	404.87
34	601.96	420.08	262.94	175.99	542.80	727.43	269.41
35	359.51	296.49	230.32	176.67	673.93	284.45	120.72
36	205.18	175.09	155.88	137.14	745.93	93.26	39.6
37	804.04	468.12	260.09	169.62	460.60	1203.06	311.98
38	511.36	389.44	261.26	179.6	593.78	545.75	176.25
39	291.04	254.49	209.89	169.47	727.48	191.68	72.3
40	158.93	143.22	131.83	119.88	794.85	58.31	22.8
41	801.3	253.06	125.27	81.32	311.78	1239.62	447.87
42	658.84	255.42	127.04	82.23	348.36	865.12	583.69
43	497.16	235.22	131.29	85.37	403.27	474.41	365.21
44	381.3	180.63	122.07	87.86	429.49	205.72	135.12
45	752.01	253.82	125.14	81.36	322.49	1165.35	484.84
46	566.24	257.24	128.02	82.4	381.96	749.63	483.07
47	383.6	222.81	133.06	87.26	469.83	373.25	265.47
48	261.57	155.86	115.44	87.31	519.41	149.99	93.78
49	696.08	256.77	125.02	81.33	337.38	1069.39	457.86
50	484.11	255.84	130.34	82.91	421.64	622.06	361.7

**Table A-1 Data Output from EVERSTRS, Cont.**

Case No.	Do (μm)	D1 (μm)	D2 (μm)	D3 (μm)	A (mm)	Strain Subgrade top (10-6)	H. Strain AC bottom (10-6)
51	301.99	204.54	132.82	89.7	538.17	278.77	177.1
52	187.63	131.99	105.45	84.17	606.48	103.31	59.88
53	630.38	261.49	125.27	81.28	359.06	947.52	383.09
54	408.75	248.23	133.89	84.35	468.79	491.98	249.46
55	239.58	181.79	128.8	91.44	605.71	198.36	110.77
56	138.9	109.74	93.12	78.21	683.36	67.99	36.04
57	557.3	265.31	126.68	81.35	389.03	803.99	290.09
58	340.41	233.08	136.94	87.16	522.73	370.83	161.48
59	190.44	156.94	120.42	90.83	669.00	135.35	66.16
60	105.11	89.88	79.88	70.08	746.28	43.23	20.84
61	618.17	129.21	59.79	39.87	255.42	751.72	477.39
62	508.4	141.02	60.17	39.8	284.95	529.61	581.42
63	388.98	141.88	65.35	40.56	330.67	294.79	354.14
64	313.01	116.48	67.71	44.39	353.37	130.27	126.78
65	574.91	131.6	59.66	39.82	264.36	709.22	487.87
66	425	146.17	60.76	39.67	315.03	460.60	467.92
67	286.48	136.39	68.37	41.66	392.42	233.80	251.72
68	202.85	99.74	65.83	45.67	435.50	96.60	86.52
69	525.83	136.16	59.44	39.75	277.30	651.64	445.59
70	353.73	149.32	62.54	39.58	352.01	383.16	343.18
71	216.77	126.51	70.74	43.63	460.43	176.03	165.37
72	138.25	84.14	61.6	45.65	524.04	67.67	54.82
73	468.5	142.78	59.28	39.64	296.75	577.35	364.81
74	290.96	148.06	65.85	39.91	397.39	304.04	233.06
75	166.5	113.21	71.03	45.93	531.72	126.53	102.46

**Table A-1 Data Output from EVERSTRS, Cont.**

Case No.	Do (μm)	D1 (μm)	D2 (μm)	D3 (μm)	A (mm)	Strain Subgrade top (10-6)	H. Strain AC bottom (10-6)
76	98.12	69.8	55.49	43.86	609.72	45.34	32.93
77	405.97	149.48	59.78	39.44	324.32	489.95	271.88
78	236.48	141.29	69.81	41.29	451.10	230.50	149.21
79	129.02	98.2	68.49	47.73	602.57	87.48	60.9
80	71.86	57.09	48.38	40.44	685.52	29.38	19.08
81	1748.75	920.5	531.73	343.7	435.47	3115.38	-178.28
82	1669.6	896.58	530.03	346.47	444.47	2836.18	141.74
83	1693.88	897.84	528.31	345.78	440.13	2989.49	31.68
84	1598.94	874.03	525.39	347.95	452.33	2684.78	316.38
85	1643.31	877.46	523.76	346.76	444.46	2872.60	195.37
86	1527.39	856.52	520.62	348.41	461.98	2522.43	408.63
87	1591.29	862.57	519.58	346.89	450.36	2745.93	294.28
88	1446.9	845.23	517.11	348.5	476.09	2325.13	416.23
89	1528.74	853.85	516.74	346.82	460.24	2582.61	324.75
90	1351.85	837.05	515.43	348.99	496.69	2076.35	363.85
91	1202.4	492.55	258.88	165.69	363.88	2234.75	-51.34
92	1156.5	485.3	259.47	166.74	370.66	2046.30	220.54
93	1174.29	485.58	258.57	166.44	367.15	2163.91	100.23
94	1112.39	478.69	258.77	167.37	377.40	1951.88	347.03
95	1146.63	479.12	257.71	166.87	370.44	2092.00	221.90
96	1062.89	474.3	257.83	167.65	386.39	1840.68	408.84
97	1112.43	474.8	256.73	166.98	375.71	2005.19	295.14
98	1001.11	473.28	257.19	167.76	400.34	1696.95	400.70
99	1064.46	473.75	256.09	166.96	385.29	1885.43	312.35
100	924.73	474.5	257.43	167.99	421.34	1511.81	342.67

**Table A-1 Data Output from EVERSTRS, Cont.**

Case No.	Do (μm)	D1 (μm)	D2 (μm)	D3 (μm)	A (mm)	Strain Subgrade top (10-6)	H. Strain AC bottom (10-6)
101	863.02	253.68	124.6	80.91	300.29	1470.95	53.84
102	836.13	252.9	124.94	81.12	304.92	1354.16	285.67
103	847.08	252.24	124.59	81.02	302.57	1434.70	156.59
104	804.76	252.12	124.84	81.19	310.55	1299.79	371.01
105	830.39	250.96	124.41	81.04	305.06	1393.65	242.31
106	766.91	252.8	124.63	81.17	318.54	1229.49	406.28
107	805.58	250.72	124.14	80.98	309.55	1338.54	293.28
108	716.43	255.98	124.45	81.09	331.50	1133.86	384.48
109	766.46	252.69	123.92	80.86	318.25	1258.33	299.04
110	652.74	261.41	124.59	81.02	351.56	1008.87	321.93
111	660.02	125.87	59.87	39.9	247.39	885.45	131.99
112	643.39	127.05	59.83	39.88	250.38	818.59	334.29
113	648.6	125.83	59.81	39.88	249.01	867.80	198.48
114	617.2	127.76	59.74	39.85	254.84	788.99	388.35
115	636.36	125.93	59.72	39.84	250.86	845.42	256.82
116	584.85	129.81	59.6	39.79	261.48	747.68	402.98
117	615.98	126.81	59.59	39.77	254.47	812.79	290.51
118	540.72	134.22	59.36	39.71	272.71	689.54	370.45
119	581.91	129.59	59.42	39.69	261.80	763.75	287.35
120	485.1	141.08	59.09	39.61	290.62	613.07	304.48

**Table A-2 EVERPAVE Output**

Case No.	Do (µm)	A (mm)	E SG MPa	ESALS (millions)	Overlay (cm)	Fatigue Damage New AC	Fatigue Damage Old AC	Rutting Damage
1	1589	455	35	1	34.00	0.536	0.275	0.910
2	1303	503	35	1	31.00	0.527	0.289	0.970
3	961	570	35	1	25.00	0.698	0.266	0.951
4	674	604	35	1	20.00	0.921	0.081	0.211
5	1500	468	35	1	33.00	0.372	0.478	0.911
6	1165	536	35	1	29.00	0.271	0.505	0.961
7	799	629	35	1	21.00	0.264	0.480	0.932
8	512	683	35	1	4.00	0.000	0.459	0.930
9	1408	484	35	1	31.00	0.205	0.710	0.976
10	1037	573	35	1	26.00	0.079	0.705	0.968
11	667	683	35	1	16.00	0.025	0.700	0.958
13	1308	506	35	1	29.00	0.063	0.756	0.914
14	912	615	35	1	23.00	0.005	0.753	0.904
15	553	733	35	1	11.00	0.000	0.848	0.988
17	1195	535	35	1	26.50	0.008	0.700	0.911
18	787	660	35	1	20.00	0.000	0.727	0.895
19	453	776	35	1	5.00	0.000	0.970	0.946
21	1105	380	70	1	28.50	0.981	0.506	0.869
22	907	423	70	1	26.00	0.930	0.465	0.802
23	675	486	70	1	22.50	0.941	0.269	0.453
24	494	517	70	1	4.50	0.708	0.509	0.979
25	1042	391	70	1	27.00	0.689	0.971	0.995
26	797	457	70	1	23.50	0.470	0.910	0.916
27	543	551	70	1	15.00	0.506	0.922	0.973
29	973	407	70	1	27.50	0.240	0.933	0.630
30	697	497	70	1	22.50	0.090	0.927	0.625
31	442	614	70	1	12.50	0.020	0.920	0.617
33	893	430	70	1	26.00	0.061	0.929	0.555
34	602	543	70	1	20.00	0.004	0.941	0.555
35	360	674	70	1	8.50	0.000	0.952	0.512

**Table A-2 EVERPAVE Output, Cont.**

Case No.	Do (μm)	A (mm)	E SG MPa	ESALS (millions)	Overlay (cm)	Fatigue Damage New AC	Fatigue Damage Old AC	Rutting Damage
37	804	461	70	1	23.00	0.005	0.964	0.682
38	511	594	70	1	17.00	0.000	0.945	0.581
39	291	727	70	1	3.00	0.000	0.967	0.397
41	801	312	140	1	27.00	0.989	0.497	0.249
42	659	348	140	1	24.50	0.991	0.443	0.226
43	497	403	140	1	22.00	0.937	0.205	0.103
45	752	322	140	1	25.50	0.680	0.960	0.290
46	566	382	140	1	21.50	0.530	0.970	0.297
47	384	470	140	1	13.00	0.601	0.987	0.319
49	696	337	140	1	25.50	0.239	0.991	0.215
50	484	422	140	1	20.50	0.092	0.985	0.208
51	302	538	140	1	10.50	0.015	0.976	0.205
53	630	359	140	1	24.00	0.055	0.988	0.193
54	409	469	140	1	18.50	0.003	0.927	0.171
55	240	606	140	1	7.00	0.000	0.915	0.150
57	557	389	140	1	21.50	0.003	0.962	0.221
58	340	523	140	1	15.50	0.000	0.945	0.181
59	190	669	140	1	1.00	0.000	0.950	0.115
61	618	255	280	1	26.00	0.959	0.470	0.042
62	508	285	280	1	24.00	0.924	0.375	0.034
63	389	331	280	1	21.50	0.954	0.167	0.015
65	575	264	280	1	24.50	0.649	0.907	0.050
66	425	315	280	1	20.50	0.541	0.909	0.051
67	286	392	280	1	12.00	0.666	0.934	0.055
69	526	277	280	1	24.50	0.219	0.921	0.037
70	354	352	280	1	19.50	0.092	0.915	0.036
71	217	460	280	1	9.00	0.010	0.998	0.040
73	469	297	280	1	23.00	0.047	0.916	0.035
74	291	397	280	1	17.00	0.003	0.950	0.034
75	167	532	280	1	5.50	0.000	0.911	0.029

**Table A-2 EVERPAVE Output, Cont.**

Case No.	Do ( $\mu\text{m}$ )	A (mm)	E SG MPa	ESALS (millions)	Overlay (cm)	Fatigue Damage New AC	Fatigue Damage Old AC	Rutting Damage
77	406	324	280	1	20.50	0.003	0.906	0.041
78	236	451	280	1	14.00	0.000	0.971	0.037
81	1749	435	35	1	35.00	0.610	0.267	0.955
82	1670	444	35	1	34.50	0.569	0.274	0.934
83	1694	440	35	1	34.50	0.505	0.468	0.960
84	1599	452	35	1	33.50	0.446	0.497	0.988
85	1643	444	35	1	33.50	0.369	0.715	0.982
86	1527	462	35	1	32.50	0.264	0.685	0.928
87	1591	450	35	1	32.00	0.209	0.900	0.993
88	1447	476	35	1	30.50	0.114	0.809	0.942
89	1529	460	35	1	30.00	0.078	0.894	0.999
90	1352	497	35	1	28.00	0.026	0.774	0.985
91	1202	364	70	1	30.50	0.943	0.421	0.748
92	1157	371	70	1	29.50	0.957	0.468	0.807
93	1174	367	70	1	29.00	0.895	0.886	0.957
94	1112	377	70	1	28.00	0.779	0.939	0.978
95	1147	370	70	1	30.00	0.452	0.939	0.633
96	1063	386	70	1	28.50	0.337	0.977	0.668
97	1112	376	70	1	29.50	0.210	0.986	0.529
98	1001	400	70	1	27.50	0.116	0.972	0.568
99	1064	385	70	1	27.50	0.073	0.977	0.561
100	925	421	70	1	25.00	0.022	0.950	0.642
101	863	300	140	1	29.00	0.929	0.415	0.218
102	836	305	140	1	28.00	0.953	0.461	0.233
103	847	303	140	1	27.00	0.956	0.970	0.316
104	805	311	140	1	26.50	0.763	0.931	0.286
105	830	305	140	1	28.00	0.460	0.998	0.211
106	767	319	140	1	27.00	0.315	0.949	0.199
107	806	310	140	1	28.00	0.189	0.940	0.161
108	716	332	140	1	26.00	0.102	0.937	0.174

**Table A-2 EVERPAVE Output, Cont.**

Case No.	Do ( $\mu\text{m}$ )	A (mm)	E SG MPa	ESALS (millions)	Overlay (cm)	Fatigue Damage New AC	Fatigue Damage Old AC	Rutting Damage
109	766	318	140	1	26.00	0.062	0.929	0.178
110	653	352	140	1	23.50	0.017	0.929	0.207
111	660	247	280	1	27.50	0.964	0.433	0.042
112	643	250	280	1	27.00	0.911	0.437	0.040
113	649	249	280	1	26.00	0.902	0.923	0.055
114	617	255	280	1	25.00	0.789	0.975	0.055
115	636	251	280	1	27.00	0.420	0.927	0.037
116	585	261	280	1	25.50	0.310	0.969	0.039
117	616	254	280	1	26.50	0.178	0.938	0.032
118	541	273	280	1	24.50	0.094	0.944	0.035
119	582	262	280	1	24.50	0.055	0.924	0.037
120	485	291	280	1	22.00	0.014	0.949	0.043
1	1589	455	35	5	42.00	0.877	0.429	0.992
2	1303	503	35	5	39.50	0.807	0.433	0.988
3	961	570	35	5	34.00	0.928	0.393	0.942
4	674	604	35	5	29.50	0.972	0.140	0.258
5	1500	468	35	5	41.00	0.646	0.744	0.988
6	1165	536	35	5	37.50	0.463	0.750	0.970
7	799	629	35	5	29.50	0.440	0.737	0.987
8	512	683	35	5	18.50	0.993	0.352	0.387
9	1408	484	35	5	40.00	0.350	0.969	0.852
10	1037	573	35	5	35.00	0.160	0.962	0.845
11	667	683	35	5	25.00	0.078	0.956	0.836
12	398	746	35	5	5.00	0.000	0.945	0.820
13	1308	506	35	5	38.50	0.127	0.985	0.684
14	912	615	35	5	32.00	0.022	0.981	0.705
15	553	733	35	5	21.00	0.001	0.943	0.622
17	1195	535	35	5	35.00	0.027	0.985	0.722
18	787	660	35	5	28.50	0.000	0.931	0.659
19	453	776	35	5	16.00	0.000	0.963	0.544

**Table A-2 EVERPAVE Output, Cont.**

Case No.	Do (µm)	A (mm)	E sg MPa	ESALS (millions)	Overlay (cm)	Fatigue Damage New AC	Fatigue Damage Old AC	Rutting Damage
21	1105	380	70	5	39.00	0.971	0.466	0.518
22	907	423	70	5	36.00	0.993	0.485	0.548
23	675	486	70	5	32.50	0.967	0.318	0.360
24	494	517	70	5	29.50	0.930	0.090	0.080
25	1042	391	70	5	37.00	0.794	0.946	0.628
26	797	457	70	5	33.00	0.623	0.995	0.663
27	543	551	70	5	25.00	0.718	0.949	0.666
28	358	605	70	5	19.00	0.982	0.232	0.118
29	973	407	70	5	37.50	0.338	0.988	0.422
30	697	497	70	5	32.50	0.157	0.981	0.418
31	442	614	70	5	22.50	0.098	0.975	0.414
32	268	683	70	5	2.50	0.000	0.961	0.403
33	893	430	70	5	36.50	0.109	0.937	0.321
34	602	543	70	5	30.00	0.018	0.961	0.335
35	360	674	70	5	18.50	0.001	0.988	0.315
37	804	461	70	5	33.00	0.020	0.963	0.359
38	511	594	70	5	26.50	0.000	0.949	0.327
39	291	727	70	5	14.00	0.000	0.940	0.244
41	801	312	140	5	37.00	0.967	0.453	0.162
42	659	348	140	5	34.50	0.964	0.424	0.153
43	497	403	140	5	31.50	0.963	0.245	0.091
44	381	429	140	5	29.00	0.967	0.061	0.190
45	752	322	140	5	35.00	0.778	0.931	0.200
46	566	382	140	5	31.00	0.664	0.963	0.209
47	384	470	140	5	22.50	0.960	0.975	0.230
48	262	519	140	5	5.50	0.286	0.970	0.238
49	696	337	140	5	35.50	0.314	0.957	0.137
50	484	422	140	5	30.50	0.153	0.955	0.146
51	302	538	140	5	20.50	0.123	0.944	0.135
52	188	606	140	5	0.50	0.000	0.975	0.157

**Table A-2 EVERPAVE Output, Cont.**

Case No.	Do ( $\mu\text{m}$ )	A (mm)	E sg MPa	ESALS (millions)	Overlay (cm)	Fatigue Damage New AC	Fatigue Damage Old AC	Rutting Damage
53	630	359	140	5	34.00	0.100	0.971	0.119
54	409	469	140	5	28.00	0.016	0.952	0.114
55	240	606	140	5	16.50	0.002	0.972	0.104
57	557	389	140	5	31.00	0.016	0.955	0.129
58	340	523	140	5	24.50	0.000	0.973	0.116
59	190	669	140	5	11.50	0.000	0.984	0.086
61	618	255	280	5	35.50	0.942	0.431	0.031
62	508	285	280	5	33.00	0.985	0.395	0.028
63	389	331	280	5	30.50	0.996	0.201	0.015
64	313	353	280	5	29.00	0.935	0.041	0.003
65	575	264	280	5	33.00	0.808	0.968	0.042
66	425	315	280	5	29.00	0.711	0.988	0.043
67	286	392	280	5	22.00	0.995	0.782	0.036
68	203	435	280	5	3.50	0.000	0.996	0.050
69	526	277	280	5	33.50	0.309	0.972	0.029
70	354	352	280	5	28.50	0.160	0.966	0.029
71	217	460	280	5	18.50	0.160	0.959	0.029
73	469	297	280	5	32.00	0.092	0.982	0.027
74	291	397	280	5	26.00	0.015	0.982	0.026
75	167	532	280	5	14.50	0.002	0.989	0.023
77	406	324	280	5	29.00	0.012	0.988	0.030
78	236	451	280	5	23.00	0.000	0.948	0.024
79	129	603	280	5	9.50	0.000	0.981	0.018
81	1749	435	35	5	43.50	0.916	0.382	0.932
82	1670	444	35	5	43.00	0.865	0.396	0.922
83	1694	440	35	5	43.00	0.783	0.672	0.933
84	1599	452	35	5	42.00	0.708	0.713	0.962
85	1643	444	35	5	42.50	0.566	0.976	0.857
86	1527	462	35	5	41.50	0.429	0.941	0.817
87	1591	450	35	5	43.00	0.280	0.979	0.584

**Table A-2 EVERPAVE Output, Cont.**

Case No.	Do (μm)	A (mm)	E sg MPa	ESALS (millions)	Overlay (cm)	Fatigue Damage New AC	Fatigue Damage Old AC	Rutting Damage
88	1447	476	35	5	40.50	0.192	0.991	0.653
89	1529	460	35	5	41.00	0.125	0.998	0.534
90	1352	497	35	5	37.50	0.062	0.992	0.660
91	1202	364	70	5	41.00	0.936	0.392	0.452
92	1157	371	70	5	40.00	0.950	0.432	0.484
93	1174	367	70	5	39.00	0.970	0.859	0.599
94	1112	377	70	5	37.50	0.934	0.980	0.675
95	1147	370	70	5	40.00	0.557	0.995	0.424
96	1063	386	70	5	39.00	0.417	0.957	0.404
97	1112	376	70	5	40.50	0.264	0.974	0.294
98	1001	400	70	5	38.00	0.177	0.998	0.333
99	1064	385	70	5	38.50	0.122	0.986	0.280
100	925	421	70	5	35.50	0.050	0.946	0.324
101	863	300	140	5	38.50	0.985	0.413	0.158
102	836	305	140	5	38.00	0.936	0.422	0.153
103	847	303	140	5	37.00	0.945	0.850	0.193
104	805	311	140	5	35.50	0.915	0.973	0.216
105	830	305	140	5	38.00	0.524	0.963	0.138
106	767	319	140	5	36.50	0.414	0.996	0.144
107	806	310	140	5	38.00	0.252	0.987	0.107
108	716	332	140	5	36.00	0.157	0.955	0.112
109	766	318	140	5	36.00	0.102	0.991	0.107
110	653	352	140	5	33.00	0.043	0.982	0.126
111	660	247	280	5	37.00	0.941	0.395	0.030
112	643	250	280	5	36.00	0.974	0.436	0.032
113	649	249	280	5	35.00	0.972	0.887	0.041
114	617	255	280	5	34.00	0.878	0.938	0.042
115	636	251	280	5	36.00	0.518	0.979	0.030
116	585	261	280	5	35.00	0.381	0.937	0.028
117	616	254	280	5	36.00	0.239	0.978	0.023
118	541	273	280	5	34.00	0.146	0.955	0.025
119	582	262	280	5	34.00	0.091	0.975	0.024
120	485	291	280	5	31.00	0.037	0.995	0.029

**Table A-2 EVERPAVE Output, Cont.**

Case No.	Do ( $\mu\text{m}$ )	A (mm)	E sg MPa	ESALS (millions)	Overlay (cm)	Fatigue Damage New AC	Fatigue Damage Old AC	Rutting Damage
1	1589	455	35	10	47.00	0.943	0.450	0.857
2	1303	503	35	10	44.00	0.924	0.491	0.937
3	961	570	35	10	39.00	0.966	0.433	0.849
4	674	604	35	10	34.50	0.941	0.170	0.263
5	1500	468	35	10	45.50	0.756	0.832	0.923
6	1165	536	35	10	41.50	0.583	0.902	0.994
7	799	629	35	10	34.00	0.506	0.848	0.949
8	512	683	35	10	23.50	0.946	0.408	0.377
9	1408	484	35	10	45.50	0.387	0.971	0.677
10	1037	573	35	10	40.50	0.188	0.964	0.671
11	667	683	35	10	30.50	0.093	0.958	0.664
12	398	746	35	10	10.50	0.139	0.948	0.653
13	1308	506	35	10	44.50	0.146	0.945	0.494
14	912	615	35	10	37.50	0.033	0.966	0.536
15	553	733	35	10	26.00	0.003	0.979	0.510
17	1195	535	35	10	40.50	0.038	0.976	0.525
18	787	660	35	10	33.00	0.001	0.995	0.553
19	453	776	35	10	21.00	0.000	0.977	0.433
21	1105	380	70	10	44.00	0.999	0.469	0.438
22	907	423	70	10	41.50	0.950	0.464	0.430
23	675	486	70	10	37.50	0.963	0.342	0.324
24	494	517	70	10	34.00	0.944	0.113	0.088
25	1042	391	70	10	42.00	0.834	0.938	0.521
26	797	457	70	10	38.00	0.662	0.997	0.553
27	543	551	70	10	30.00	0.724	0.967	0.565
28	358	605	70	10	23.50	0.979	0.281	0.125
29	973	407	70	10	43.00	0.362	0.951	0.329
30	697	497	70	10	38.00	0.179	0.945	0.327
31	442	614	70	10	28.00	0.110	0.939	0.323
32	268	683	70	10	7.50	0.029	0.988	0.345
33	893	430	70	10	41.50	0.135	0.980	0.270
34	602	543	70	10	35.00	0.028	0.974	0.275
35	360	674	70	10	23.50	0.003	0.995	0.256

**Table A-2 EVERPAVE Output, Cont.**

Case No.	D <sub>0</sub> (μm)	A (mm)	E <sub>SG</sub> (MPa)	ESALS (millions)	Overlay (cm)	Fatigue Damage New AC	Fatigue Damage Old AC	Rutting Damage
37	804	461	70	10	38.00	0.030	0.979	0.281
38	511	594	70	10	31.00	0.000	0.984	0.274
39	291	727	70	10	19.00	0.000	0.942	0.198
41	801	312	140	10	42.00	0.956	0.439	0.137
42	659	348	140	10	39.50	0.946	0.420	0.131
43	497	403	140	10	36.00	0.989	0.273	0.088
44	381	429	140	10	33.50	0.955	0.074	0.021
45	752	322	140	10	39.50	0.840	0.954	0.180
46	566	382	140	10	35.50	0.699	0.996	0.188
47	384	470	140	10	27.50	0.918	0.944	0.192
48	262	519	140	10	24.00	0.933	0.181	0.028
49	696	337	140	10	40.50	0.344	0.947	0.116
50	484	422	140	10	35.50	0.176	0.941	0.115
51	302	538	140	10	25.00	0.149	1.000	0.124
52	188	606	140	10	5.00	0.000	0.987	0.121
53	630	359	140	10	39.00	0.121	0.972	0.099
54	409	469	140	10	32.50	0.025	0.996	0.102
55	240	606	140	10	21.50	0.005	0.952	0.085
57	557	389	140	10	35.50	0.024	0.997	0.110
58	340	523	140	10	29.00	0.000	0.978	0.098
59	190	669	140	10	16.50	0.000	0.967	0.071
61	618	255	280	10	40.00	0.963	0.433	0.028
62	508	285	280	10	37.50	0.997	0.404	0.026
63	389	331	280	10	35.00	0.988	0.217	0.015
64	313	353	280	10	33.00	0.981	0.052	0.003
65	575	264	280	10	37.50	0.839	0.952	0.038
66	425	315	280	10	33.50	0.737	0.981	0.039
67	286	392	280	10	26.50	0.988	0.792	0.033
68	203	435	280	10	24.00	0.962	0.126	0.004
69	526	277	280	10	38.00	0.347	0.990	0.027

**Table A-2 EVERPAVE Output, Cont.**

Case No.	D <sub>0</sub> (μm)	A (mm)	E <sub>SG</sub> (MPa)	ESALS (millions)	Overlay (cm)	Fatigue Damage New AC	Fatigue Damage Old AC	Rutting Damage
70	354	352	280	10	33.00	0.186	0.984	0.027
71	217	460	280	10	23.00	0.193	0.978	0.026
73	469	297	280	10	37.00	0.108	0.942	0.022
74	291	397	280	10	30.50	0.023	0.989	0.023
75	167	532	280	10	19.50	0.007	0.938	0.019
77	406	324	280	10	33.50	0.020	0.988	0.026
78	236	451	280	10	27.00	0.000	1.000	0.023
79	129	603	280	10	14.50	0.000	0.946	0.015
81	1749	435	35	10	48.50	0.980	0.401	0.804
82	1670	444	35	10	47.50	0.989	0.443	0.866
83	1694	440	35	10	47.00	0.958	0.798	0.944
84	1599	452	35	10	46.00	0.873	0.848	0.974
85	1643	444	35	10	48.00	0.598	0.978	0.680
86	1527	462	35	10	47.00	0.465	0.946	0.652
87	1591	450	35	10	49.00	0.298	0.964	0.436
88	1447	476	35	10	46.50	0.212	0.962	0.478
89	1529	460	35	10	47.50	0.135	0.948	0.357
90	1352	497	35	10	43.50	0.076	0.958	0.455
91	1202	364	70	10	46.00	0.966	0.396	0.385
92	1157	371	70	10	45.00	0.979	0.436	0.411
93	1174	367	70	10	44.00	1.000	0.851	0.496
94	1112	377	70	10	42.50	0.967	0.965	0.554
95	1147	370	70	10	45.50	0.569	0.958	0.331
96	1063	386	70	10	44.00	0.463	0.985	0.344
97	1112	376	70	10	46.00	0.287	0.978	0.234
98	1001	400	70	10	43.50	0.200	0.987	0.259
99	1064	385	70	10	44.50	0.124	0.948	0.198
100	925	421	70	10	40.50	0.067	0.991	0.261
101	863	300	140	10	43.50	0.972	0.399	0.133
102	836	305	140	10	42.50	0.993	0.438	0.140

**Table A-2 EVERPAVE Output, Cont.**

Case No.	D <sub>0</sub> (μm)	A (mm)	E <sub>SG</sub> (MPa)	ESALS (millions)	Overlay (cm)	Fatigue Damage New AC	Fatigue Damage Old AC	Rutting Damage
103	847	303	140	10	42.00	0.939	0.810	0.159
104	805	311	140	10	40.00	0.976	0.988	0.192
105	830	305	140	10	43.00	0.549	0.953	0.117
106	767	319	140	10	41.50	0.443	0.982	0.121
107	806	310	140	10	43.50	0.265	0.948	0.084
108	716	332	140	10	41.00	0.182	0.968	0.094
109	766	318	140	10	41.50	0.115	0.966	0.081
110	653	352	140	10	38.00	0.056	0.983	0.100
111	660	247	280	10	41.50	0.963	0.396	0.028
112	643	250	280	10	40.50	0.993	0.435	0.029
113	649	249	280	10	39.50	0.993	0.871	0.037
114	617	255	280	10	38.00	0.972	0.993	0.040
115	636	251	280	10	40.50	0.558	0.997	0.027
116	585	261	280	10	39.50	0.421	0.958	0.026
117	616	254	280	10	41.00	0.257	0.962	0.020
118	541	273	280	10	38.50	0.174	0.995	0.023
119	582	262	280	10	39.00	0.106	0.970	0.020
120	485	291	280	10	36.00	0.048	0.951	0.023

**Table A-3 Comparison of Overlay Required: EVERPAVE vs Equation**

Case No.	Do (microns)	A (mm)	E <sub>SG</sub> MPa	ESALS (millions)	Overlay EVERPAVE (cm)	Overlay equation (cm)	Percent Difference	Absolute Difference (cm)
1	1589	455	35	1	34.00	33.65	1%	0.35
2	1303	503	35	1	31.00	29.87	4%	1.13
3	961	570	35	1	25.00	23.15	7%	1.85
4	674	604	35	1	20.00	12.19	39%	7.81
5	1500	468	35	1	33.00	32.50	2%	0.50
6	1165	536	35	1	29.00	28.05	3%	0.95
7	799	629	35	1	21.00	19.86	5%	1.14
8	512	683	35	1	4.00	6.42	60%	2.42
9	1408	484	35	1	31.00	31.39	1%	0.39
10	1037	573	35	1	26.00	26.16	1%	0.16
11	667	683	35	1	16.00	16.18	1%	0.18
13	1308	506	35	1	29.00	30.25	4%	1.25
14	912	615	35	1	23.00	23.91	4%	0.91
15	553	733	35	1	11.00	11.77	7%	0.77
17	1195	535	35	1	26.50	28.94	9%	2.44
18	787	660	35	1	20.00	21.04	5%	1.04
19	453	776	35	1	5.00	6.48	30%	1.48
21	1105	380	70	1	28.50	30.09	6%	1.59
22	907	423	70	1	26.00	26.67	3%	0.67
23	675	486	70	1	22.50	20.78	8%	1.72
24	494	517	70	1	4.50	11.43	154%	6.93
25	1042	391	70	1	27.00	29.04	8%	2.04
26	797	457	70	1	23.50	24.74	5%	1.24
27	543	551	70	1	15.00	17.25	15%	2.25
29	973	407	70	1	27.50	27.95	2%	0.45
30	697	497	70	1	22.50	22.78	1%	0.28
31	442	614	70	1	12.50	13.54	8%	1.04
33	893	430	70	1	26.00	26.73	3%	0.73
34	602	543	70	1	20.00	20.51	3%	0.51
35	360	674	70	1	8.50	9.25	9%	0.75
37	804	461	70	1	23.00	25.31	10%	2.31
38	511	594	70	1	17.00	17.71	4%	0.71
39	291	727	70	1	3.00	4.19	40%	1.19

**Table A-3 Comparison of Overlay Required: EVERPAVE vs Equation, Cont.**

Case No.	Do (microns)	A (mm)	E <sub>SG</sub> MPa	ESALS (millions)	Overlay EVERPAVE (cm)	Overlay equation (cm)	Percent Difference	Absolute Difference (cm)
41	801	312	140	1	27.00	27.56	2%	0.56
42	659	348	140	1	24.50	24.31	1%	0.19
43	497	403	140	1	22.00	19.17	13%	2.83
45	752	322	140	1	25.50	26.43	4%	0.93
46	566	382	140	1	21.50	22.02	2%	0.52
47	384	470	140	1	13.00	15.07	16%	2.07
49	696	337	140	1	25.50	25.19	1%	0.31
50	484	422	140	1	20.50	19.78	4%	0.72
51	302	538	140	1	10.50	11.11	6%	0.61
53	630	359	140	1	24.00	23.77	1%	0.23
54	409	469	140	1	18.50	17.34	6%	1.16
55	240	606	140	1	7.00	6.81	3%	0.19
57	557	389	140	1	21.50	22.09	3%	0.59
58	340	523	140	1	15.50	14.49	7%	1.01
59	190	669	140	1	1.00	1.90	90%	0.90
61	618	255	280	1	26.00	27.20	5%	1.20
62	508	285	280	1	24.00	23.91	0%	0.09
63	389	331	280	1	21.50	19.36	10%	2.14
65	575	264	280	1	24.50	25.76	5%	1.26
66	425	315	280	1	20.50	20.90	2%	0.40
67	286	392	280	1	12.00	14.21	18%	2.21
69	526	277	280	1	24.50	24.18	1%	0.32
70	354	352	280	1	19.50	18.10	7%	1.40
71	217	460	280	1	9.00	9.65	7%	0.65
73	469	297	280	1	23.00	22.35	3%	0.65
74	291	397	280	1	17.00	15.24	10%	1.76
75	167	532	280	1	5.50	5.07	8%	0.43
77	406	324	280	1	20.50	20.25	1%	0.25
78	236	451	280	1	14.00	12.13	13%	1.87
81	1749	435	35	1	35.00	35.60	2%	0.60
82	1670	444	35	1	34.50	34.62	0%	0.12
83	1694	440	35	1	34.50	34.81	1%	0.31
84	1599	452	35	1	33.50	33.66	0%	0.16
85	1643	444	35	1	33.50	34.04	2%	0.54

**Table A-3 Comparison of Overlay Required: EVERPAVE vs Equation, Cont.**

Case No.	Do (microns)	A (mm)	E <sub>SG</sub> MPa	ESALS (millions)	Overlay EVERPAVE (cm)	Overlay equation (cm)	Percent Difference	Absolute Difference (cm)
86	1527	462	35	1	32.50	32.73	1%	0.23
87	1591	450	35	1	32.00	33.32	4%	1.32
88	1447	476	35	1	30.50	31.81	4%	1.31
89	1529	460	35	1	30.00	32.62	9%	2.62
90	1352	497	35	1	28.00	30.82	10%	2.82
91	1202	364	70	1	30.50	31.71	4%	1.21
92	1157	371	70	1	29.50	30.93	5%	1.43
93	1174	367	70	1	29.00	31.16	7%	2.16
94	1112	377	70	1	28.00	30.14	8%	2.14
95	1147	370	70	1	30.00	30.60	2%	0.60
96	1063	386	70	1	28.50	29.31	3%	0.81
97	1112	376	70	1	29.50	29.99	2%	0.49
98	1001	400	70	1	27.50	28.37	3%	0.87
99	1064	385	70	1	27.50	29.26	6%	1.76
100	925	421	70	1	25.00	27.27	9%	2.27
101	863	300	140	1	29.00	28.95	0%	0.05
102	836	305	140	1	28.00	28.33	1%	0.33
103	847	303	140	1	27.00	28.54	6%	1.54
104	805	311	140	1	26.50	27.58	4%	1.08
105	830	305	140	1	28.00	28.09	0%	0.09
106	767	319	140	1	27.00	26.71	1%	0.29
107	806	310	140	1	28.00	27.50	2%	0.50
108	716	332	140	1	26.00	25.63	1%	0.37
109	766	318	140	1	26.00	26.66	3%	0.66
110	653	352	140	1	23.50	24.30	3%	0.80
111	660	247	280	1	27.50	28.48	4%	0.98
112	643	250	280	1	27.00	27.96	4%	0.96
113	649	249	280	1	26.00	28.07	8%	2.07
114	617	255	280	1	25.00	27.06	8%	2.06
115	636	251	280	1	27.00	27.63	2%	0.63
116	585	261	280	1	25.50	26.00	2%	0.50
117	616	254	280	1	26.50	26.94	2%	0.44
118	541	273	280	1	24.50	24.61	0%	0.11
119	582	262	280	1	24.50	25.86	6%	1.36
120	485	291	280	1	22.00	22.89	4%	0.89

**Table A-3 Comparison of Overlay Required: EVERPAVE vs Equation, Cont.**

Case No.	Do (microns)	A (mm)	E <sub>SG</sub> MPa	ESALS (millions)	Overlay EVERPAVE (cm)	Overlay equation (cm)	Percent Difference	Absolute Difference (cm)
1	1589	455	35	5	42.00	43.57	4%	1.57
2	1303	503	35	5	39.50	39.80	1%	0.30
3	961	570	35	5	34.00	33.07	3%	0.93
4	674	604	35	5	29.50	22.11	25%	7.39
5	1500	468	35	5	41.00	42.43	3%	1.43
6	1165	536	35	5	37.50	37.97	1%	0.47
7	799	629	35	5	29.50	29.79	1%	0.29
8	512	683	35	5	18.50	16.34	12%	2.16
9	1408	484	35	5	40.00	41.32	3%	1.32
10	1037	573	35	5	35.00	36.08	3%	1.08
11	667	683	35	5	25.00	26.11	4%	1.11
12	398	746	35	5	5.00	10.19	104%	5.19
13	1308	506	35	5	38.50	40.18	4%	1.68
14	912	615	35	5	32.00	33.84	6%	1.84
15	553	733	35	5	21.00	21.69	3%	0.69
17	1195	535	35	5	35.00	38.86	11%	3.86
18	787	660	35	5	28.50	30.96	9%	2.46
19	453	776	35	5	16.00	16.41	3%	0.41
21	1105	380	70	5	39.00	40.01	3%	1.01
22	907	423	70	5	36.00	36.59	2%	0.59
23	675	486	70	5	32.50	30.70	6%	1.80
24	494	517	70	5	29.50	21.35	28%	8.15
25	1042	391	70	5	37.00	38.96	5%	1.96
26	797	457	70	5	33.00	34.67	5%	1.67
27	543	551	70	5	25.00	27.18	9%	2.18
28	358	605	70	5	19.00	15.12	20%	3.88
29	973	407	70	5	37.50	37.87	1%	0.37
30	697	497	70	5	32.50	32.70	1%	0.20
31	442	614	70	5	22.50	23.46	4%	0.96
32	268	683	70	5	2.50	8.82	253%	6.32
33	893	430	70	5	36.50	36.66	0%	0.16
34	602	543	70	5	30.00	30.43	1%	0.43
35	360	674	70	5	18.50	19.17	4%	0.67
37	804	461	70	5	33.00	35.23	7%	2.23
38	511	594	70	5	26.50	27.63	4%	1.13

**Table A-3 Comparison of Overlay Required: EVERPAVE vs Equation, Cont.**

Case No.	Do (microns)	A (mm)	E <sub>SG</sub> MPa	ESALS (millions)	Overlay EVERPAVE (cm)	Overlay equation (cm)	Percent Difference	Absolute Difference (cm)
39	291	727	70	5	14.00	14.12	1%	0.12
41	801	312	140	5	37.00	37.48	1%	0.48
42	659	348	140	5	34.50	34.24	1%	0.26
43	497	403	140	5	31.50	29.09	8%	2.41
44	381	429	140	5	29.00	21.56	26%	7.44
45	752	322	140	5	35.00	36.35	4%	1.35
46	566	382	140	5	31.00	31.95	3%	0.95
47	384	470	140	5	22.50	25.00	11%	2.50
48	262	519	140	5	5.50	14.47	163%	8.97
49	696	337	140	5	35.50	35.12	1%	0.38
50	484	422	140	5	30.50	29.71	3%	0.79
51	302	538	140	5	20.50	21.04	3%	0.54
52	188	606	140	5	0.50	7.77	1454%	7.27
53	630	359	140	5	34.00	33.69	1%	0.31
54	409	469	140	5	28.00	27.26	3%	0.74
55	240	606	140	5	16.50	16.73	1%	0.23
57	557	389	140	5	31.00	32.02	3%	1.02
58	340	523	140	5	24.50	24.41	0%	0.09
59	190	669	140	5	11.50	11.83	3%	0.33
61	618	255	280	5	35.50	37.13	5%	1.63
62	508	285	280	5	33.00	33.84	3%	0.84
63	389	331	280	5	30.50	29.29	4%	1.21
64	313	353	280	5	29.00	23.65	18%	5.35
65	575	264	280	5	33.00	35.68	8%	2.68
66	425	315	280	5	29.00	30.82	6%	1.82
67	286	392	280	5	22.00	24.14	10%	2.14
68	203	435	280	5	3.50	15.14	332%	11.64
69	526	277	280	5	33.50	34.11	2%	0.61
70	354	352	280	5	28.50	28.02	2%	0.48
71	217	460	280	5	18.50	19.58	6%	1.08
73	469	297	280	5	32.00	32.27	1%	0.27
74	291	397	280	5	26.00	25.16	3%	0.84
75	167	532	280	5	14.50	15.00	3%	0.50
77	406	324	280	5	29.00	30.17	4%	1.17
78	236	451	280	5	23.00	22.05	4%	0.95

**Table A-3 Comparison of Overlay Required: EVERPAVE vs Equation, Cont.**

Case No.	Do (microns)	A (mm)	E <sub>SG</sub> MPa	ESALS (millions)	Overlay EVERPAVE (cm)	Overlay equation (cm)	Percent Difference	Absolute Difference (cm)
79	129	603	280	5	9.50	10.07	6%	0.57
81	1749	435	35	5	43.50	45.53	5%	2.03
82	1670	444	35	5	43.00	44.55	4%	1.55
83	1694	440	35	5	43.00	44.73	4%	1.73
84	1599	452	35	5	42.00	43.58	4%	1.58
85	1643	444	35	5	42.50	43.96	3%	1.46
86	1527	462	35	5	41.50	42.65	3%	1.15
87	1591	450	35	5	43.00	43.25	1%	0.25
88	1447	476	35	5	40.50	41.73	3%	1.23
89	1529	460	35	5	41.00	42.55	4%	1.55
90	1352	497	35	5	37.50	40.74	9%	3.24
91	1202	364	70	5	41.00	41.63	2%	0.63
92	1157	371	70	5	40.00	40.86	2%	0.86
93	1174	367	70	5	39.00	41.08	5%	2.08
94	1112	377	70	5	37.50	40.07	7%	2.57
95	1147	370	70	5	40.00	40.52	1%	0.52
96	1063	386	70	5	39.00	39.23	1%	0.23
97	1112	376	70	5	40.50	39.91	1%	0.59
98	1001	400	70	5	38.00	38.30	1%	0.30
99	1064	385	70	5	38.50	39.19	2%	0.69
100	925	421	70	5	35.50	37.20	5%	1.70
101	863	300	140	5	38.50	38.88	1%	0.38
102	836	305	140	5	38.00	38.26	1%	0.26
103	847	303	140	5	37.00	38.46	4%	1.46
104	805	311	140	5	35.50	37.50	6%	2.00
105	830	305	140	5	38.00	38.02	0%	0.02
106	767	319	140	5	36.50	36.64	0%	0.14
107	806	310	140	5	38.00	37.43	2%	0.57
108	716	332	140	5	36.00	35.55	1%	0.45
109	766	318	140	5	36.00	36.58	2%	0.58
110	653	352	140	5	33.00	34.22	4%	1.22
111	660	247	280	5	37.00	38.40	4%	1.40
112	643	250	280	5	36.00	37.89	5%	1.89
113	649	249	280	5	35.00	37.99	9%	2.99
114	617	255	280	5	34.00	36.99	9%	2.99

**Table A-3 Comparison of Overlay Required: EVERPAVE vs Equation, Cont.**

Case No.	Do (microns)	A (mm)	E <sub>SG</sub> MPa	ESALS (millions)	Overlay EVERPAVE (cm)	Overlay equation (cm)	Percent Difference	Absolute Difference (cm)
115	636	251	280	5	36.00	37.55	4%	1.55
116	585	261	280	5	35.00	35.93	3%	0.93
117	616	254	280	5	36.00	36.87	2%	0.87
118	541	273	280	5	34.00	34.54	2%	0.54
119	582	262	280	5	34.00	35.78	5%	1.78
120	485	291	280	5	31.00	32.81	6%	1.81
1	1589	455	35	10	47.00	47.85	2%	0.85
2	1303	503	35	10	44.00	44.07	0%	0.07
3	961	570	35	10	39.00	37.35	4%	1.65
4	674	604	35	10	34.50	26.39	24%	8.11
5	1500	468	35	10	45.50	46.70	3%	1.20
6	1165	536	35	10	41.50	42.25	2%	0.75
7	799	629	35	10	34.00	34.06	0%	0.06
8	512	683	35	10	23.50	20.62	12%	2.88
9	1408	484	35	10	45.50	45.59	0%	0.09
10	1037	573	35	10	40.50	40.36	0%	0.14
11	667	683	35	10	30.50	30.38	0%	0.12
12	398	746	35	10	10.50	14.46	38%	3.96
13	1308	506	35	10	44.50	44.45	0%	0.05
14	912	615	35	10	37.50	38.11	2%	0.61
15	553	733	35	10	26.00	25.97	0%	0.03
17	1195	535	35	10	40.50	43.14	7%	2.64
18	787	660	35	10	33.00	35.24	7%	2.24
19	453	776	35	10	21.00	20.68	2%	0.32
21	1105	380	70	10	44.00	44.29	1%	0.29
22	907	423	70	10	41.50	40.87	2%	0.63
23	675	486	70	10	37.50	34.98	7%	2.52
24	494	517	70	10	34.00	25.63	25%	8.37
25	1042	391	70	10	42.00	43.24	3%	1.24
26	797	457	70	10	38.00	38.94	2%	0.94
27	543	551	70	10	30.00	31.45	5%	1.45
28	358	605	70	10	23.50	19.40	17%	4.10
29	973	407	70	10	43.00	42.15	2%	0.85
30	697	497	70	10	38.00	36.98	3%	1.02
31	442	614	70	10	28.00	27.74	1%	0.26

**Table A-3 Comparison of Overlay Required: EVERPAVE vs Equation, Cont.**

Case No.	Do (microns)	A (mm)	E <sub>SG</sub> MPa	ESALS (millions)	Overlay EVERPAVE (cm)	Overlay equation (cm)	Percent Difference	Absolute Difference (cm)
32	268	683	70	10	7.50	13.10	75%	5.60
33	893	430	70	10	41.50	40.93	1%	0.57
34	602	543	70	10	35.00	34.71	1%	0.29
35	360	674	70	10	23.50	23.45	0%	0.05
37	804	461	70	10	38.00	39.51	4%	1.51
38	511	594	70	10	31.00	31.91	3%	0.91
39	291	727	70	10	19.00	18.39	3%	0.61
41	801	312	140	10	42.00	41.76	1%	0.24
42	659	348	140	10	39.50	38.51	3%	0.99
43	497	403	140	10	36.00	33.37	7%	2.63
44	381	429	140	10	33.50	25.84	23%	7.66
45	752	322	140	10	39.50	40.63	3%	1.13
46	566	382	140	10	35.50	36.22	2%	0.72
47	384	470	140	10	27.50	29.27	6%	1.77
48	262	519	140	10	24.00	18.75	22%	5.25
49	696	337	140	10	40.50	39.39	3%	1.11
50	484	422	140	10	35.50	33.98	4%	1.52
51	302	538	140	10	25.00	25.31	1%	0.31
52	188	606	140	10	5.00	12.04	141%	7.04
53	630	359	140	10	39.00	37.97	3%	1.03
54	409	469	140	10	32.50	31.54	3%	0.96
55	240	606	140	10	21.50	21.01	2%	0.49
57	557	389	140	10	35.50	36.29	2%	0.79
58	340	523	140	10	29.00	28.69	1%	0.31
59	190	669	140	10	16.50	16.10	2%	0.40
61	618	255	280	10	40.00	41.40	4%	1.40
62	508	285	280	10	37.50	38.11	2%	0.61
63	389	331	280	10	35.00	33.56	4%	1.44
64	313	353	280	10	33.00	27.93	15%	5.07
65	575	264	280	10	37.50	39.96	7%	2.46
66	425	315	280	10	33.50	35.10	5%	1.60
67	286	392	280	10	26.50	28.41	7%	1.91
68	203	435	280	10	24.00	19.41	19%	4.59
69	526	277	280	10	38.00	38.38	1%	0.38
70	354	352	280	10	33.00	32.30	2%	0.70

**Table A-3 Comparison of Overlay Required: EVERPAVE vs Equation, Cont.**

Case No.	Do (microns)	A (mm)	E <sub>SG</sub> MPa	ESALS (millions)	Overlay EVERPAVE (cm)	Overlay equation (cm)	Percent Difference	Absolute Difference (cm)
71	217	460	280	10	23.00	23.85	4%	0.85
73	469	297	280	10	37.00	36.55	1%	0.45
74	291	397	280	10	30.50	29.44	3%	1.06
75	167	532	280	10	19.50	19.27	1%	0.23
77	406	324	280	10	33.50	34.45	3%	0.95
78	236	451	280	10	27.00	26.33	2%	0.67
79	129	603	280	10	14.50	14.35	1%	0.15
81	1749	435	35	10	48.50	49.80	3%	1.30
82	1670	444	35	10	47.50	48.82	3%	1.32
83	1694	440	35	10	47.00	49.01	4%	2.01
84	1599	452	35	10	46.00	47.86	4%	1.86
85	1643	444	35	10	48.00	48.24	0%	0.24
86	1527	462	35	10	47.00	46.93	0%	0.07
87	1591	450	35	10	49.00	47.52	3%	1.48
88	1447	476	35	10	46.50	46.01	1%	0.49
89	1529	460	35	10	47.50	46.82	1%	0.68
90	1352	497	35	10	43.50	45.02	3%	1.52
91	1202	364	70	10	46.00	45.91	0%	0.09
92	1157	371	70	10	45.00	45.13	0%	0.13
93	1174	367	70	10	44.00	45.36	3%	1.36
94	1112	377	70	10	42.50	44.34	4%	1.84
95	1147	370	70	10	45.50	44.80	2%	0.70
96	1063	386	70	10	44.00	43.51	1%	0.49
97	1112	376	70	10	46.00	44.19	4%	1.81
98	1001	400	70	10	43.50	42.57	2%	0.93
99	1064	385	70	10	44.50	43.46	2%	1.04
100	925	421	70	10	40.50	41.47	2%	0.97
101	863	300	140	10	43.50	43.15	1%	0.35
102	836	305	140	10	42.50	42.53	0%	0.03
103	847	303	140	10	42.00	42.74	2%	0.74
104	805	311	140	10	40.00	41.78	4%	1.78
105	830	305	140	10	43.00	42.29	2%	0.71
106	767	319	140	10	41.50	40.91	1%	0.59
107	806	310	140	10	43.50	41.70	4%	1.80
108	716	332	140	10	41.00	39.83	3%	1.17

**Table A-3 Comparison of Overlay Required: EVERPAVE vs Equation, Cont.**

Case No.	Do (microns)	A (mm)	E <sub>SG</sub> MPa	ESALS (millions)	Overlay EVERPAVE (cm)	Overlay equation (cm)	Percent Difference	Absolute Difference (cm)
109	766	318	140	10	41.50	40.86	2%	0.64
110	653	352	140	10	38.00	38.50	1%	0.50
111	660	247	280	10	41.50	42.68	3%	1.18
112	643	250	280	10	40.50	42.16	4%	1.66
113	649	249	280	10	39.50	42.27	7%	2.77
114	617	255	280	10	38.00	41.26	9%	3.26
115	636	251	280	10	40.50	41.83	3%	1.33
116	585	261	280	10	39.50	40.20	2%	0.70
117	616	254	280	10	41.00	41.14	0%	0.14
118	541	273	280	10	38.50	38.81	1%	0.31
119	582	262	280	10	39.00	40.06	3%	1.06
120	485	291	280	10	36.00	37.09	3%	1.09
						Total	4310%	461.71
						Average	13%	1.411971

## APPENDIX B GRAPHS

### B.1 INTRODUCTION

The best way to see if there is a relationship between two parameters is to graph one versus the other on an x-y scatter plot. A regression equation defines the “best-fit” straight line that represents the relationship between the two variables. Often, variables relate to each other in a non-linear fashion. In this case, transformations can be made to one or both of the variables in order to create a more linear relationship. Figure B-1 shows four typical relationships between two parameters. For each of these examples, a generic equation can be written. These relationships and their equations are:

- a. Linear                    $y = b_0 + b_1x$
- b. Exponential              $y = b_0b_1^x$
- c. Power                    $y = b_0x^{b_1}$
- d. Hyperbolic              $y = b_0 + b_1\left(\frac{1}{x}\right)$

where  $b_0$  and  $b_1$  are adjusted to best represent the relationship between x and y.

### B.2 GRAPHS

Figures B-2 through B-11 show the graphs produced during the first stage of research for this thesis. These graphs relate different measured pavement responses such as  $D_0$  and Area Parameter to the critical strains,  $\epsilon_t$  and  $\epsilon_v$ .

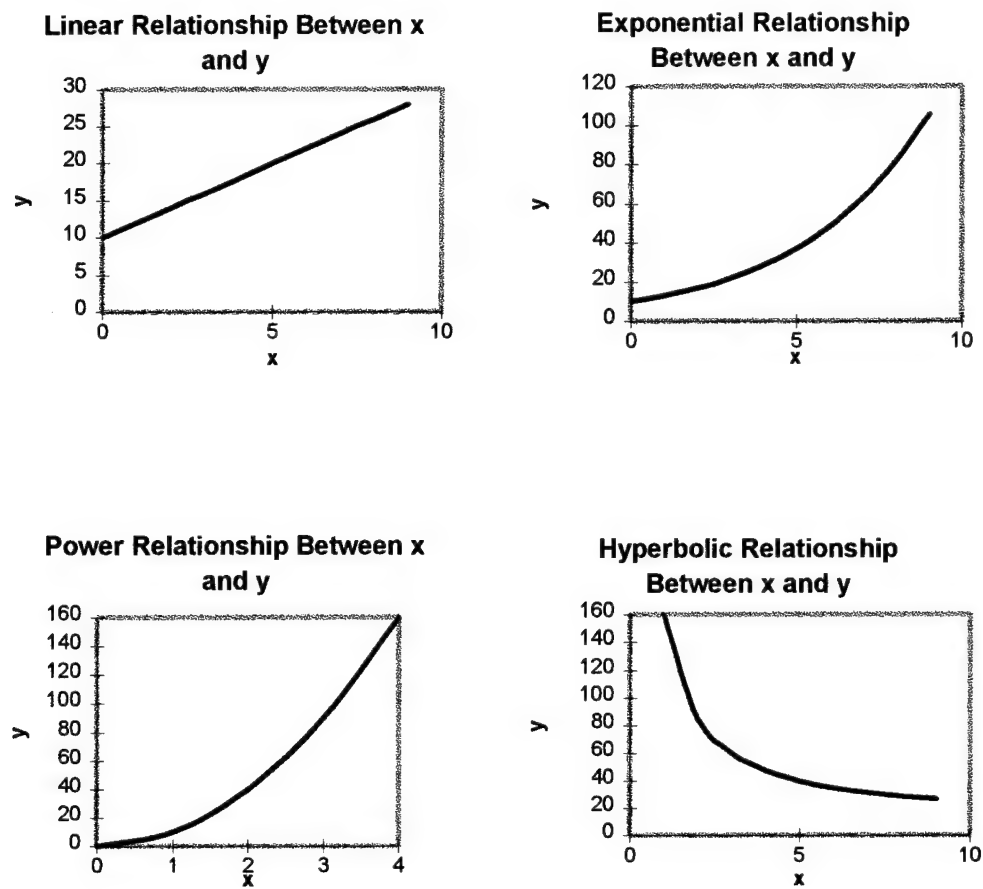


**Figure B-1 Typical Relationships Between Variables (after Mahoney, 1994)**

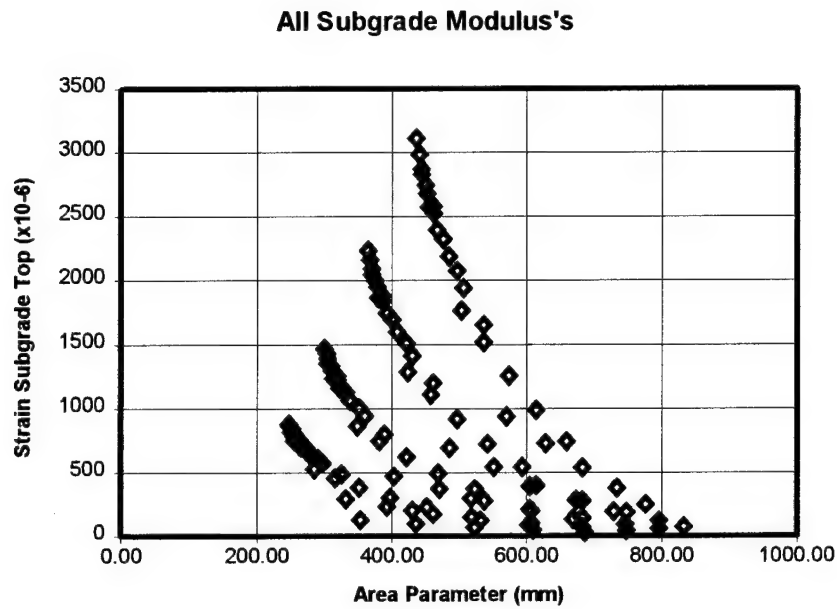


**Figure B-2 Area Parameter vs  $\varepsilon_v$  for All Subgrades**

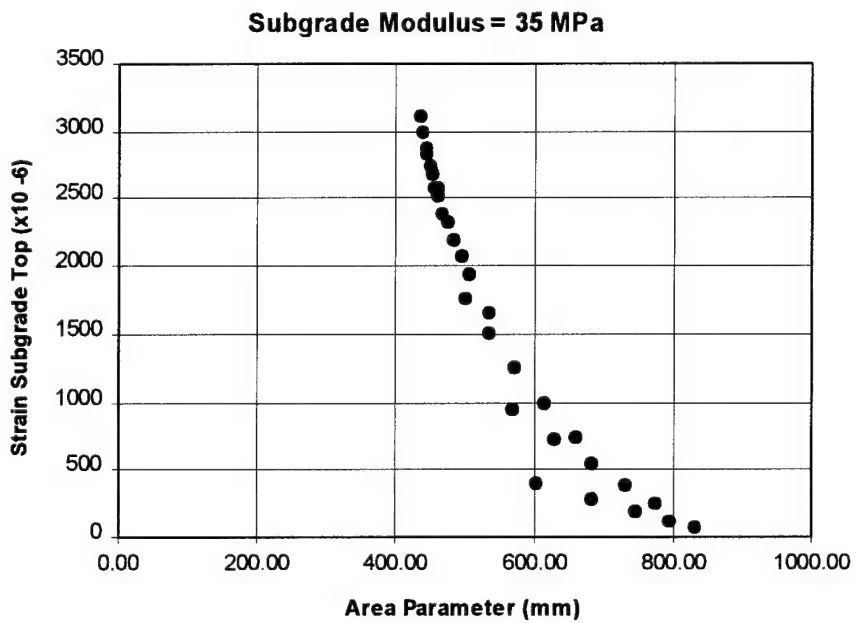


**Figure B-3 Area Parameter vs  $\varepsilon_v$  for Subgrades with Modulus = 35 MPa**

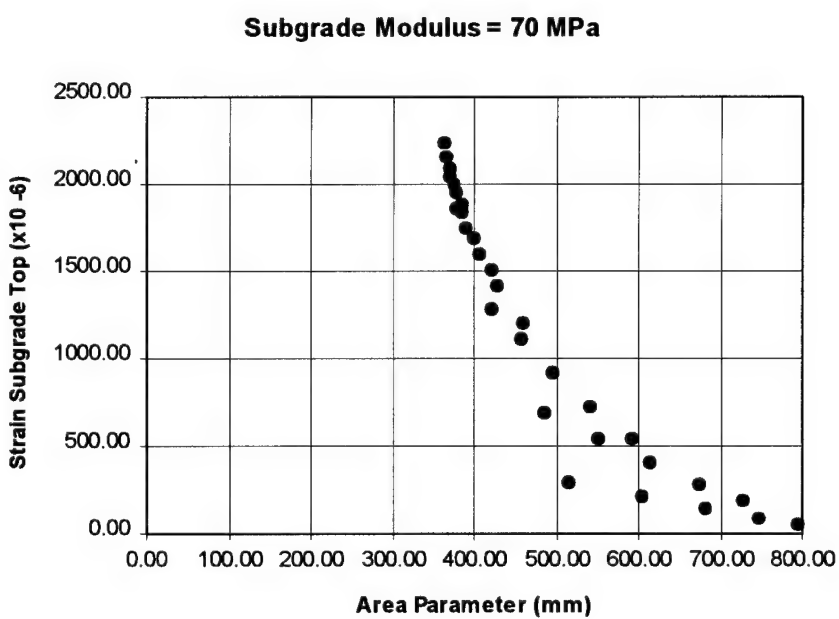


**Figure B-4 Area Parameter vs  $\varepsilon_v$  for Subgrades with Modulus = 70 MPa**

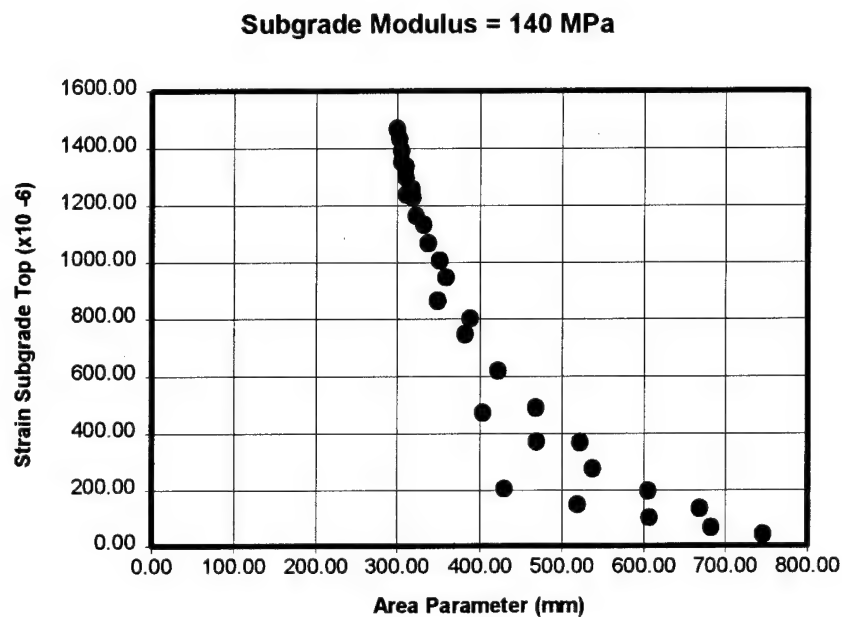


**Figure B-5 Area Parameter vs  $\epsilon_v$  for Subgrades with Modulus = 140 MPa**

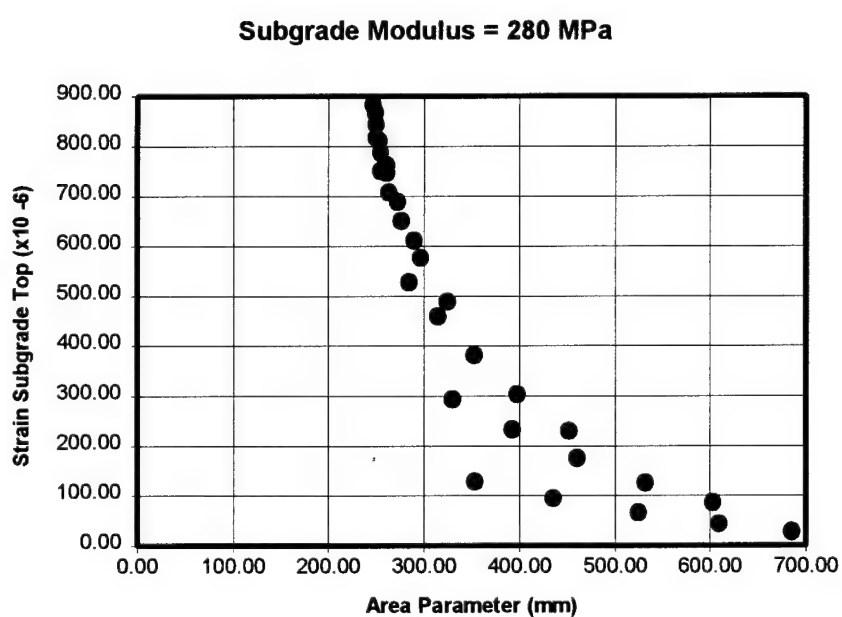


**Figure B-6 Area Parameter vs  $\epsilon_v$  for Subgrades with Modulus = 280 MPa**

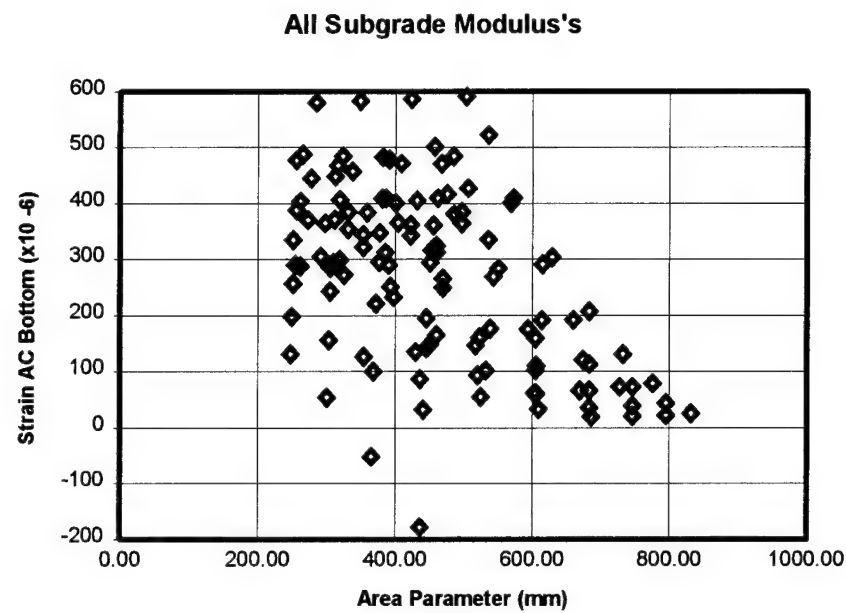


**Figure B-7 Area Parameter vs  $\varepsilon_t$  for All Subgrades**

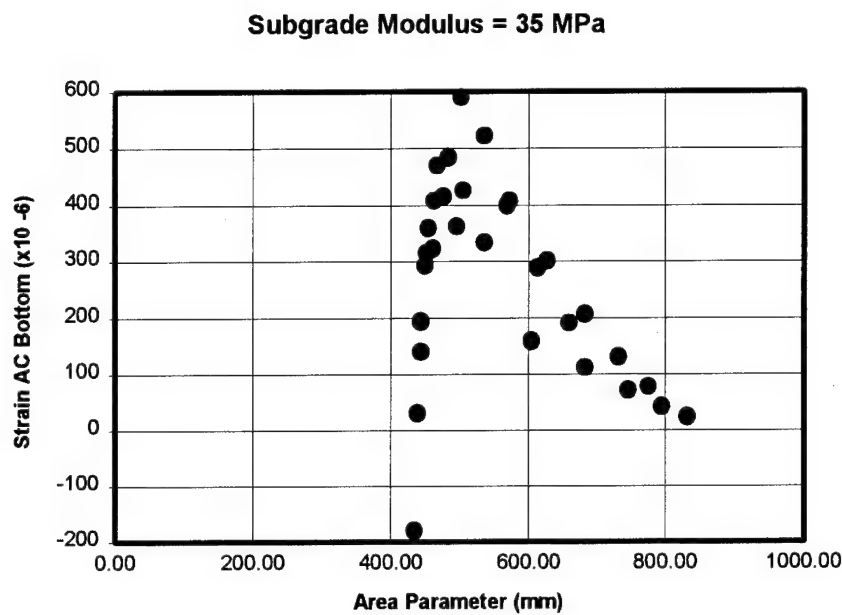


**Figure B-8 Area Parameter vs  $\varepsilon_t$  for Subgrades with Modulus = 35 MPa**

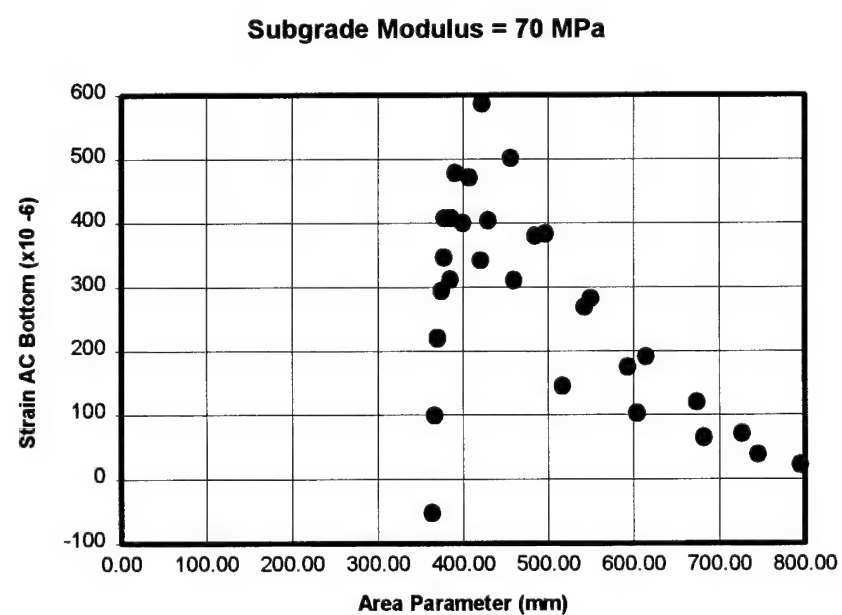


**Figure B-9 Area Parameter vs  $\varepsilon_t$  for Subgrades with Modulus = 70 MPa**

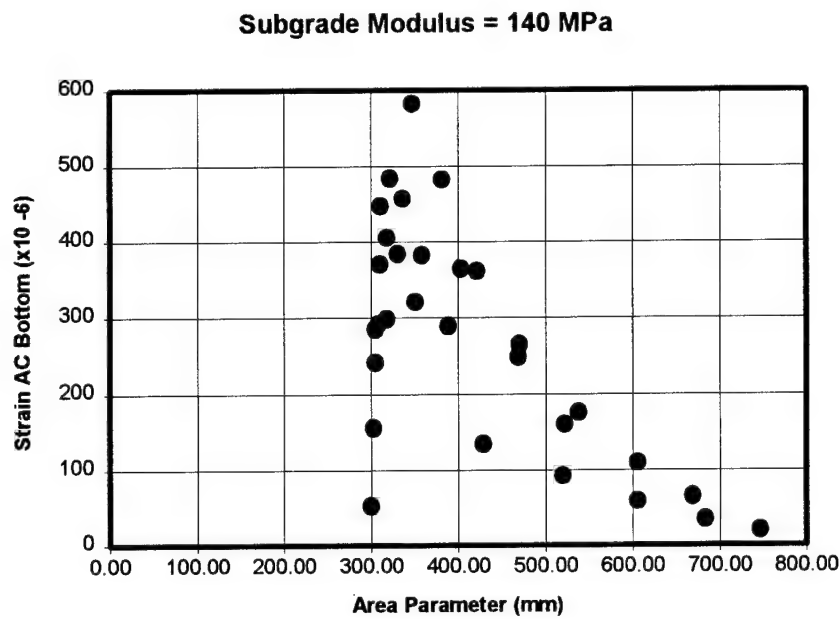


**Figure B-10 Area Parameter vs  $\varepsilon_t$  for Subgrades with Modulus = 140 MPa**

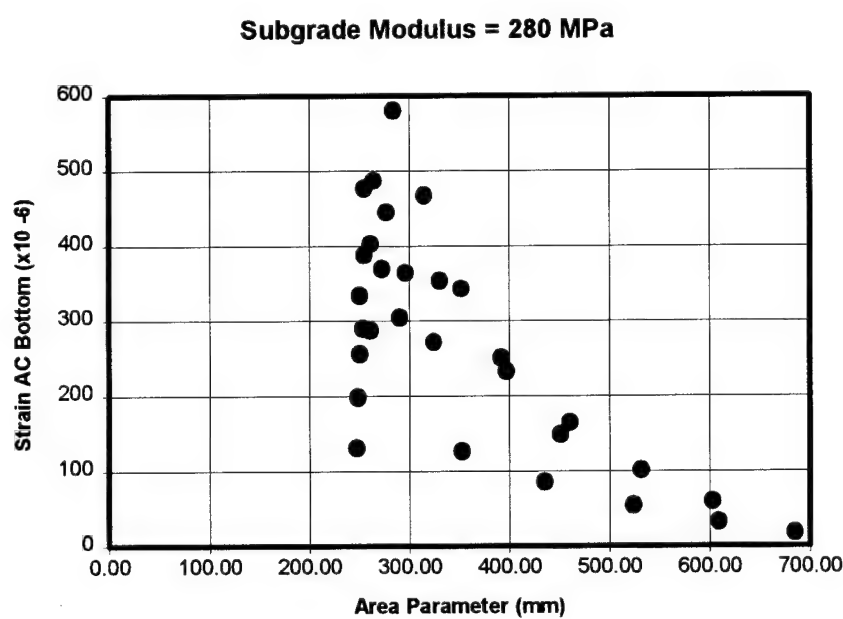


**Figure B-11 Area Parameter vs  $\varepsilon_t$  for Subgrades with Modulus = 280 MPa**

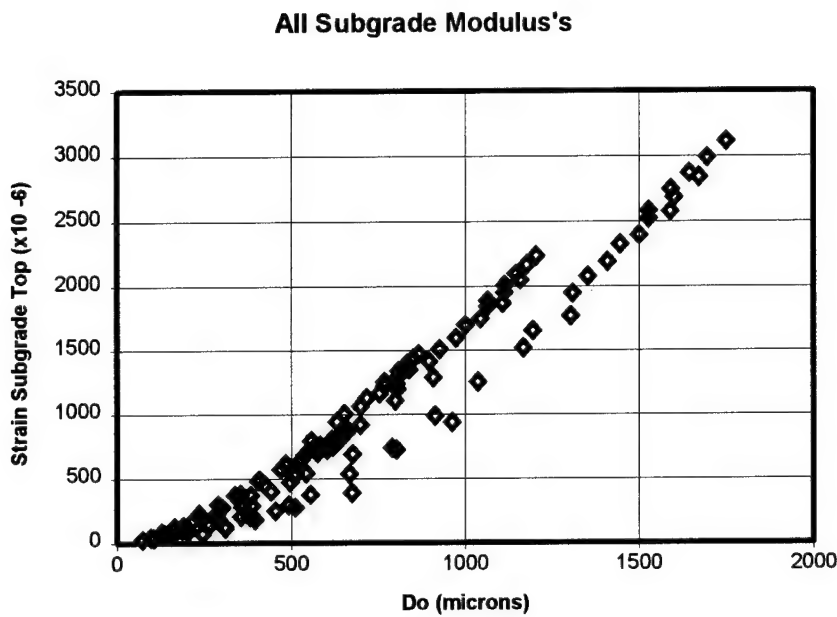


**Figure B-12  $D_0$  vs  $\varepsilon_v$  for All Subgrades**

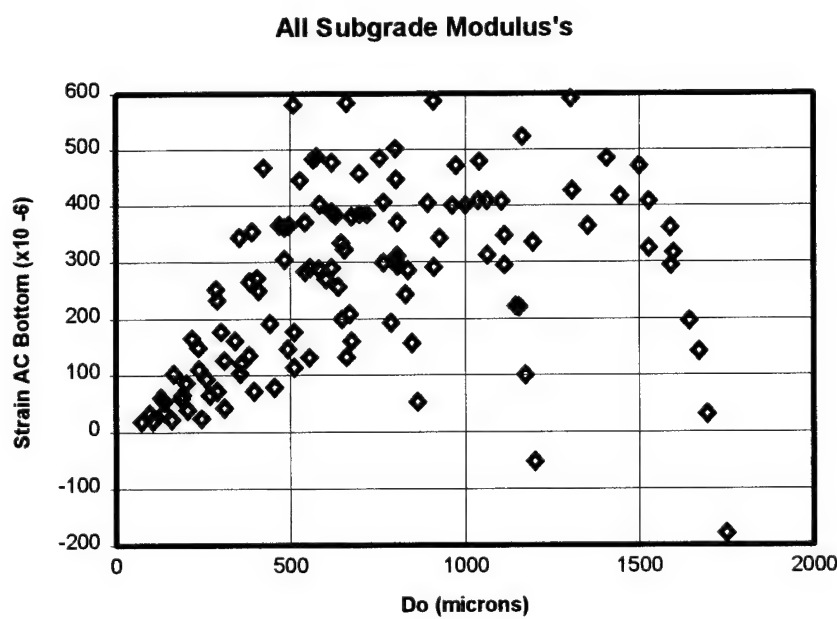


**Figure B-13  $D_0$  vs  $\varepsilon_t$  for All Subgrades**

## **APPENDIX C**

### **REGRESSION ANALYSIS**

#### **C.1 INTRODUCTION**

Regression analysis is a powerful tool used to establish relationships that exist in a set of data. Regression analysis is used extensively in this thesis therefore, this Appendix is included to provide a cohesive explanation of the regression analysis procedure. Section 3.2.2 provides a brief description of regression analysis. This section will go into greater detail.

#### **C.2 CORRELATION**

Correlation is a method of quantifying the association of two variables. The Pearson product moment correlation coefficient,  $r$ , is commonly used. The basic equation for  $r$  is (Ryan et al., 1985):

$$r = \frac{\sum (x - \bar{x})(y - \bar{y})}{\sqrt{(x - \bar{x})^2(y - \bar{y})^2}}$$

while the formula normally used to compute  $r$  is (Ryan et al., 1985):

$$r = \frac{\sum xy - \frac{\sum x \sum y}{n}}{\left[ \left( \sum x^2 - \frac{(\sum x)^2}{n} \right) \left( \sum y^2 - \frac{(\sum y)^2}{n} \right) \right]^{1/2}}$$

Its value is always between -1 and +1. On an x-y plot of the data, a positive correlation indicates y tends to increase as x increases, commonly known as a positive slope in

mathematics. The converse is true for a negative correlation. It indicates a negative slope:  $y$  tends to decrease as  $x$  increases. If no trend can be seen at all,  $r$  will equal 0; although, an  $r$  equal to 0 does not always indicate a lack of association between  $x$  and  $y$ . It indicates a lack of a linear association between  $x$  and  $y$ . A curved association is an example of a relationship that cannot be identified by the correlation coefficient. Because of this limitation, a plot of the data on an  $x$ - $y$  scatter plot provides an excellent picture of any association that exists between the variables. The correlation coefficient should not be used exclusively to determine if two variables are related by some function.

### C.3 REGRESSION

Whereas correlation provides a quantitative measure of relationship between two variables, regression provides the equation to describe the relationship mathematically. Simple regression involves only two variables and is the most straightforward to explain. Simple regression calculates the “best-fit” line on an  $x$ - $y$  plot of the two variables. Figure C-1 illustrates the “best-fit” line using an example of height vs weight for 5 people.

The method of least squares is used to calculate the “best-fit” line. The equation for any straight line follows the form  $y = a + bx$ , where  $x$  and  $y$  are the variables and  $a$  and  $b$  are the constants defining the relationship. Using the least squares method,  $a$  and  $b$  are calculated by (Ryan et al., 1985):

$$b = \frac{\sum (x - \bar{x})(y - \bar{y})}{\sum (x - \bar{x})^2}$$

$$a = \bar{y} - b\bar{x}$$

## Height vs Weight

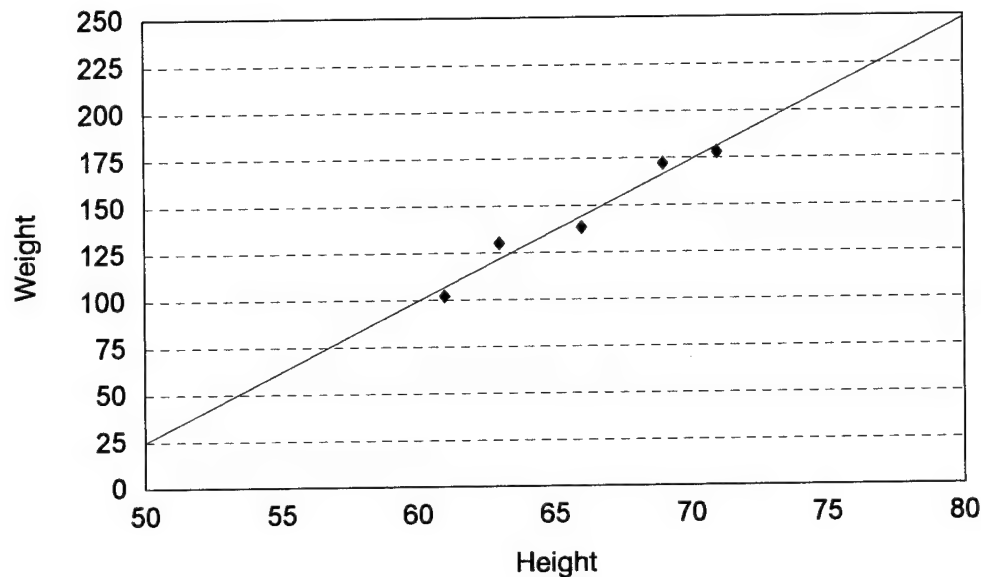


**Figure C-1 Illustration of the “Best Fit” Line**

Multiple regression involves more than two variables. The development of a regression equation is more rigorous using multiple variables; therefore, statistical computer programs such as Minitab are used to calculate the equation. Most of the equations developed in this thesis utilized multiple regression, they can be found in Appendix D.

The parameters used to quantify the usefulness of a regression equation are explained in Chapter 3, Section 3.2.2. These are  $R^2$ , RMSE and N.

## APPENDIX D

### MINITAB OUTPUT

**Table D-1 Regression Equations for  $\varepsilon_t$  and  $\log \varepsilon_t$**

Equation	$R^2$	RMSE	N
$\varepsilon_t = 984 - 1.13 A - 1.10 E_{SG}$	70.4	80.51	41
$\varepsilon_t = -79.9 + 0.434 D_0 + 0.373 E_{SG}$	89.3	48.46	41
$\log \varepsilon_t = -4.23 + 1.80 \log D_0 + 0.898 \log E_{SG}$	97.6	0.06465	41
$\log \varepsilon_t = -2.31 + 1.60 \log D_0 + 0.00273 E_{SG}$	93.2	0.1080	41
$\log \varepsilon_t = 5.91 - 0.00353 A - 0.877 \log E_{SG}$	89.3	0.1358	41
$\log \varepsilon_t = 4.59 - 0.00351 A - 0.00335 E_{SG}$	85.2	0.1593	41
$\log \varepsilon_t = 18.0 - 5.12 \log A - 0.863 \log E_{SG}$	87.4	0.1470	41
$\log \varepsilon_t = 16.6 - 5.10 \log A - 0.00330 E_{SG}$	83.6	0.1678	41
$\log \varepsilon_t = 3.88 - 0.00290 A$	43.3	0.3081	41

**Table D-2 Regression Equations for  $\log \varepsilon_v$**

Equation	$R^2$	RMSE	N
$\log \varepsilon_v = 7.04 - 0.00339A - 1.34 \log E_{SG}$	94.4	0.01148	120
$\log \varepsilon_v = 15.3 - 3.67 \log A - 1.42 \log E_{SG}$	91.0	0.1450	120
$\log \varepsilon_v = 12.7 - 3.52 \log A - 0.00485 E_{SG}$	86.7	0.1765	120
$\log \varepsilon_v = 4.88 - 0.00323A - 0.00451E_{SG}$	88.8	0.1616	120
$\log \varepsilon_v = 1.89 + 0.00112 D_0 - 0.000833 E_{SG}$	81.6	0.2075	120
$\log \varepsilon_v = 6.0 - 0.00284 A - 1.03 \log E_{SG} + 0.000233 D_0$	120	0.1100	120
$\log \varepsilon_v = 8.73 - 0.150 (A)^{0.5} - 1.38 \log E_{SG}$	120	0.1247	120

**Table D-3 Regression Equations for  $\epsilon_v$** 

<b>Equation</b>	<b>R<sup>2</sup></b>	<b>RMSE</b>	<b>N</b>
$\epsilon_v = 3964 - 4.3 A - 7.54 E_{SG}$	69.5	450.2	120
$\epsilon_v = 5994 - 1.88 (A)^{0.5} - 7.74 E_{SG}$	68.2	460.0	120
$\epsilon_v = -511 + 1.97 D_0 + 0.788 E_{SG}$	96.0	163.9	120
$\epsilon_v = -88.5 + 1.83 D_0 - 0.472 A$	96.1	161.6	120
$\epsilon_v = -204 + 1.87 D_0 - 0.359 A + 0.252 E_{SG}$	96.1	161.9	120
$\epsilon_v = -337 + 1.88 D_0$	95.4	174.5	120

**Table D-4 Regression Equations for Area Parameter Load Adjustment**

<b>Case Number</b>	<b>Equation</b>	<b>N</b>	<b>R<sup>2</sup></b>	<b>RMSE</b>
50	A = 380 + 0.968 (Load)	7	98.8	3.337
70	A = 310 + 0.982 (Load)	7	99.2	2.792
55	A = 567 + 0.835 (Load)	7	95.8	5.503
65	A = 217 + 1.16 (Load)	7	99.9	1.406
115	A = 201 + 1.23 (Load)	7	99.8	1.527
1	A = 395 + 1.36 (Load)	7	97.9	6.297
40	A = 761 + 0.715 (Load)	7	93.1	6.155
89	A = 410 + 1.18 (Load)	7	98.9	3.915
10	A = 485 + 1.37 (Load)	7	90.3	14.18
13	A = 468 + 0.888 (Load)	7	99.1	2.674

Range of slope of line: 0.715 - 1.37

Average slope: 1.069

Use average slope as Area Parameter adjustment factor for load

**Table D-5 Regression Equations for  $D_0$  Load Adjustment**

<b>Case Number</b>	<b>Equation</b>	<b>N</b>	<b>R<sup>2</sup></b>	<b>RMSE</b>
50	$D_0 = 76.8 + 9.93 \text{ (Load)}$	7	99.8	12.95
70	$D_0 = 73.3 + 6.78 \text{ (Load)}$	7	99.7	11.97
55	$D_0 = 20.8 + 5.42 \text{ (Load)}$	7	100	2.672
65	$D_0 = 225 + 8.13 \text{ (Load)}$	7	98.7	30.00
115	$D_0 = 303 + 7.65 \text{ (Load)}$	7	98.2	32.38
1	$D_0 = 316 + 31.0 \text{ (Load)}$	7	99.8	40.87
40	$D_0 = 8.01 + 3.76 \text{ (Load)}$	7	100	0.7115
89	$D_0 = 259 + 30.9 \text{ (Load)}$	7	99.8	42.97
10	$D_0 = 85.5 + 23.5 \text{ (Load)}$	7	100	15.35
13	$D_0 = 151 + 28.4 \text{ (Load)}$	7	99.9	28.74

Range of slope of line: varies with initial value of  $D_0$   
 Develop equation to predict the slope of the line based on load.

**Table D-6 Regression Equations for Slope of  $D_0$  Adjustment for Load**

<b>Equation</b>	<b>N</b>	<b>R<sup>2</sup></b>	<b>RMSE</b>
slope = -0.91 + 0.0369 ( $D_0$ ) <sub>20</sub>	10	90.2	3.788
slope = -1.01 + 0.0265 ( $D_0$ ) <sub>30</sub>	10	93.8	3.022
slope = -0.98 + 0.0209 ( $D_0$ ) <sub>40</sub>	10	95.9	2.463
slope = -0.92 + 0.0174 ( $D_0$ ) <sub>50</sub>	10	97.2	2.030
slope = -0.83 + 0.0149 ( $D_0$ ) <sub>60</sub>	10	97.8	1.686
slope = -0.737 + 0.0131 ( $D_0$ ) <sub>70</sub>	10	98.7	1.402
slope = -0.643 + 0.0117 ( $D_0$ ) <sub>80</sub>	10	99.1	1.164
1/pslope = 8.51 + 0.970 (Load)	7	99.9	0.5917
intercept = -1.13 + 0.00535 (Load) (all loads)	7	75.4	0.0722
intercept = -1.27 + 0.00758 (Load) (loads 30-80 kN)	7	97.4	0.02611

Use the equation **slope = intercept + pslope (Load)** to calculate the slope of the Load Adjustment Factor for  $D_0$

Where intercept = -1.27 + 0.00758 (Load) for loads 30-80 kN

intercept = -0.91 for 20 kN load

and pslope = 1/ (8.51 + 0.970 (Load)) for all loads

**Figure D-7 Regression Equations for Temperature Shift Factor for A**

Equation	R <sup>2</sup>	RMSE	N
A <sub>SF</sub> = 4.96 + 0.0375 E <sub>SG</sub>	34.1	5.107	24
A <sub>SF</sub> = -11.2 + 10.6 log E <sub>SG</sub>	34.9	5.075	24
A <sub>SF</sub> = 14.5 - 345(1/E <sub>SG</sub> )	30.1	5.258	24
A <sub>SF</sub> = 7.09 + 0.000107(E <sub>SG</sub> ) <sup>2</sup>	30.4	5.258	24
A <sub>SF</sub> = 0.45 + 0.880(E <sub>SG</sub> ) <sup>0.5</sup>	35.2	5.063	24
A <sub>SF</sub> = -2.77 + 0.880(E <sub>SG</sub> ) <sup>0.5</sup> + 0.238 T <sub>AC</sub>	62.4	3.949	24
A <sub>SF</sub> = 6.24 + 0.880(E <sub>SG</sub> ) <sup>0.5</sup> - 33.3(1/T <sub>AC</sub> )	87.9	2.236	24
A <sub>SF</sub> = -6.64 + 0.880(E <sub>SG</sub> ) <sup>0.5</sup> + 2.16(T <sub>AC</sub> ) <sup>0.5</sup>	70.5	3.496	24
log A <sub>SF</sub> = 0.849 + 0.0361(E <sub>SG</sub> ) <sup>0.5</sup> - 1.93(1/T <sub>AC</sub> )	92.9	0.08642	24

**Table D-8 Regression Equations for Area Temperature Shift Factor Calculation**

<b>E<sub>SG</sub></b>	<b>T<sub>AC</sub></b>	<b>Regression Equation</b>	<b>R<sup>2</sup></b>	<b>RMSE</b>	<b>N</b>
35	2.5	$1/A = 0.00219 + 0.000002(\text{Temp})$	97.9	8.3E <sup>-6</sup>	5
70	2.5	$1/A = 0.00262 + 0.000002(\text{Temp})$	94.3	1.6E <sup>-5</sup>	5
140	2.5	$1/A = 0.00318 + 0.000003(\text{Temp})$	92.2	2.4E <sup>-5</sup>	5
280	2.5	$1/A = 0.00387 + 0.000003(\text{Temp})$	90.5	3.1E <sup>-5</sup>	5
35	3.75	$1/A = 0.00205 + 0.000004(\text{Temp})$	97.2	1.8E <sup>-5</sup>	5
70	3.75	$1/A = 0.00242 + 0.000005(\text{Temp})$	96.4	2.8E <sup>-5</sup>	5
140	3.75	$1/A = 0.00291 + 0.000007(\text{Temp})$	95.7	4.2E <sup>-5</sup>	5
280	3.75	$1/A = 0.00353 + 0.000009(\text{Temp})$	94.9	5.8E <sup>-5</sup>	5
35	5.0	$1/A = 0.00191 + 0.000005(\text{Temp})$	98.6	1.8E <sup>-5</sup>	5
70	5.0	$1/A = 0.00223 + 0.000007(\text{Temp})$	98.3	2.7E <sup>-5</sup>	5
140	5.0	$1/A = 0.00265 + 0.000010(\text{Temp})$	98.1	4.0E <sup>-5</sup>	5
280	5.0	$1/A = 0.00319 + 0.000013(\text{Temp})$	97.8	5.7E <sup>-5</sup>	5
35	10.0	$1/A = 0.00154 + 0.000008(\text{Temp})$	100.0	3.7E <sup>-6</sup>	5
70	10.0	$1/A = 0.00172 + 0.000011(\text{Temp})$	99.9	7.0E <sup>-6</sup>	5
140	10.0	$1/A = 0.00196 + 0.000015(\text{Temp})$	99.9	1.1E <sup>-5</sup>	5
280	10.0	$1/A = 0.00229 + 0.000021(\text{Temp})$	100.0	1.3E <sup>-5</sup>	5
35	20.0	$1/A = 0.00129 + 0.000007(\text{Temp})$	97.8	3.2E <sup>-5</sup>	5
70	20.0	$1/A = 0.00138 + 0.000011(\text{Temp})$	97.6	4.8E <sup>-5</sup>	5
140	20.0	$1/A = 0.00150 + 0.000016(\text{Temp})$	97.6	7.0E <sup>-5</sup>	5
280	20.0	$1/A = 0.00167 + 0.000022(\text{Temp})$	97.9	9.2E <sup>-5</sup>	5
35	40.0	$1/A = 0.00119 + 0.000007(\text{Temp})$	94.6	4.9E <sup>-5</sup>	5
70	40.0	$1/A = 0.00124 + 0.000011(\text{Temp})$	94.7	7.2E <sup>-5</sup>	5
140	40.0	$1/A = 0.00132 + 0.000016(\text{Temp})$	95.1	1.0E <sup>-4</sup>	5
280	40.0	$1/A = 0.00144 + 0.000022(\text{Temp})$	96.0	1.3E <sup>-4</sup>	5

**Table D-9 Regression Equations for  $D_0$  Temperature Shift Factor Calculation**

<b>E<sub>SG</sub></b>	<b>T<sub>AC</sub></b>	<b>Regression Equation</b>	<b>R<sup>2</sup></b>	<b>RMSE</b>	<b>N</b>
35	2.5	$D_0 = 1547 + 3.50(\text{Temp})$	99.8	3.89	5
70	2.5	$D_0 = 1081 + 2.18(\text{Temp})$	98.5	7.65	5
140	2.5	$D_0 = 782 + 1.51(\text{Temp})$	95.9	8.80	5
280	2.5	$D_0 = 596 + 1.22(\text{Temp})$	94.1	8.60	5
35	3.75	$D_0 = 1382 + 5.08(\text{Temp})$	99.6	9.37	5
70	3.75	$D_0 = 952 + 3.71(\text{Temp})$	98.7	12.05	5
140	3.75	$D_0 = 676 + 2.93(\text{Temp})$	97.9	12.05	5
280	3.75	$D_0 = 506 + 2.53(\text{Temp})$	97.7	11.00	5
35	5.0	$D_0 = 1229 + 6.33(\text{Temp})$	99.7	9.08	5
70	5.0	$D_0 = 833 + 4.83(\text{Temp})$	99.5	9.96	5
140	5.0	$D_0 = 581 + 3.93(\text{Temp})$	99.4	8.91	5
280	5.0	$D_0 = 426 + 3.42(\text{Temp})$	99.4	7.27	5
35	10.0	$D_0 = 817 + 8.29(\text{Temp})$	100.0	4.51	5
70	10.0	$D_0 = 531 + 6.36(\text{Temp})$	99.9	6.49	5
140	10.0	$D_0 = 353 + 5.12(\text{Temp})$	99.7	8.49	5
280	10.0	$D_0 = 245 + 4.37(\text{Temp})$	99.3	10.21	5
35	20.0	$D_0 = 467 + 8.14(\text{Temp})$	99.1	22.11	5
70	20.0	$D_0 = 297 + 6.14(\text{Temp})$	98.3	22.77	5
140	20.0	$D_0 = 191 + 4.88(\text{Temp})$	97.3	23.05	5
280	20.0	$D_0 = 126 + 4.13(\text{Temp})$	96.2	23.32	5
35	40.0	$D_0 = 244 + 6.83(\text{Temp})$	97.0	34.20	5
70	40.0	$D_0 = 154 + 5.30(\text{Temp})$	95.6	32.18	5
140	40.0	$D_0 = 97.5 + 4.35(\text{Temp})$	94.1	30.90	5
280	40.0	$D_0 = 62.7 + 3.79(\text{Temp})$	92.6	30.20	5

**Table D-10 Regression Equations for Overlay, N = 327  
(without zero values for overlay required)**

Equation	N	R <sup>2</sup>	RMSE
overlay = -135 + 45logD <sub>0</sub> + 14.9logE <sub>SG</sub> + 14.2logESALs	327	93.7	2.686
overlay = -541 + 84.9logD <sub>0</sub> + 82.4logA + 54.3logE <sub>SG</sub> + 14.5logESALs	327	95.7	2.239
overlay = 111 - 0.084A - 26.3logE <sub>SG</sub> + 13.8logESALs	327	90.7	3.273
overlay = -167 + 50.8logD <sub>0</sub> + 0.0113A + 20.4logE <sub>SG</sub> + 14.2logESALs	327	93.8	2.682

**Table D-11 Regression Equations for Overlay, N = 360  
(including zero values for overlay required)**

Equation	N	R <sup>2</sup>	RMSE
overlay = -8.06 + 0.0291D <sub>0</sub> + 0.0501E <sub>SG</sub> + 1.53ESALs	360	77.2	6.42
overlay = -137 + 45.4logD <sub>0</sub> + 15.4logE <sub>SG</sub> + 13.8logESALs	360	93.8	3.337
log(overlay) = -2.53 + 1.06logD <sub>0</sub> + 0.413logE <sub>SG</sub> + 0.231logESALs	360	66.5	0.1591
overlay = -109 + 44.1logD <sub>0</sub> + 0.0505E <sub>SG</sub> + 1.53ESALs	360	91.6	3.906
overlay = -429 + 72.6logD <sub>0</sub> + 61.4logA + 43.2logE <sub>SG</sub> + 13.8logESALs	360	94.9	3.032
overlay = 69.8 - 0.0846A - 0.0893E <sub>SG</sub> + 1.53ESALs	360	84.9	5.224
overlay = 115 - 0.089A - 27.4logE <sub>SG</sub> + 1.53ESALs	360	89.9	4.266
log(overlay) = 3.24 - 0.00194A - 0.551logE <sub>SG</sub> + 0.024logESALs	360	61.0	0.1717
overlay = 83 - 0.0874A - 2.2(E <sub>SG</sub> ) <sup>0.5</sup> + 1.53ESALs	360	88.1	4.641
overlay = 61.6 - 0.0788A - 0.0002(E <sub>SG</sub> ) <sup>2</sup> + 1.53ESALs	360	78.8	6.192
overlay = -6.82 + 16410(1/A) - 0.102E <sub>SG</sub> + 1.53ESALs	360	75.9	6.602
overlay = 274 - 91.6logA - 0.0976E <sub>SG</sub> + 1.53ESALs	360	82.2	5.684
overlay = 48.4 - 0.00008(A) <sup>2</sup> - 0.0798E <sub>SG</sub> + 1.53ESALs	360	84.5	5.302

**Table D-11 Regression Equations for Overlay, N = 360  
(including zero values for overlay required), cont.,**

Equation	N	R <sup>2</sup>	RMSE
overlay = 110 - 3.73A <sup>0.5</sup> - 0.0937E <sub>SG</sub> + 1.53ESALs	360	84.0	5.384
overlay = 46.6 - 0.0863A + 918(1/E <sub>SG</sub> ) + 1.53ESALs	360	87.6	4.730
overlay = 159 - 3.91A <sup>0.5</sup> - 28.5logE <sub>SG</sub> + 1.53ESALs	360	88.8	4.506
overlay = 331 - 95.7logA - 29.4logE <sub>SG</sub> + 1.53ESALs	360	86.5	4.944
overlay = 38.2 + 16834(1/A) - 29.8logE <sub>SG</sub> + 1.53ESALs	360	78.8	6.200
overlay = 88.3 - 0.00008A <sup>0.5</sup> - 24.8logE <sub>SG</sub> + 1.53ESALs	360	89.4	4.377
(overlay) <sup>2</sup> = 4810 - 3.83A - 1295logE <sub>SG</sub> + 87.1ESALs	360	89.2	207.4
overlay = 115 - 0.0890A - 27.4logE <sub>SG</sub> + 13.8logESALs	360	91.0	4.045
overlay = 129 - 0.0890A - 27.4logE <sub>SG</sub> - 14.0(1/ESALs)	360	89.9	4.274
overlay = 109 - 0.0890A - 27.4logE <sub>SG</sub> + 6.52(ESALs) <sup>0.5</sup>	360	90.8	4.071
overlay = 118 - 0.0890A - 27.4logE <sub>SG</sub> + 0.123(ESALs) <sup>2</sup>	360	87.2	4.808

## **APPENDIX E**

### **NONDESTRUCTIVE TESTING DEVICES**

#### **E.1 INTRODUCTION**

Many summaries of pavement nondestructive testing devices have been written. This appendix is included as a general overview of the most commonly used devices; past, present, and future. As a reminder, only devices that can measure the deflection basin can be used to calculate the Area Parameter used frequently in this thesis. Most devices are able to measure the maximum deflection at the center of the load ( $D_0$ ). Chapter 2 includes a summary of which devices are most commonly used in the United States (Table 2-1).

#### **E.2 STATIC DEFLECTION EQUIPMENT**

Devices that measure the pavement's response to a slowly applied load are classified as static deflection equipment. The Benkelman Beam was the most widely used static deflection device resulting in much of the earlier deflection based overlay designs being based on Benkelman Beam data (Smith and Lytton, 1984).

##### **E.2.1 Benkelman Beam**

The Benkelman Beam consists of a 3.66 meter (12 ft) beam with a probe on one end that rests on the pavement between the rear dual tires of a loaded truck axle. The other end is supported by stationary legs that are ideally outside the influence of the truck load. There is a pivot point 2.44 meters (8 ft) from the probe and the remaining 1.22

meters (4 ft) of the beam activates a dial gauge for measuring the displacement. The displacement is read from the dial as the truck is slowly driven away from the probe. The maximum dial reading is recorded as the rebound deflection (Newcomb, 1986, p. 8).

#### **E.2.2 Plate Bearing Test**

The plate bearing test loads a circular plate on the pavement using a hydraulic jacking system that reacts against the frame of a truck. The plate's deflection is measured by a dial gauge which is mounted on a stand placed as far away from the plate as possible. Curvature in the plates is reduced by using a stack of successively smaller diameter steel plates (Smith and Lytton, 1984).

### **E.3 AUTOMATED BEAM DEFLECTION EQUIPMENT**

This category of deflection equipment automates the Benkelman Beam process.

#### **E.3.1 La Croix Deflectograph**

The La Croix Deflectograph consists of a truck with a pivot/beam assembly mounted on it. The length and geometry of the beam vary with different wheel bases for different trucks. The measurement process begins with the beam being placed in front of the wheel. As the truck's wheel approaches the beam tip, the beam rotates about the pivot. The rotation is measured until the wheel has gone approximately 21.9 cm (0.72 ft) past the beam tip. The beams and frame are then repositioned to be in front of the wheel again to begin another measurement. Measurements can be made every 3.5 to 6 meters (11.4 to 19.7 ft) depending on the particular truck (Smith and Lytton, 1984). This device was used extensively in Europe but did not gain popularity in the United States.

### **E.3.2 California Traveling Deflectometer**

The California Traveling Deflectometer is very similar to the La Croix Deflectograph and has been used extensively by the California Department of Transportation. It basically consists of two Benkelman Beam probes mounted on a semi-trailer. The measurement is conducted in much the same manner as the La Croix Deflectograph..

## **E.4 STEADY STATE DYNAMIC DEFLECTION EQUIPMENT**

This class of deflection equipment uses dynamic force generators to produce a sinusoidal vibration in the pavement. The most commonly used models are the Dynaflect and the Road Rater.

### **E.4.1 Dynaflect**

The Dynaflect transmits a load to the pavement through two 16 inch diameter rubber-coated steel wheels, 10 centimeters (4 in) wide, spaced 50.8 centimeters (20 in) center to center. The dynamic force is created by counter-rotating, eccentric flywheels which generate a 4448 newton (1,000 pound) peak-to-peak dynamic force which is offset by the machine's static weight of approximately 746.5 kilograms (2,000 pounds). Surface deflections are measured by five geophones spaced at 30.5 centimeter (1 ft) intervals from the center of the load. Deflection measurements are recorded by a computer located inside the tow vehicle. The vibration frequency and load cannot be changed (Newcomb, 1986) (Smith and Lytton, 1984).

#### **E.4.2 Road Rater**

The Road Rater, like the Dynaflect, is a steady state dynamic device. The load is applied to the pavement surface through a steel loading plate which is approximately 10 centimeters by 18 centimeters (4 in by 7 in). Three models are available from Foundation Mechanics, Inc., the 400B with a maximum static load of 10,676 newtons (2,400 pounds), the model 2000 with a maximum static load of 16,903 newtons (3,800 pounds) and the model 2008 with a maximum static load of 25,800 newtons (5,800 pounds). The static load is created by a hydraulic system acting on the trailer weight while the dynamic force is produced by a hydraulic actuator oscillating a steel, lead-filled mass. Each Road Rater model has the capability of adjusting the loads and the frequency. Four geophones spaced at 30.5 centimeter (1 ft) intervals from the center of the loading plate measure the pavement deflections (Smith and Lytton, 1984) (Newcomb, 1986).

#### **E.5 IMPULSE DEFLECTION EQUIPMENT**

This category of equipment contains all Falling Weight Deflectometers, different models of which are manufactured by Dynatest, KUAB, and Phoenix. These machines all deliver a transient force impulse to the pavement, simulating the passage of a truck wheel over the pavement section.

##### **E.5.1 Falling Weight Deflectometer**

The FWD is a very precise measurement system which has been shown to closely model the effects of truck loading on pavements. A heavy load is dropped from a

predetermined height onto a rubber buffer system creating a load pulse in approximately a half-sine wave form of 25 to 30 millisecond duration. The load is transmitted to the pavement through a load distributing steel plate situated directly on the pavement. The plate typically measured 30 centimeters (11.8 in) in diameter, however other diameter plates are also available (Smith and Lytton, 1984). An array of geophones or accelerometers is placed from the center of the load plate radially outward along the load axis. Depending on whether the sensors measure the velocity or acceleration of the impulse waves, the data is integrated once or twice respectively to compute the deflections due to the loading. The array of sensors capture data which provides a picture of the deflection basin due to the load. Figure E-1 shows the layout of a typical FWD configuration.

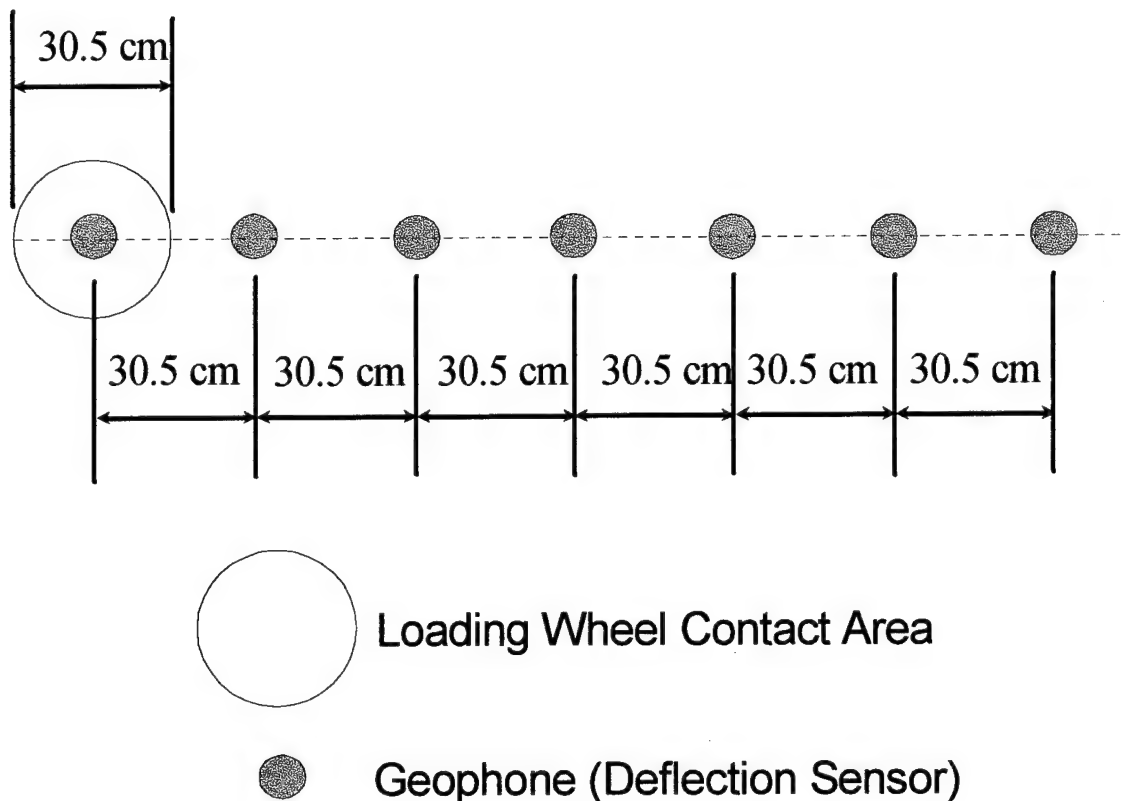


**Figure E-1: Typical FWD Configuration of Loading Plate and Geophones  
(WSDOT Guide, 1995)**

Figure E-2 illustrates a deflection basin measured by a FWD. This figure also shows how different layers affect different parts of the deflection basin, i.e. the surface course stiffness is most related to  $D_0$  while the subbase quality is reflected in  $D_3$ .

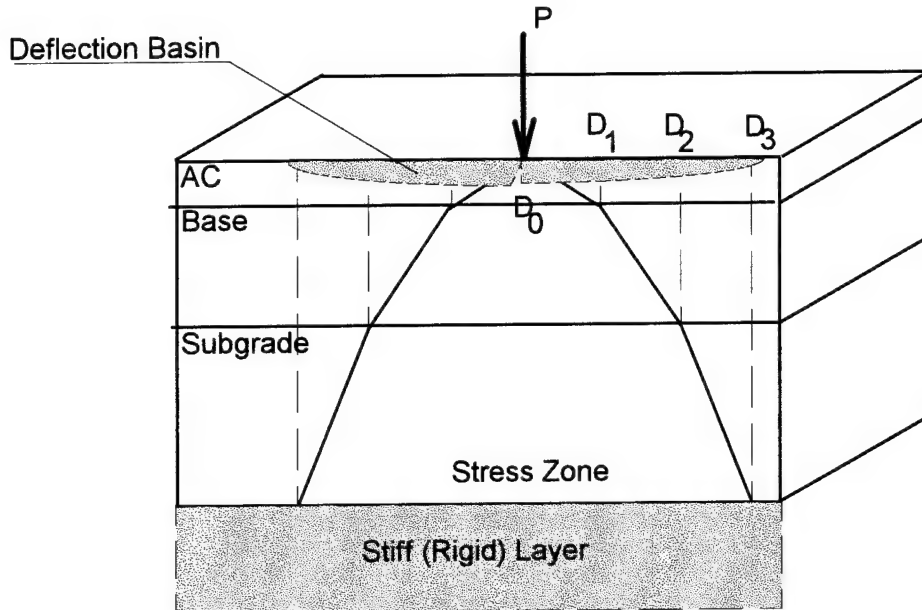


**Figure E-2 Illustration of FWD Deflection Basin (after WSDOT Guide, 1995)**

If the structure of the pavement is known (thickness and material in each layer) the elastic modulus of each layer can be estimated through the iterative process of backcalculation which will be discussed in greater detail later in this chapter.

## **E.6 LASER ROLLING WEIGHT DEFLECTOMETER**

A rolling wheel pavement deflectometer was first reported and tested in the mid 1970's (Johnson, 1995). Harr began work in the 1970's with several graduate students evaluating the use of the deflection basin to evaluate airfield pavements. They began the process of developing a system that could measure pavement deflections from a noncontact sensor mounted on a beam moving above the pavement. A rigid beam was constructed with light-emitting diodes (LEDs), however, ambient light was found to adversely affect the performance of the LEDs so they were subsequently replaced with lasers (Bush, et al., 1983). In 1984 Bush, Cox and Hall researched a system of four sensors on a rigid beam. Other efforts by Harr (1975) and Bush et al. (1983) used the four sensors on a beam approach, however, critical errors due to beam deflections were unresolved (Johnson, 1995). What was needed was a beam long enough to establish a reference elevation of the pavement outside the deflection basin, yet rigid enough not to create error due to the deflection in the beam itself (or some method of calculating the beam deflection at any given time and adjusting the pavement deflection accordingly).

### **E.6.1 Two-Point Deflection Measurement**

The principle for measuring pavement deflections using a beam passing over the pavement is to determine two heights from a floating reference datum; one on the unloaded pavement and the second at the **same point** on the pavement at the time the loaded wheel passes (Johnson, 1995). The deflection is then the difference between these two calculated heights. The Transportation and Road Research Laboratory (TRRL) in

Crowthorne, England, conducted research on a high-speed profilometer using 4 sensors on a rigid beam. The solution to the noncontact measurement system used by many rolling deflectometers was derived from this TRRL research (Bush et al., 1983)..

In order to measure the distance from the reference datum to the undeflected pavement, three sensors are required outside the influence of the applied load (beyond the deflection basin). Bush, Hall and Harr (1983) described the profile algorithm used to measure the undeflected pavement profile. The description of the algorithm that follows uses nomenclature consistent with that used by Johnson (1995) in the RWD Final Report. The undeflected height above the pavement is calculated from an initial set of measurements recorded from the three equally spaced lead sensors, termed sensors A, B, C as shown in Figure E-3. The height measured by sensors A, B and C are termed *A*, *B*, and *C* respectively. Using similar triangles and a level reference datum, a virtual height, *h*, can be calculated at sensor C by the equation:

$$A - (A-B) = C-h + (A-B)$$

solving for *h*:

$$h = A-2B+C$$

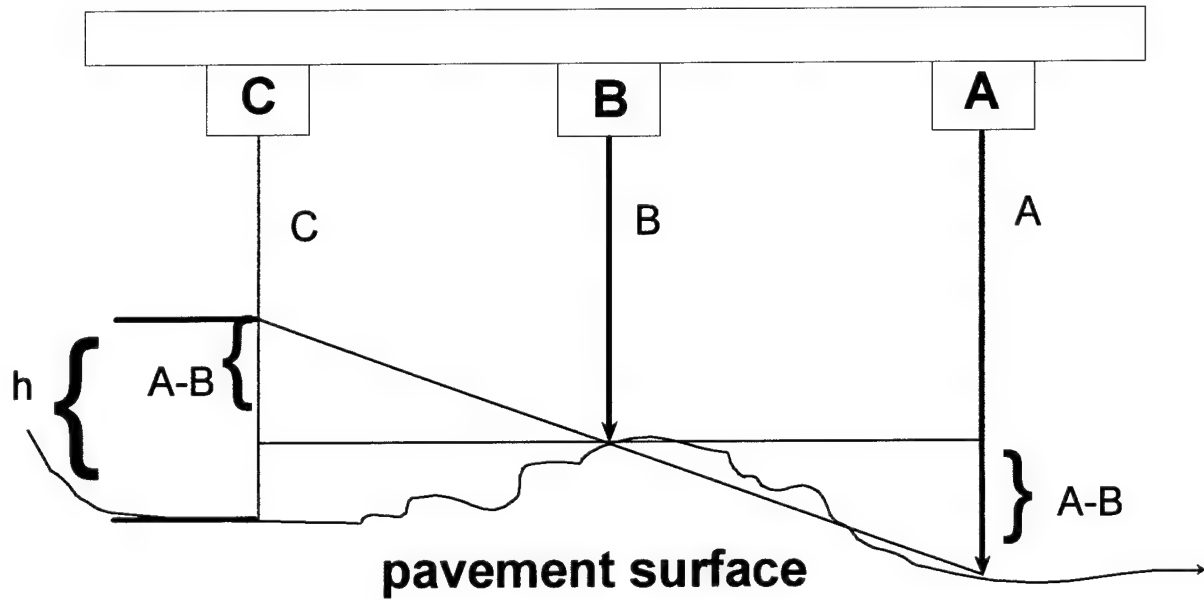


**Figure E-3 First Point Measurement (after Johnson, 1995)**

A fourth sensor, D is located adjacent to the load wheel and measures the deflection due to the applied load. The RWD is designed so that all four sensors are set at 9 ft spacing.

The virtual deflected height,  $h'$  is calculated when sensor D is directly over the spot sensor C was at when  $h$  was calculated as shown in Figure E-4.

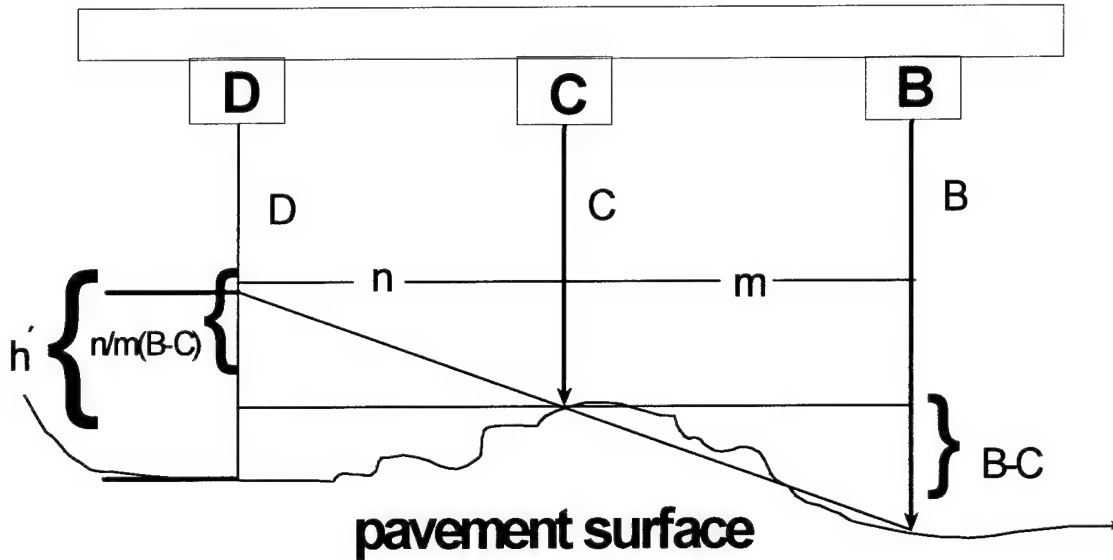


**Figure E-4 Second Point Measurement (after Johnson, 1995)**

Again, using similar triangles and a level reference datum the equation to calculate  $h'$  is

$$B - (B-C) = D - h' + ((n/m)(B-C))$$

solving for  $h'$  when  $n/m = 1$  (reflects spacing of RWD sensors):

$$h' = B - 2C + D$$

Consequently, the deflection at that point on the pavement due to the applied load is:

$$d = h - h'$$

This algorithm is completely independent of variations in the beam angle and beam height above the pavement (remember,  $h$  and  $h'$  are virtual heights).

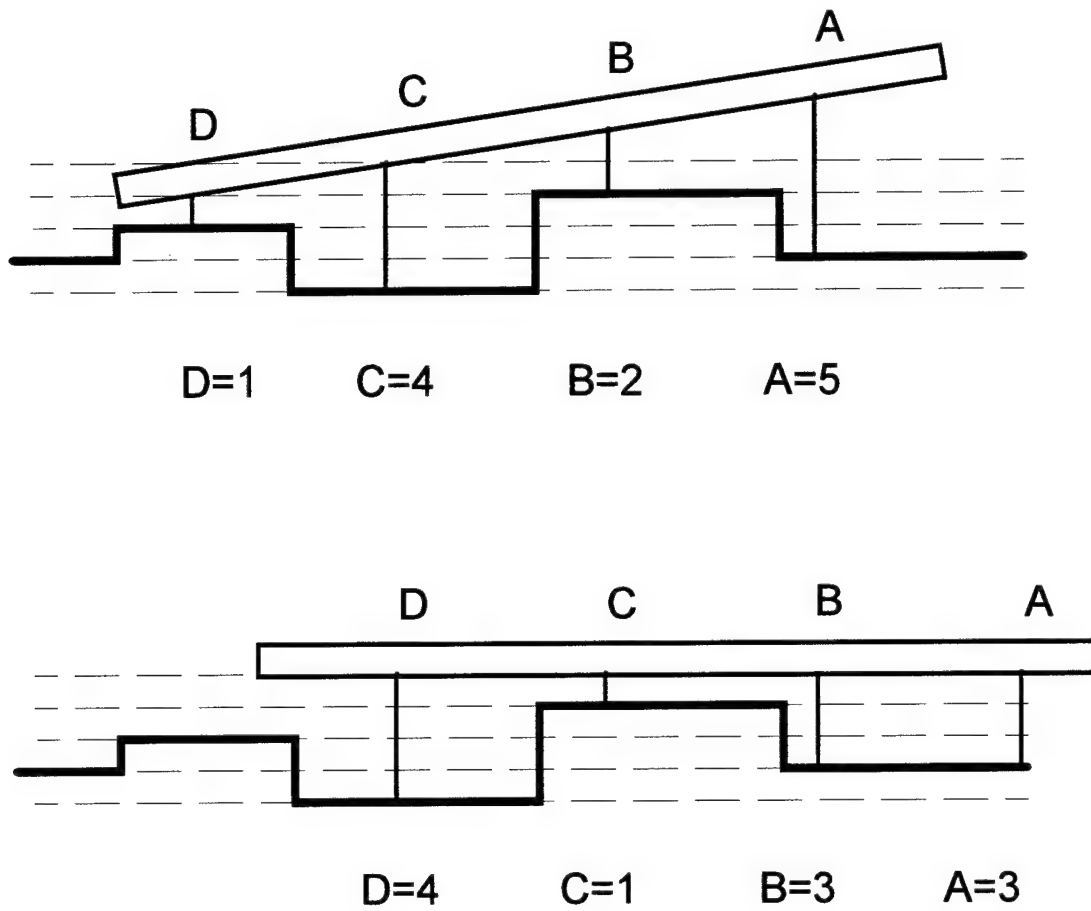


**Figure E-5 Variable Beam Angle and Height (after Johnson, 1995)**

Figure E-5 provides an example of how beam angle and height above the pavement do not effect the ability to measure deflections in the pavement. In the top figure of Figure E-5, the virtual height,  $h$  can be calculated as:  $h = A - 2B + C = 5 - 2(2) + 4 = 5$  and the bottom figure of Figure E-5 where the beam has moved forward by one sensor, the virtual height  $h'$  can be calculated as:  $h' = B - 2C + D = 3 - 2(1) + 4 = 5$  from this, it is clear that the measured deflection,  $h - h'$  is equal to 0.

## APPENDIX F

### TEMPERATURE ADJUSTMENT

#### **F.1 INTRODUCTION**

The temperature adjustment procedure developed as part of this thesis is presented in an appendix rather than in Chapter 4 with the load adjustment because this procedure is not required when using the regression equations presented in Chapters 3 and 5. The procedure is presented in this section to provide a record for future use in redeveloping regression equations with a constant AC moduli as recommended in Chapter 6.

A temperature adjustment is required if the testing will occur at other than a standard pavement temperature of 25 degrees Celsius. Deflections and the Area Parameter calculated by those deflections will increase as the pavement temperature increases. The pavement is stiffer at colder temperatures and therefore will deflect less than at higher temperatures. Section 2.6.3 in Chapter 2 discussed other research on temperature effects.

#### **F.2 METHODOLOGY**

##### **F.2.1 Data Generation**

The following relationship between pavement stiffness,  $E_{AC}$ , and temperature,  $T$ , is well accepted and used (WSDOT Pavement Guide, 1995):

$$E_{AC} = e^{9.1242 - 0.04456(T)}$$

Based on this equation, Table F-1 shows the range of temperatures associated with the asphalt concrete stiffness' used for the initial 120 pavement scenarios.

**Table F-1 Ranges of  $E_{AC}$  Used vs Temperature**

$E_{AC}$ (MPa)	Temperature (°C)
690	58.0
1380	42.5
2760	27.0
5520	11.4
11040	-4.0

Based on this information alone, it would seem that temperature differences were already included in the data that generated the relationships using the pavement responses from the initial pavement scenarios. However, another factor affects pavement stiffness. The level of fatigue will affect the pavement stiffness. The temperature vs  $E_{AC}$  equation is based on unfatigued pavement, however, once a pavement begins to fatigue (crack) the stiffness will also reduce.

In order to proceed with generating temperature shift factors, an assumption was made to clarify the source of the data. The original data from the 120 pavement scenarios is assumed to be at a constant temperature of 25 degrees Celsius meaning the AC stiffness ranges are due to fatigue levels only. This assumption clarifies that

temperature adjustments are not already embedded in the data due to the range of stiffness' used.

#### **F.2.2 Regression Analysis**

For the next step, all data is assumed to be for unfatigued pavement at different temperatures that correlate to the AC stiffness' as noted in Table F-1. In this manner, the same data can be used to see the effects of temperature on  $D_0$  and Area Parameter. Each combination of AC Thickness and  $E_{SG}$  (24 combinations possible) was used to plot Temperature vs 1/A and Temperature vs. Do. These are the relationships that correlate closest to a straight line based on plots on Minitab. The regression equation for the "best-fit" line was generated for each of the 24 combinations and can be found in Appendix D. The slope of this line is the temperature adjustment for that combination and is shown in Table F-2 for Area Parameter and in Table F-3 for  $D_0$ .

**Table F-2 Temperature Shift Factors for 1/A**

$E_{SG}$ (MPa)	AC Thickness (cm)					
	2.5	3.75	5.0	10.0	20.0	40.0
35	$2 \times 10^{-6}$	$4 \times 10^{-6}$	$5 \times 10^{-6}$	$8 \times 10^{-6}$	$7 \times 10^{-6}$	$7 \times 10^{-6}$
70	$2 \times 10^{-6}$	$5 \times 10^{-6}$	$7 \times 10^{-6}$	$11 \times 10^{-6}$	$11 \times 10^{-6}$	$11 \times 10^{-6}$
140	$3 \times 10^{-6}$	$7 \times 10^{-6}$	$10 \times 10^{-6}$	$15 \times 10^{-6}$	$16 \times 10^{-6}$	$16 \times 10^{-6}$
280	$3 \times 10^{-6}$	$9 \times 10^{-6}$	$13 \times 10^{-6}$	$21 \times 10^{-6}$	$22 \times 10^{-6}$	$22 \times 10^{-6}$

**Table F-3 Temperature Shift Factors for  $D_0$** 

$E_{SG}$ (MPa)	AC Thickness (cm)					
	2.5	3.75	5.0	10.0	20.0	40.0
35	3.5	5.08	6.33	8.29	8.14	6.83
70	2.18	3.71	4.83	6.36	6.14	5.30
140	1.51	2.93	3.93	5.12	4.88	4.35
280	1.22	2.53	3.42	4.37	4.13	3.79

**F.3 RESULTS**

The shift factors in Table F-2 and Table F-3 were then correlated against subgrade modulus,  $E_{SG}$ , and AC thickness,  $T_{AC}$ , to see if a relationship exists to be able to predict the temperature shift factor for any pavement scenario. The best equation for each shift factor follows. Additional equations attempted can be found in Appendix D.

$$\log A_{SF} = 0.849 + 0.0361(E_{SG})^{0.5} - 1.93\left(\frac{1}{T_{AC}}\right)$$

$$R^2 = 92.9\% \quad RMSE = 0.08642 \quad N = 24$$

$$D_{0_{SF}}^{0.5} = 2.13 + 28.6\left(\frac{1}{E_{SG}}\right) - 2.47\left(\frac{1}{T_{AC}}\right)$$

$$R^2 = 90.8\% \quad RMSE = 0.1445 \quad N = 24$$

where  $A_{SF}$  = Shift factor for 1/Area Parameter

$D_{0_{SF}}$  = Shift Factor for  $D_0$  ( $\mu m$ )

$E_{SG}$  = Subgrade Modulus (MPa)

$T_{AC}$  = AC Thickness (cm)

Once a shift factor is calculated, the adjusted  $D_0$  and  $A$  are calculated by the equations:

$$A_{adjusted} = A_{temp} + (25-temp)(A_{SF})$$

$$D_{0_{adjusted}} = D_{0_{temp}} + (25-temp)(D_{0_{SF}})$$

where  $D_{0(\text{temp})}$  and  $A_{\text{temp}}$  are the values measured in the field and temp is the pavement temperature during field testing.

The adjusted value for A will be greater than the measured value of A when the temperature during testing is less than 25 °C. The same relationship will exist for  $D_0$ .